THE IMPACT OF VARIABLE SPEED DRIVES ON ENERGY EFFICIENT INDUCTION MOTORS

by

Ernest Ohene Anyang

A thesis submitted to the University of Cape Town in full fulfilment of the requirements for the degree of

MSc Electrical Engineering

December 2011

DECLARATION

This is to certify that this dissertation has not been previously submitted to this or any other university for any degree. I understand the meaning of plagiarism and declare that all the work in the document, except that which is properly acknowledged, is my own.

……..

Ernest Ohene Anyang

……..

Date

ACKNOWLEDGEMENT

It has taken more than the effort of a single person for this work to come to fruition. I would therefore want to acknowledge the following personalities for their help and support during my study.

My sincere gratitude and appreciation goes to the Almighty God for all the favour and grace he showered me during my study. Surely, it is not of him that wills, nor of him that runs, but of God that shows mercy. I am forever indebted to him for the strength he gives me daily.

I would want to thank my supervisor, Prof. Mohamed Azeem Khan and my co-superviser Dr Paul Barendse for their invaluable contributions to my research work. Their criticisms and corrections have been my backbone, and they have been more than supervisors to me throughout my period of study.

I am extremely thankful to Dr Richard Okou for taking the time to read through this work. His inputs have been instrumental in getting this work to this standard.

I am very grateful to Mr C. Wozniak and Mr P. Titus for their support and guidance in the laboratory. The experimental work would have been impossible without these men.

To my colleagues of Room 3.34.2 Menzies: Hartmut Jagau, John Wangiku, Ashwill Van Wyk, Barbara Herndler, Manuella d'Oliviera Pio, Oelof De Meyer and Akrama Khan, thanks a lot for all the care, love and support you offered during my studies. To the other members of the AMES group; Derishni Reddi, Jacques De La Bat, Chetan Gajjar, Chris de Beer, Po-Heng Liu and Anesu Tichagwa, it has been a great pleasure knowing you and I will forever remember the mark you each made in my life.

To my family in Cape Town, I don't know how MSc. would have been without you.

I want to acknowledge the National Research Foundation for their financial support.

This section would be incomplete without me saying thank you to my parents for their support and motivation. Truly, a good man leaves an inheritance for his

children’s children. I owe every word in this thesis to you for everything you have spent on my education since infancy.

ABSTRACT

In an era when the world is faced with diminishing resources and energy security concerns, the slightest energy savings can prove essential in energy conservation. Induction motors and motorised loads consume an estimated 60% of the total energy required in the South African industry. This figure stands at 40% worldwide. Energy Efficient induction motors have proven to be an effective solution in the quest to reduce energy consumption. In South Africa, there have been efforts to replace the standard motors already in operation with energy efficient motors. The South African Utility, ESKOM, through its energy efficiency motor programme, has been providing incentives to its industrial customers to speed up this process.

Variable speed drives (VSDs) are used in industry together with induction motors for variable torque, fan, pump, blowers, compressors and other induction motor applications. They have proven to be more efficient than other systems of varying process speed like dampers and valves. The influx of energy efficient induction motors into the industry implies that there is the need to study and understand the operations of VSDs with energy efficient motors in order to maximize the energy savings.

To be able to quantify the differences between using a VSD on an energy efficient motor and on a standard motor, the differences between standard and energy efficient motors in terms of design and performance have been compared. Eight standard and energy efficient motors were tested in the laboratory using internationally accepted standards. The efficiency results from these evaluations have been presented. Variations in induction motor losses resulting from these different standards are also presented.

In the presence of harmonics, more sophisticated methods are needed to accurately predict the input power of the induction machine. Definition of power from the first principles is considered and some methods of measuring power are compared. It is concluded that using the wattmeter to measure power in the presence of harmonics is prone to error.

This study further tests these induction motors by using two industrial drives. The performances of the motors are monitored while operated under the VSD supply. The efficiency of the motor was also estimated using harmonic equivalent circuits that are developed from the fundamental per phase equivalent circuit of the induction motor. The resulting efficiencies are compared with the case when the motors are operated without the VSD. The switching frequency of the VSDs used was varied and the tests repeated to examine the impact of varying VSD switching frequency on the motor efficiency.

This study confirms that there is a drop in induction motor efficiency under VSD supply. Also the induction motor efficiency increases with increase in the VSD switching frequency. The increase in switching frequency has negative consequences on the frequency converter (losses and heat). Valuable recommendations are made for further research.

LIST OF FIGURES

LIST OF TABLES

GLOSSARY

%VU	Percentage Voltage Unbalance
%VUF	Percentage Voltage Unbalance Factor
A/D	Analogue to Digital
AC	Alternating Current
DC	Direct Current
AS/NZ	Australian/New Zealand Standard
CSV	Comma Separated Values
Dq	Direct - Quadrature
EE	Energy Efficient
EPAct	Energy Policy Act
ESKOM	Electricity Supply Commission
IEC	International Electrotechnical Commission
IEEE	Institute Of Electrical And Electronics Engineers
IGBT	Insulated Gate Bipolar Transistor
IP	Ingress Proteection
JEC	Japanese Electrotechnical Committee
LV	Low Voltage
MATLAB	Matrix Laboratory
NEMA	National Electrical Manufacturers Association
PC	Personal Computer
Premium +	Premium Plus
PWM	Pulse-Width Modulation
SANS	South African National Standards
SLL	Stray Load Loss
SVPWM	Space Vector Pulse-Width Modulation
TEFC	Totally Enclosed Fan Cooled
USB	Universal Serial Bus
VSD	Variable Speed Drive
VSI	Voltage Source Inverter
VU	Voltage Unbalance

VUF	Voltage Unbalance Factor

TABLE OF CONTENTS

CHAPTER ONE: INTRODUCTION

1.1 Background

Induction motors contribute to a large percentage of the industrial energy requirements and it is estimated that about 60% of the industrial energy is used by motors and motorized loads in South Africa. Globally, this figure stands at 40%. A report issued by ESKOM Demand Side Management in October 2009 states that an estimated 100,000 electric motors are installed in South African industries with their power ratings ranging from 1.5kW up to 36MW [1]. These motors altogether represent about 10GW of installed capacity. In a period when the world is faced with energy problems, a reduction in the energy consumed by motors will greatly influence the cost of energy. A small improvement on the efficiency of induction motors will further reduce the burden on the supply utilities. An example of this is the energy efficiency motor programme by ESKOM which seeks to realize energy savings by providing incentives to industrial customers to replace standard motors with energy efficient motors.

Over the years, drive systems consisting of induction machine(s) attached to a variable speed drive have been useful for variable torque, fan, pump, blowers, compressors and other induction motor applications. They have proven to be more efficient than other systems of varying process speed like dampers and valves.

With the upsurge of energy efficient motors in the industry, there is the need to look into the usage of variable speed drives with energy efficient motors since the harmonic loss mechanisms are not fully understood. The return on the combination of variable speed drives and energy efficient motors for specific applications can be very rewarding. This notwithstanding, the harmonics generated through the use of variable speed drives have effects on induction motors which need to be critically looked at, so as to guarantee the effectiveness of this application. Hence there is the need for thorough investigation into the effects of VSD applications on operations of EE motors and the system efficiency as a whole.

1.2 Research Questions

The purpose of this research is to consider the effects of using variable speed drives on energy efficient induction motors. In view of this the following research questions were considered:

- What are the differences between standard and EE motors?
- How can power measurement be carried out accurately in the presence of harmonics?
- What effects are observed on EE and standard motors when they are operated with a variable speed drive?

1.3 Aims and Objectives

The main aims and objectives of this research include:

- To compare and contrast between standard and EE motors in terms of their design and steady-state performance.
- Accurately measure power in the presence of harmonics.
- Determine the impact of variable speed drive operations on the performance of both standard and EE motors.
- Quantify the efficiency differences between standard and EE motors with and without VSD supply.
- Make relevant recommendations for future research.

1.4 Methodology

The research involves both experimental and analytical procedures. A set of eight induction motors were tested in the laboratory according to the IEEE 112, IEC 60034-2-1 standards and references made to the IEC 60034-2-3 standard when the machines were tested under VSD supply. These motors are all three-phase, four-pole, 50Hz, totally enclosed fan cooled induction motors from the same vendor with power ratings of 3kW, 7.5kW, 11kW and 15kW. Two industrial drives with power ratings of 7.5kW and 15kW were used in testing these motors. The motors were first tested from a generator set in the absence of the VSDs and then with the VSD

connected between the motors and the generator set. Because of the harmonics associated with using VSDs, special care was taken in measurement of the power into the motor in order to accurately account for the harmonic powers involved. A harmonic equivalent circuit developed for each of the motors was used to estimate the efficiency of the machines using programmes developed in MATLAB. The results from the tests were analysed and from that conclusions made.

1.5 Scope and Limitations

The experimental work and simulations are limited to induction machines from the same vendor (WEG) and the power ratings are 3kW, 7.5kW, 11kW and 15kW.

This study is limited to LV induction motors and hence low power VSDs. These have the typical topologies discussed.

The industrial drives used in the experimental work provide a limited amount of flexibility in terms of control and hence analysis is limited to the performance of drives with this level of flexibility and control.

1.6 Thesis Structure

The remainder of the thesis is structured as follows:

Chapter Two

This chapter takes a look at induction motor efficiency. The various ways of defining motor efficiency are considered and the various factors that affect induction motor efficiency are also examined. This is followed by an assessment of the different methods available for induction machine efficiency testing. The chapter also considers the various ways of measuring power in the presence of harmonics and some different methods of carrying out this process are compared.

Chapter Three

This section of the thesis gives a general overview of variable speed drives and the harmonics associated with them. A detailed look is taken at the PWM VSI. The harmonic equivalent circuit of an induction motor is developed from the

fundamental equivalent circuit. The various equations of torque, slip, power and currents associated with these circuits are also developed. The chapter also explores the effects of VSD operations on induction motor losses and other motor performance as available in literature. Some harmonic mitigation techniques are also considered in this chapter

Chapter Four

The various test procedures that were undertaken in the laboratory and the test equipment used are presented in detail in this chapter.

Chapter Five

This chapter presents the experimental results obtained from the tests carried out in the laboratory. Analytical results from the harmonic equivalent circuits are also presented. Analysis of these results is also carried out in this chapter.

Chapter Six

The conclusions based on the work done in the research are presented in this chapter. Recommendations are made based on the results and towards future research.

1.7 Review of relevant Literature

A great deal of research is continuously being conducted in the field of inverter fed induction machines. Below are some of the materials published in this field.

- Alexander Eigeles Emanuel [2]

  The writer talks of the effects of temperature rise in squirrel cage motors from randomly varying the harmonic voltages. He proves theoretically that the harmonic losses in per unit of the rated or base loss can be approximately by the series

$$\Delta P_H/\Delta P_R \approx 35 \sum_{h=5,7,11\ldots} (1/h)(V_h/V_R)^2 \qquad (1.1)$$

  Where

ΔP_R is the basic electrical loss at rated current and voltage

V_R is the rated voltage (rms)

V_h is the harmonic voltage of the order h (rms)

He comes up with different modules by which temperature variations with harmonic voltages can be calculated.

- Fernand G. G. De Buck [3]

  The writer conducts a study on the theoretical performance of electric motors that are supplied with unfiltered pulsewidth modulated inverter. He states in his work that the PWM principle can be employed to eliminate all harmonics lower than the pulse frequency. However, with higher frequencies, the losses are considerable increased. In his work, the writer concludes that based on factors such as the winding design, the degree of filtering and the fundamental frequency, PWM-induced copper losses can increase for more than 50%. He further stated that aside high frequency torques, small motors or motors with high number of pole pairs may experience low frequency torques within a wide speed range.

- K. Venkatesan and James F. Lindsay [4]

  This publication calculates the losses in an induction motor fed from a six-step voltage and current source inverters and compares the efficiencies when supplied by these different sources. It then goes on to calculate the copper losses using the equivalent circuit that includes the effects of space harmonics and corrected for skin effect in rotor bars. It concludes by stating that with constant air gap flux, the efficiency of an induction motor supplied by a six-step voltage or current converter is the same irrespective of the type of source employed. In the case where there is reduced torque, the efficiency of the motor is higher when it is supplied by a current source inverter than when it is supplied by a voltage source inverter. Conversely, when there is increased torque, the motor records a higher efficiency in the situation whereby it is supplied by a voltage source inverter than when it is supplied by a current source inverter.

- Fernand G. G. De Buck, Paul Gistelinck, and Dirk De Backer [5]

  This publication presents a semiempirical loss model of an induction motor developed as a function of motor power rating. Similar to all other publications, the purpose of this model is to estimate the losses caused by voltage and current supplies that are distorted by harmonics. The publication presents an experimentally verified penalization factor for time harmonics. This factor is a function of the motor size and is quasi-linearly dependent on the harmonic frequency. This model estimates the stator, rotor I^2R as well as the iron losses separately and subsequently combined and simplified. It concludes that the iron plus stray load loss contributions become very relevant as soon as the frequency exceeds 250-2500Hz.

- Daniel S. Kirschen, Donald W. Novotny and Warin Suwanwisoot [6]

  In this publication, the optimal operating point which results in minimum power loss in induction motor operations is determined using the complete speed and torque range of the motor. The publication concludes that substantial power savings are achieved using the optimal operating point than in the case of the conventional programmed voltage/hertz control. Similar to what has been stated in previous literature, it states that the main flux saturation has an essential role in determining the optimal operating point. Using the models developed in the publication, the writers conclude that the power loss in an induction motor can be reduced either by an increase in flux for large loads or a decrease in flux for light loads.

CHAPTER TWO: INDUCTION MACHINE EFFICIENCY

This chapter takes a look at the definition of induction machine efficiency and compares the more important standards available for testing the efficiency of induction machines. The various methods of determining power in the presence of harmonics have been considered and experimental results presented.

2.1 Definition of Efficiency

A system's efficiency is defined as the ratio of the output power to the input power. An electric motor's efficiency represents the machine's ability to convert electric power at the input to mechanical power at the output [7] as shown in equation (2.1):

$$\eta = \frac{P_{Mechanical}}{P_{Electrical}} \tag{2.1}$$

Where

$P_{Mechanical}$ is the output power at the motor shaft

$P_{Electrical}$ is the electrical power absorbed from the main supply

In practice, the efficiency of a motor is less than 100% due to the losses in the machine, which are dissipated as heat. Efficiency can therefore be expressed in terms of the total losses as shown in equation (2.2) [7], [8]:

$$\eta = \frac{P_{Mechanical}}{P_{Mechanical} + \sum Losses} = 1 - \frac{\sum Losses}{P_{Electrical}} \tag{2.2}$$

Because the input and output power quantities are almost equal numerically, the direct determination of efficiency using equation (2.1) is error prone since a small error in measuring either of the two quantities significantly influences the efficiency [8]. Therefore, equation (2.2) is preferred when determining efficiency.

2.2 Factors affecting induction machine efficiency

In order to quantify how much of the input power in an induction machine is put to use on the shaft; it is necessary to examine the various factors that influence the efficiency of the machine under consideration. Some of the factors considered within

the scope of this study include losses in the machine, quality of power supply, load profile and in some cases, repair of the machine.

2.2.1 Quality of Power Supply

Though the efficiencies stated on the nameplates of induction motors are determined under ideal supply conditions in terms of voltage and frequency, these conditions seldom exist during normal operation conditions. The power quality issues that exist ranges from voltage unbalance, presence of harmonics and voltage variations. These will be discussed in further detail below.

- **Voltage Unbalance**

Voltage unbalance in a three-phase system occurs when the magnitude of line or phase voltages and/or phase angles vary from the values at balanced conditions. Voltage unbalance is the non-equality of voltage magnitudes and /or phase angles among the three-phases at any given point of time [9].

There are different definitions of voltage unbalance, and the chosen definition will result in different percentage unbalances for a specific voltage condition. These include

National Electrical Manufacturers Association (NEMA) defines voltage unbalance (VU) as [10], [11], [12], [13]:

$$\%\,\mathrm{VU} = \frac{\text{maximum deviation from average line voltage}}{\text{average line voltage}} \times 100\% \qquad (2.3)$$

Though this definition only makes use of line voltages and neglects the phase angles, it is widely used in the industry because it is easy to use.

Alternatively, the IEEE definition of voltage unbalance makes use of phase voltages. It defines voltage unbalance as [10], [11], [13]:

$$\%\,\mathrm{VU} = \frac{\text{maximum deviation from average phase voltage}}{\text{average phase voltage}} \times 100\% \qquad (2.4)$$

In terms of phase angle, the IEEE definition is similar to that of the NEMA definition. The phase angle is neglected in the definition.

The IEC definition, which is referred to as the true definition of voltage unbalance, defines voltage unbalance as the ratio of the negative to the positive sequence voltage. The percentage voltage unbalance factor (%VUF) is given as [9], [11], [10], [13]:

$$\%\text{VUF} = \frac{\text{negative sequence voltage component}}{\text{positive sequence voltage component}} \times 100\% \tag{2.5}$$

Either phase or line voltage can be used in this definition. The positive and negative sequence voltage components are obtained by resolving three-phase unbalanced line voltages (or phase voltages) into two symmetrical balanced components of the line (or phase voltages) [11]. The two balanced components are given by

$$\mathrm{V_p} = \frac{\mathrm{V_{ab}} + \mathrm{a} \cdot \mathrm{V_{bc}} + \mathrm{a}^2 \cdot \mathrm{V_{ca}}}{3} \tag{2.6}$$

$$\mathrm{V_n} = \frac{\mathrm{V_{ab}} + \mathrm{a}^2 \cdot \mathrm{V_{bc}} + \mathrm{a} \cdot \mathrm{V_{ca}}}{3} \tag{2.7}$$

Where:

$\mathrm{a} = 1\angle 120°$

$\mathrm{a}^2 = 1\angle 240°$

The effects of voltage unbalance on an induction machine can be ascertained considering the effect of the positive (V_p) and negative (V_n) sequence voltages independently on the induction machine. Using the theory of superposition, the effects of V_p and V_n and their associated; slips *s* and (2-s) respectively, can be added to find the total effect on the machine [11], [13].

The total output power (per phase) is given as:

$$\mathrm{P_m} = \mathrm{I_p^2 r_2}\left[\frac{(1-\mathrm{s})}{\mathrm{s}}\right] - \mathrm{I_n^2 r_2}\left[\frac{(1-\mathrm{s})}{(2-\mathrm{s})}\right] \tag{2.8}$$

and the torque per phase is given as:

$$\mathrm{T} = \mathrm{r_2}\frac{\left[\frac{\mathrm{I_p^2}}{\mathrm{s}} - \frac{\mathrm{I_n^2}}{(2-\mathrm{s})}\right]}{\omega_{\mathrm{syn}}} \tag{2.9}$$

Where

r_2 is the per phase rotor resistance

ω_{syn} is the synchronous speed in radians per second

I_p and I_n are the per phase positive and negative sequence rotor currents respectively given as [11], [13]:

$$I_p = \frac{V_p}{\sqrt{\left\{\left[r_1 + \left(\frac{r_2'}{s}\right)\right]^2 + (x_1 + x_2')^2\right\}}} \tag{2.10}$$

$$I_n = \frac{V_n}{\sqrt{\left\{\left[r_1 + \frac{r_2'}{(2-s)}\right]^2 + (x_1 + x_2')^2\right\}}} \tag{2.11}$$

It can be seen from the preceding equations (2.8) and (2.9) that the presence of the negative sequence current results in a reduction of the total output power and torque. The machine therefore takes longer to run up in the presence of unbalanced voltages. There is an increase in thermal stress which could result in failure [11]. The reduced torque also forces the motor to operate at higher slip. This results in increased rotor current and loss in the form of heat dissipation and as a result, further decrease in efficiency [13].

- **Voltage Variation**

Voltage variation is random variation of voltage magnitude [9]. The variation of voltages can result in balanced over-voltages or balanced under-voltages. Balanced over voltage is whereby the three-phase voltages are individually and equally greater than the rated voltage value. Balanced under-voltage on the other hand is when the three-phase voltages are individually and equally lesser than the rated voltage value [9]. Figure 2.1 illustrates the effects of variation of voltage on the performance of induction motors. From the figure, though there exist a linear relationship individually between the torque and the starting current with the voltage variation, the situation is different in the case of the power factor, efficiency and full load current.

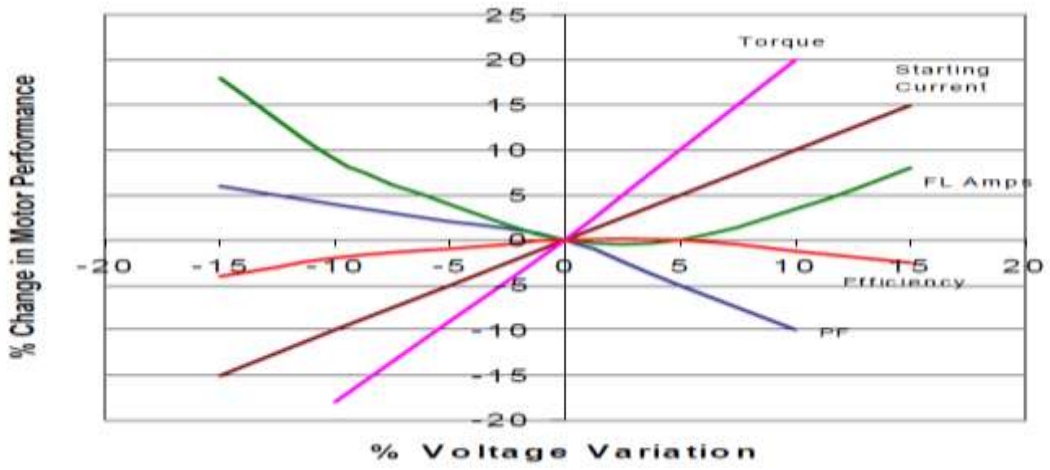

Figure 2.1 Effect of Voltage Variation on Induction Motors [14]

2.2.2 Harmonics

Harmonics are sinusoidal components of a periodic waveform having a frequency that are integral multiples of the fundamental frequency [15]. Harmonics are produced by the application of a non sinusoidal voltage to a circuit containing linear or non linear impedance or the application of a sinusoidal voltage to a circuit containing non linear impedance.

The presence of voltage and current harmonics from the supply impacts the load under the supply considerably. The presence of voltage harmonics in the supply results in an increase in the core losses in the induction machine. The copper losses in the induction machine increase as a result of the current harmonics. Based on the order of the harmonics available, there are resulting pulsating torques associated with the harmonics. The effect of the harmonic torques on the fundamental can be additive or subtractive based on whether the harmonics are forward rotating or reverse rotating respectively.

When induction machines are controlled via voltage or current inverters, the current to the machines are non-sinusoidal. They consist of the fundamental and harmonic components of the current. The rotating fields produced by these harmonic currents rotate at speeds that are higher than that of the fields produced by the fundamental current and as a result produce parasitic torques in the machine. Another major effect of time harmonics in electric machines is increased heating which affects the machine efficiency [15]**.** The actual effect of these harmonics on induction machines

depends on the reactance since at high frequencies; the impedance is dominated by the reactance.

Space harmonics are the harmonic fluxes produced by the distributed winding of an induction machine. The mmf produced when current flows through the distributed winding of an induction machine is non-sinusoidally distributed in the air gap. As a result, the air gap flux is made up of the fundamental and harmonic components of the flux; which are called the space harmonics. Space harmonics affect the speed-torque characteristics of the machine. Though space harmonics cannot be avoided since they are generated by the magnetic interaction of the various phase windings in their bid to produce rotating magnetic fields, optimization of the machine design can reduce space harmonics in the machine.

2.2.3 Loading of the Machine

The nameplate efficiency of induction motors are stated at rated load conditions. Most motors used in industry operate at 60% of their rated load since many motors operate at higher than the rated load conditions [16]. Hence, the stated nameplate efficiencies are typically not applicable to the normal operation of the motor. A critical look at the efficiency versus load curve of an induction motor, places the maximum efficiency of the motor between 50% and 80% of the rated load depending on the size and design of the motor [17] . Below the 50% loading point, the efficiency of most motors drop drastically with a reduction in load [8], [18]. Figure 2.2 shows a variation of motor efficiency with load.

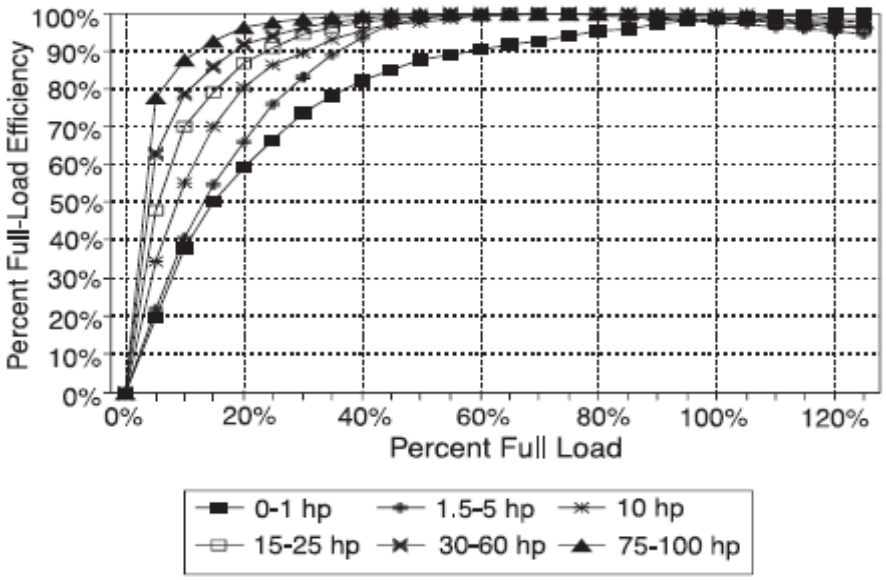

Figure 2.2 Variation of Motor Efficiency with Load [13]

Though over sizing of motors has effects on operating cost and the environment, operating motors at reduced loads has the following advantages [17]:

- It accommodates any load fluctuations and unbalance.
- It makes provision for safety margin, since it provides the capacity of meeting the requirements even when the actual mechanical load is uncertain.
- It allows for increasing motor load in the future.

Conversely, over loading a motor causes a rise in the motor temperature. This results in a reduction in its efficiency and also reduces its service life.

A study of over and under loading of motors will provide the user with the optimum region of operation; striking a balance between operating the motor at the optimum efficiency and the service life of the motor.

2.2.4 Losses in the Machine

The difference between the input electric power at the motor terminals and the output mechanical power on its shaft is defined as losses. Losses greatly influence the efficiency of the motor and therefore needs to be examined critically. The losses in a motor are generally categorised as load dependent and load independent losses [8]. The load dependent losses include the I^2R losses in both the stator and the rotor, and the stray load losses. The load independent losses comprise of the core losses and the friction and windage losses. The power flow diagram in Figure 2.3 identifies the various losses at play between the input and the output of the motor.

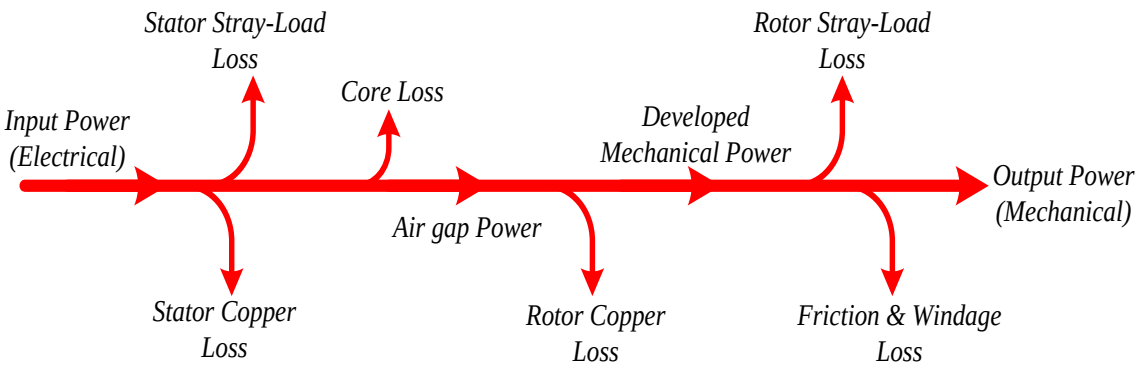

Figure 2.3 Power Flow in an Induction Motor

According to [8] and [17], the efficiency of a motor is maximum when the load dependent losses equals the load independent losses.

The following section examines the various losses and how they adversely affect efficiency.

- **Stator Copper Losses**

  These are also referred to as the stator winding resistance losses. These losses depend on the current flowing through the stator windings and the value of the resistance (which depends on temperature, the cross-sectional area, length of winding and the winding material) [19]. They make up 35% to 40% of the total losses in the motor [8]. In order to reduce these losses, the stator winding resistance in an induction motor can be reduced by increasing the volume of copper wire in the stator, through improved stator slot design and/or by using thinner insulation.

- **Rotor Copper Losses**

  Also known as rotor winding resistance losses, they are copper losses in the rotor conductive bars [19]. They make up 15% to 20% of the total losses in the induction motor [8]. By increasing the size of the rotor conducting bars and end rings, the conductor resistance is decreased and as a result the associated rotor losses are reduced [20].

- **Core Losses**

  The core losses encompass the hysteresis and the eddy current losses in the iron laminations of the machine [19]. Hysteresis losses in the core are due to the hysteresis effect. Hysteresis losses can be reduced by improving the permeability of the steel, extending the length of the core, or using thinner laminations [21]. Eddy current losses result from the rapid change of flux density through the core [19]. These losses are reduced by using a high-resistivity core material or by using thin laminated core [19]. The core losses make up 15% to 20% of the total losses in the machine.

- **Friction and Windage Losses**

  They make up 5% to 10% of the total losses in the machine [8]. The friction and windage losses are as a result of the movement of air and friction in the motor. They are significant in totally enclosed fan-cooled or high speed motors [21]. These losses are considered constant by all standards from no-load to full load conditions. They can be reduced by lowering bearing friction and also by improving fan design to enhance air flow.

- **Stray Load Losses**

  Though stray load losses make up 10% to 15% of the total losses present in the induction machine [8], they are the most complex of all the losses when it comes to loss estimation. Stray load losses; also known as additional losses are expressed as the difference between the total losses in the machine and the summation of all the conventional losses; already described in the preceding sections. Thus stray load loss (P_{SLL}) can be expressed as [22]:

$$P_{SLL} = P_{Input} - (P_{Output} + P_{Cu\ Stator} + P_{Cu\ Rotor} + P_{Core} + P_{FW}) \quad (2.12)$$

  Where

  P_{Input} is the input electrical power

  P_{Output} is the output mechanical power

  $P_{Cu\ Stator}$ is the stator copper losses

  $P_{Cu\ Rotor}$ is the rotor copper losses

P_{Core} is the iron losses and

P_{FW} is the friction and windage losses

Stray load losses mainly originate from pulsations of flux in the stator and rotor teeth and in the air gap [23]. They also include losses due to active iron and other metal parts other than conductors [24].

2.2.5 Machine Repair

The effect of rewinding a damaged motor on the efficiency of the motor needs to be considered. When a motor experiences damage to the windings, it is a common practise in industry to rewind it in a quest to restore it to its original state. However, this typically has a negative impact on the motors' efficiency [17]. The decision to repair a machine should take into consideration the procedures employed by the rewind company. The procedures have over the years been known to alter the winding and slot designs, the choice of winding, insulation performance and operating temperature. Due to the effects of rewinding a damaged motor on the losses associated with the machine, there is summative effect on the overall efficiency. Studies by [17] and [7] show a decrease in efficiency after the motors are rewound. In special cases however, when motors are rewound under controlled conditions, there can be an increase in the efficiency.

2.3 International Standards for Induction Motor Testing

The extent of research carried out in the field of testing electric machinery has necessitated the standardisation of testing procedures. Fortunately, numerous standards exist worldwide for testing electric machines. Notable among these are the IEEE 112 [25], the IEC 60034-2 [26] , the Japanese standard JEC 2137, the Canadian standard C390, the Australian/New Zealand standard AS/NZ 1359.5, and the more recent IEC 60034-2-1 [27]. The IEEE standard is primarily used in North America and the IEC is used in Europe. South Africa adopted the IEC 60034-2-1 in 2008 as the SANS 34-2-1 [28].

Though all these standards exist, the values of efficiency stated on nameplates of induction machines or given in catalogues by the manufacturers are measured or

calculated according to the IEEE 112-B or the IEC 60034-2 (indirect method) [24]. The JEC 2137 neglects the stray load losses in the determination of efficiency and therefore produces higher efficiency values [7], [10]. A summary of the differences and similarities between the IEEE and IEC standards are shown in Table 2.1.

Table 2.1 Summary of the Main Differences and Similarities between IEEE 112-B, IEC 34-2 and IEC 61972 [24]

		IEC 34 – 2 (Indirect Method)	**IEEE 112 – B**	**IEC 61972 (Direct Method)**
Type of measurement		Summation of losses	Direct	Direct
Segregation of losses		Yes	Yes	Yes
Core losses with voltage drop compensation		No	No	Yes
SLL using regression analysis		No	Yes	Yes
Temperature correct winding (I^2R) losses (both in the rotor and in the stator)		No	Yes	Yes
Thermal equilibrium at rated load		No	Yes	Yes
Stabilization of no-load losses		No	Yes	Yes
Dynamometer torque correction		No	Yes	Yes
Instrumentation accuracy (+/- % of full scale)	Electrical	1.0	0.2	0.2
	Instrument transform	1.0	0.2	0.2
	Frequency	1.0	0.1	0.1
	Speed	1.0	1 rpm	0.1
	Torque	1.0	0.2	0.2
	Resistance	0.5	**0.2**	0.2

The next two sub-sections further reviews the two main standards in Table 2.1 .

2.3.1 IEEE 112 - 2004

The IEEE 112 consists of five main methods of efficiency determination for polyphase induction motors and generators; Methods A, B, C, E and F. Method A employs the direct method in determining the efficiency as expressed in equation (2.1); where efficiency is the ratio of the output and input powers. Method B employs the input-output with segregation of losses in determining efficiency. It

however uses a direct method in determining the stray load losses. During the load test, this method requires the temperature of the stator winding to be within 10ºC of the hottest temperature recorded during the rated load temperature test. Method C uses a back to back machine test. A separation of losses is applied to obtain the total stray load losses for both the motor and the generator. The stray load losses are then apportioned between the two machines based on the rotor currents. Method E uses electrical power measurement with loss segregation. The stray load loss is determined using the direct method. Method E1 however uses assumed values of stray load losses based on the power rating of the motor under test. Method F uses the equivalent circuit in determining the efficiency and direct measurement to determine the stray load losses. Method F1 like E1 assumes values for the stray load loss. In determining the core loss, the IEEE 112 does not compensate for voltage drop in the stator winding. Ideally, the core loss is constant and independent of the load. The IEEE 112 employs a linear regression for smoothing the stray load loss by expressing it as a function of the square of the load torque. A satisfactory test, depicting correct instrumentation and test readings is achieved if the correlation coefficient of the linear regression is higher than 0.9. Another concern of the IEEE 112 is the measurement of winding temperature and resistance. It requires the measurement of the cold winding temperature and resistance. These readings are used as the basis for applying temperature corrections, whereby the temperature is measured at every load point.

2.3.2 IEC 60034-2 and IEC 60034-2-1

Both the IEC 60034-2 and the IEC 60034-2-1 use the separation of losses in determining efficiency. The IEC 60034-2 however does not compensate for the voltage drop in the stator windings when obtaining the core losses; unlike the IEC 60034-2-1 which determines the core losses by accounting for voltage drop in the stator windings at each loading point using equation (2.13):

$$U_r = \sqrt{\left(V - \frac{\sqrt{3}}{2} \times I \times R_{LL} \times \cos\varphi\right)^2 + \left(\frac{\sqrt{3}}{2} \times I \times R_{LL} \times \sin\varphi\right)^2} \qquad (2.13)$$

Where:

U_r is the voltage accounting for the resistive drop (V)

V is the rated line voltage (V)

I is the rated line current (A)

R_{LL} is the line to line resistance (Ω)

φ is the power factor angle

The IEC 60034-2 does not take into account temperature correlation of the copper losses to the specific temperature point. It therefore does not require the installation of temperature sensors. It does not require the stabilisation of the friction losses in the bearing at the operating condition before performing the no-load test. Furthermore, in determining the stray load loss, the IEC 60034-2 directly attributes 0.5% of the input power absorbed by the motor as the stray load loss.

The IEC 60034-2-1 is very similar to the IEEE 112. Previously known as IEC 61972 [10], it determines the stray load losses using either direct or indirect methods. In the direct method, it determines the stray load losses similarly to the method employed in the IEEE 112-B. But in smoothing the stray load loss it requires a correlation factor of not less than 0.95. In determining the stray load losses indirectly, it assigns a preset value from a predefined curve based on the machine's power rating.

Studies have shown that expected difference between efficiency results determined using the IEEE and the IEC standards is approximately 1% [24]. This is evident for 89 motors with ratings between 2hp and 100 tested under 60Hz supply.

2.4 Measurement of power in the presence of harmonics

In the presence of harmonics, the different definitions of power produce different numerical values due to the contribution of the harmonic powers to the total power. The process of using a wattmeter to measure active power is susceptible to error in the presence of harmonics. Therefore, this method of measuring power is only valid in the absence of harmonics [29].

2.4.1 Power from first principles

For a balanced three phase system, power is defined as [19]:

$$P = \sqrt{3} \times V_{l-l} \times I_l \times \cos\theta \tag{2.14}$$

Where

V_{l-l} is the line to line voltage

I_l is the line current

θ is the angle between the voltage and current phasors

Equation (2.14) is only valid when all line voltages and currents are identical in magnitude and phase displaced by 120 degrees. Unfortunately, this condition is not always available. Hence power per phase can be calculated as

$$P = \frac{1}{T}\int v(t)i(t)\,dt \tag{2.15}$$

Where

v(t) is the magnitude of the instantaneous voltage

i(t) is the magnitude of the instantaneous current

T is the period

The total power is the sum of either two or all of the per phase powers derived from equation (2.15).

The product of *v(t)* and *i(t)* gives the instantaneous power. Summing this product over a cycle and averaging gives the average real power over the period [30].

In the presence of harmonics,

$$v(t) = \sum_{n=1}^{\infty} V_n \sin(n\omega t + \theta_n) \tag{2.16}$$

Where

V_n is the amplitude of the voltage harmonic

n is the voltage harmonic order

θ_n is the phase angle of the voltage harmonic

$$i(t) = \sum_{m=1}^{\infty} I_m \sin(m\omega t + \phi_m) \tag{2.17}$$

Where

I_m is the amplitude of the current harmonic

m is the current harmonic order

ϕ_m is the phase angle of the current harmonic

$$\text{Real power} = \frac{1}{T}\int_0^T vi\, dt = \frac{2\pi}{\omega}\int_0^{\frac{2\pi}{\omega}} v(\omega t)i(\omega t)dt \tag{2.18}$$

Since $\int_0^{2\pi} sin(nt)sin(mt)dt = 0$, for all n ≠ m and $\int_0^{2\pi} sin(nt)cos(mt)dt = 0$, for all m and n, real power will be the sum of the real power of the fundamental and the real power for each of the harmonic components in the presence of harmonics [30].

The afore-mentioned theorem can be confirmed based on the Parseval's theorem; which states that for a power signal $f_p(t)$ with Fourier coefficient $F(n)$, the average power in the waveform is [31]

$$P = \frac{1}{T_0}\int_{\frac{-T_0}{2}}^{\frac{T_0}{2}} \left|f_p(t)\right|^2 dt \tag{2.19}$$

For a voltage signal $f_p(t)$, the power through a purely resistive load $R\Omega$ *is* given as

$$P = \frac{\left|f_p(t)\right|^2}{R} \tag{2.20}$$

The power equation remains unchanged for a 1Ω resistor even when $f_p(t)$ is a current signal. Therefore for a 1Ω resistance, power is given as

$$P = \left|f_p(t)\right|^2 \tag{2.21}$$

Energy (E) flow per period is given as

$$E = \int_{\frac{-T_0}{2}}^{\frac{T_0}{2}} \left| f_p(t) \right|^2 dt \tag{2.22}$$

Hence average power is as given by equation (2.19).

It is possible to measure the magnitude of *v* and *i* several times over the cycle, each measurement is called a sample. However, the sampling frequency should be greater than twice the highest frequency.

It can be shown that the average power is [32]:

$$P_{avg} = \sum_{n=1}^{\infty} V_n I_n \cos\theta_n \tag{2.23}$$

Where the right hand side of the equation sums power in the presence of harmonics [29].

Using A/D converters, it is possible to digitize the voltage every *T* seconds. Similarly, the current is synchronously digitized with the voltage. The quantities *V(t)* and *I(t)* are multiplied and the products summed across the cycle. If *N* samples are taken, the average power is [29]

$$P_{avg} = \frac{1}{N} \sum_{i=1}^{N} V(i\Delta T) I(i\Delta T) \tag{2.24}$$

2.4.2 Comparison of methods of power determination

Using a Yokogawa WT 1600 Power Analyser, the power drawn by an induction motor under variable speed drive supply was measured using three different methods. These three different methods employed equations (2.14), (2.23) and (2.24). The power meter uses equation (2.14) during its normal operation mode. The voltage and current used in the equation are true rms values. The true rms voltage (V_{rms}) or true rms current (I_{rms}) is defined as [33]:

$$V_{rms} \text{ or } I_{rms} = \sqrt{\frac{1}{T} \int_0^T f(t)^2 \, dt} \tag{2.25}$$

Where

f(t) is the input signal (voltage or current) as a function of time

T is the period of the input signal

In the case of equation (2.23), the harmonic voltages, harmonic currents and their associated power factors were recorded when the power meter was in operated in the harmonic mode. These parameters were multiplied to obtain the power associated with each individual harmonic and the sum of these powers produced the total power as obtained in equation (2.23). To calculate the total power using equation (2.24), the power meter was used to trace the voltage and current waveforms. The different sample points of the voltage waveforms are multiplied by the respective points of the current waveform. These products are summed up and the resulting sum divided by the number of sample points to obtain the power as described by equation (2.24). A 7.5kW EE motor was operated with the VSD, and at any given load, the power drawn by the motor under the VSD supply is calculated using these different methods. The resulting values of input power are plotted against the load. Figure 2.4 presents the input power versus load for the 7.5kW EE motor.

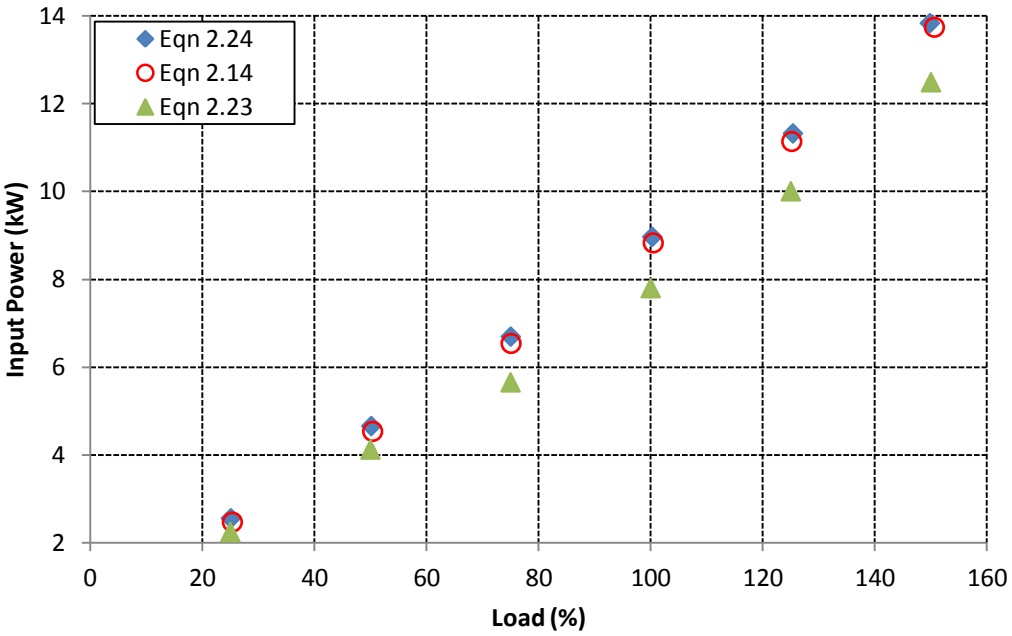

Figure 2.4 Input power versus load for 7.5kW EE motor using different methods of power measurement

From Figure 2.4, it can be observed that using equation (2.24) yields the highest values of input power for any given load. This is because this method properly accounts for harmonic powers and as a result it records the highest input power reading. Determining power using equation (2.14); which is based on readings from the normal operations of the power meter on the other hand, would have been more accurate if there were no harmonics involved. Though equation (2.23) makes use of the harmonic powers in calculating the power, the accuracy of this method depends on the instrumentation available, and hence gives the lowest power readings.

Since the tests involved in this work covers motors under VSD supply, the method of measuring power using equation (2.24) will be employed in subsequent calculations. This method takes instantaneous points along the voltage and current waveforms and finds the average of their products.

CHAPTER THREE: EFFECTS OF VSDs ON INDUCTION MOTOR PERFORMANCE

This chapter gives a general overview of variable speed drives and the harmonics associated with them. Specific focus is given towards PWM VSI, since these are most common. The space and time harmonic equivalent circuits of an induction motor are developed from the fundamental equivalent circuit. The various equations for torque, slip, power and currents associated with these circuits are also developed. Finally, the impact of VSD's operations on induction motor losses and other induction motor performance parameters are explored.

3.1 Overview of Variable Speed Drives

The VSDs used in low powered applications, typically have a front-end rectifier to convert the mains supply to a DC- voltage, and an inverter from the DC-bus, to obtain the desired output AC voltages and currents, adjustable in magnitude and frequency. A generic block diagram of the variable speed drive is as shown in the Figure 3.1.

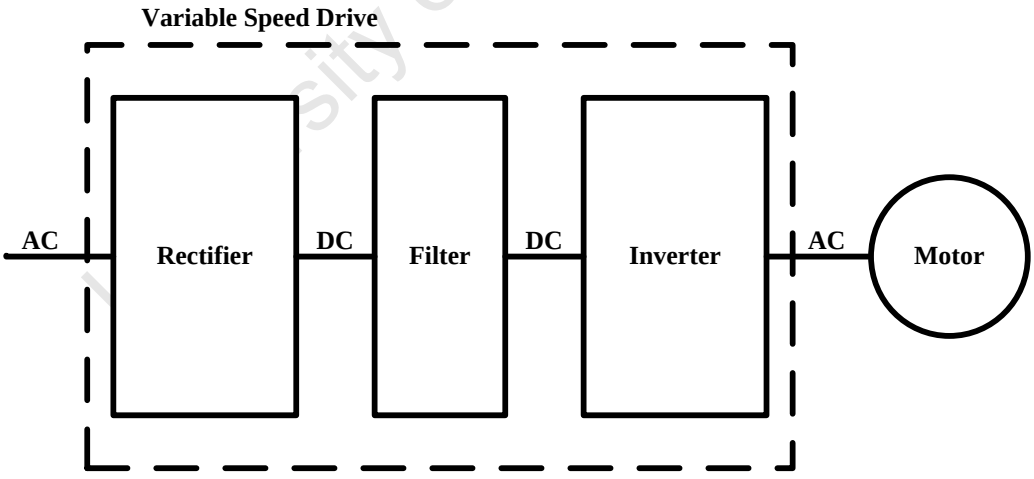

Figure 3.1 Block Diagram of a Variable Speed Drive

These drives are classified according to the selection of inverters and rectifiers used. The most prevalent VSDs are pulse-width modulated voltage source inverter (PWM VSI) with a diode rectifier, square-wave voltage source inverter (square wave VSI) with a thyristor rectifier and a current source inverter with a thyristor rectifier [34].

The main difference between a voltage source inverter and a current source inverter is that, in a voltage source inverter, the dc input appears as a voltage source to the inverter with ideally no internal impedance, but in a current source inverter, the dc input appears as a current source to the inverter with an infinite internal impedance [34].

In addition to controlling voltage and frequency, current source inverters control the amount of current delivered to the motor. Current source inverters are mostly used in applications that require very large horsepower. Current source inverters are usually designed for specific motor applications and require a better match between the inverter and the motor [34].

Voltage source inverters control voltage and frequency usually independent of the motor impedance [35]. The more dominant type of the voltage source inverters in industry today are the PWM drives [35], [36]. They have become the industry drive of choice. The variable speed drive used in the laboratory for the purpose of this study employed the PWM technology. Since PWMs are the most common drives applied, a detailed look at these PWM VSIs will be taken in the next subsection.

The orders and magnitudes of harmonics present in a VSD driven system depends on the inverter type and the controlling technique employed. Generally, the order of the harmonics present is related by the number of pulses as indicated by equation (3.1) [37].

$$h = (m \times p) \pm 1 \tag{3.1}$$

Where:

h is the harmonic order

m is an integer

p is the number of pulses in the circuit

The magnitude of the harmonic is inversely proportional to the harmonic order.

Deducing from the preceding equation, a three phase, full wave converter with six pulses will produce harmonics of the order 5,7,11,13,17,19…

The flux produced by harmonic voltages rotates in the air gap at speeds which equals the product of the harmonic order and the fundamental synchronous speed. The direction of rotation of the flux however can be the same or opposite the direction of rotation of the rotor [34]. For any integer *m*, harmonics of the order (6m + 1) produce flux that have the same phase rotation as the fundamental. The flux rotates in the same direction as the rotor and are therefore referred to as forward rotating harmonics. On the other hand, harmonics of the order (6m – 1) are known as the reverse rotating harmonics because they produce a flux rotation opposite to the direction of the rotor.

There are two basic control types employed in the inverters used in variable speed drives. These are scalar and vector control.

Scalar control maintains constant flux in the machine by keeping the ratio of rms supply voltage to frequency constant. It is mostly applied when there is no need for fast responses to speed and torque commands, and when a single drive is connected to several motors [38].

Fast responses and high level of precision on motor speed and torque is achieved by means of vector control. Vector control uses a two-axis (dq) model of an induction machine and achieves independent control of the flux and torque producing components of stator current, similar to that of a separately excited DC motor. Good dynamic response is achievable through this control technique [38].

3.2 PWM VSI Drives

This section explores the PWM VSI drives and how some drive properties influence the induction motor performance.

A schematic representation of a PMW-VSI is given in Figure 3.2:

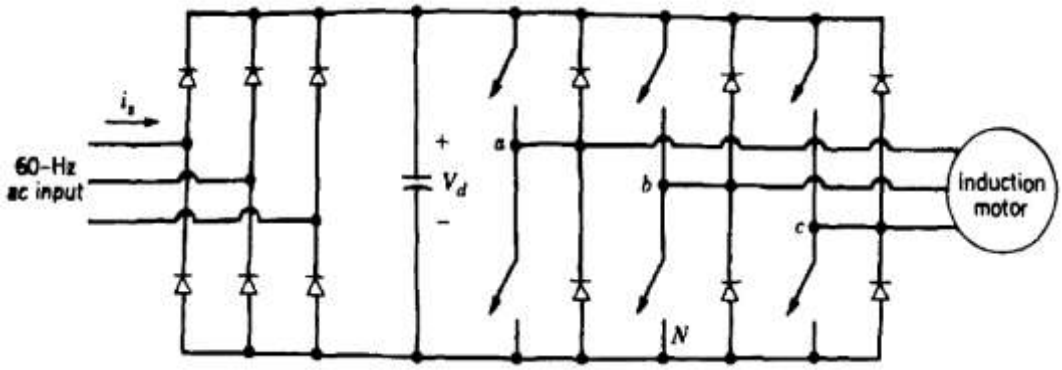

Figure 3.2 PWM VSI Drive [34]

The waveform associated with this converter is shown in Figure 3.3

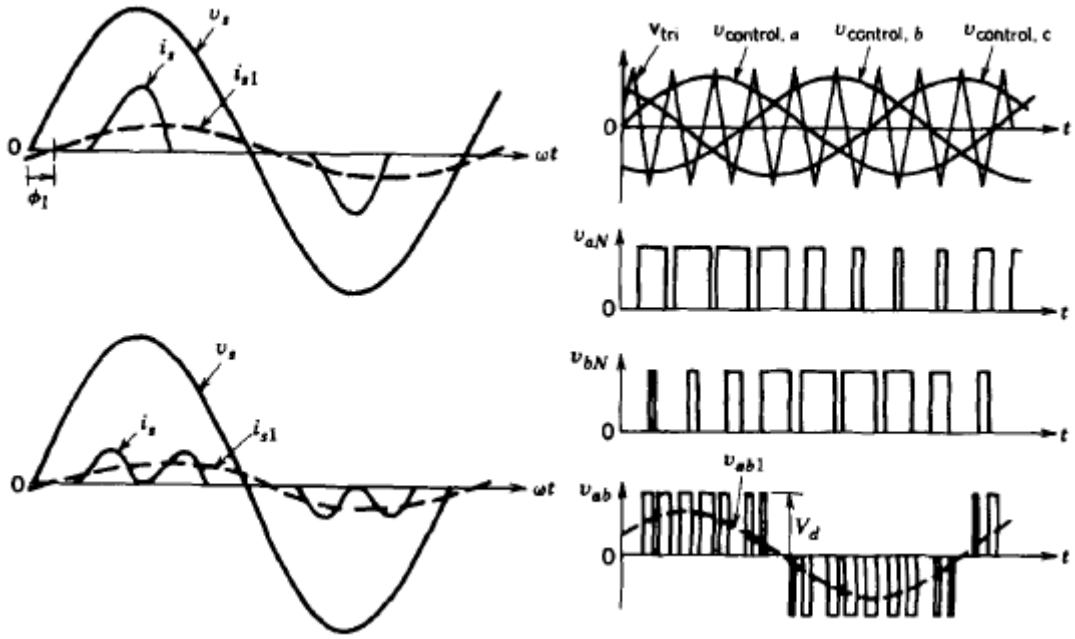

Figure 3.3 Waveform associated with a PWM VSI [34]

The following sections take a look at some PWM switching techniques and how some PWM characteristics affect induction motors.

3.2.1 PWM Switching Techniques

Under a non-sinusoidal supply, a motor experiences the usual losses associated with sinusoidal supply and additional losses introduced by harmonics. For a PWM inverter-fed induction motor, a variation of inverter properties like modulation index, switching frequency and modulation frequency impacts the harmonic losses on the machine, and hence the total losses.

Some of the switching techniques applied for a PWM inverter include the sinusoidal PWM and the Space Vector PWM (SVPWM).

- **Sinusoidal PWM**

Sinusoidal PWM seeks to produce a sinusoidal output waveform of a desired frequency. A control signal which is sinusoidal at the desired frequency is compared with a triangular waveform. Based on which of these waveforms is larger in magnitude, the dedicated switch is turned on. This is illustrated in Figure 3.4 .

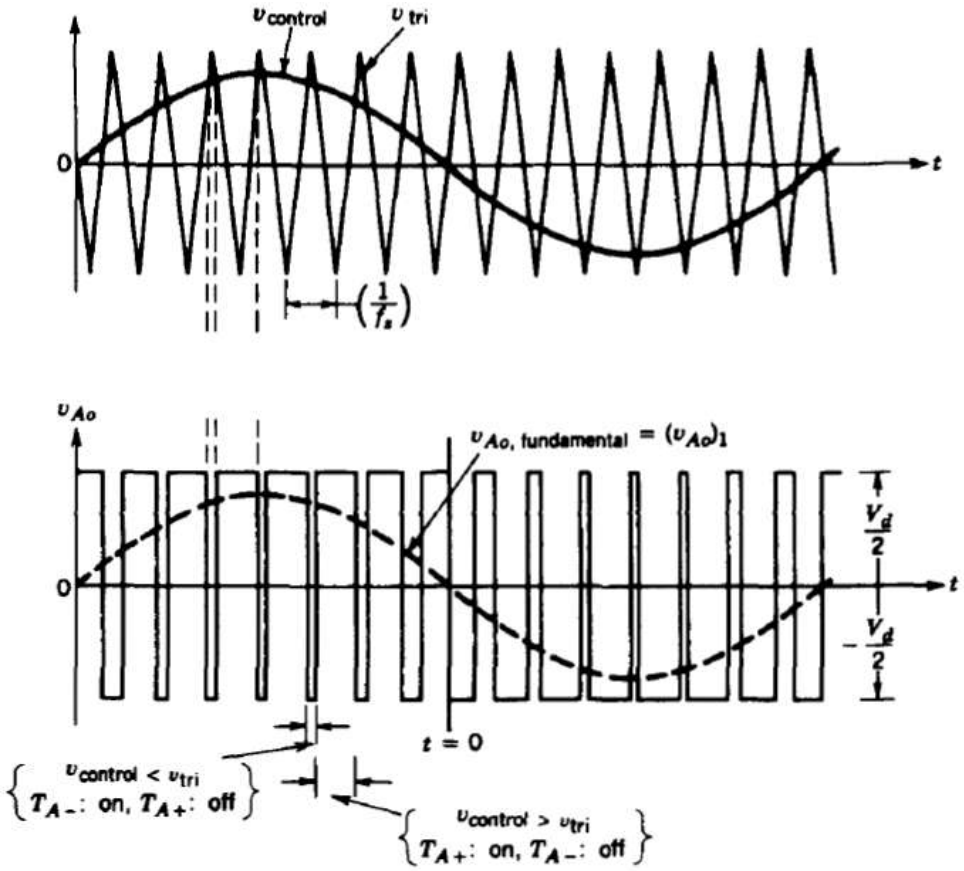

Figure 3.4 Pulse-width modulation [34]

The effect of dead time during switching is necessary as it prevents short circuit of the power supply of the PWM inverter and prevents the switches in each leg from being on at the same time [39] . The inverter switches at a frequency f_s which is the frequency of the triangular waveform. With the advancement in technologies for IGBTs and other switching devices, it is possible to operate the inverter at high switching frequencies since they are able to withstand these frequencies. Because of the relative ease of filtering out harmonic voltages at high frequencies, it is desirable to use as high a switching frequency as possible, though this increases the switching losses in the inverter switches.

- **Space Vector PWM**

Space Vector PWM (SVPWM) is a newer technique of producing PWM to control the output frequency and voltage of an inverter. It treats the sinusoidal voltage as a constant amplitude vector rotating at constant frequency. It allows the user to place the vector at a specified point in the α-β reference frame. This is shown in Figure 3.5.

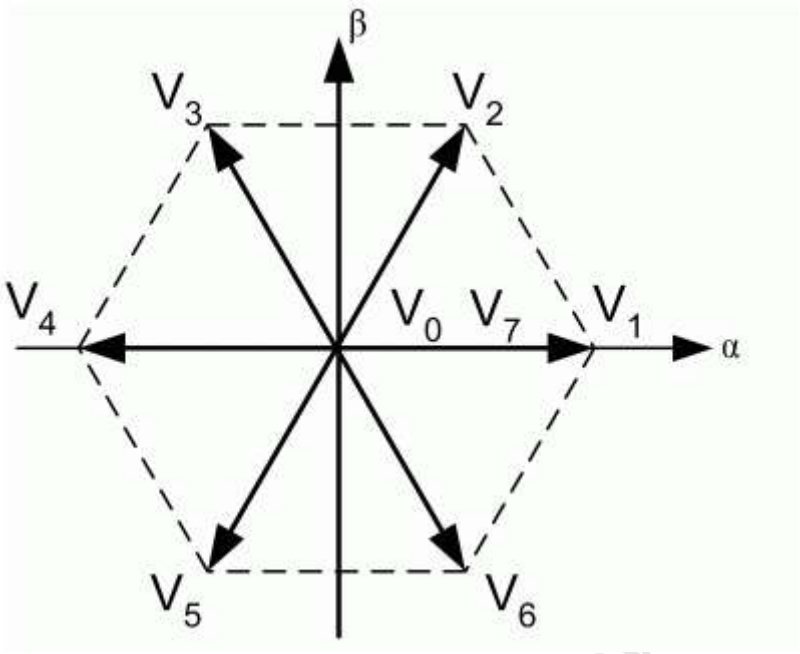

Figure 3.5 Space Vector Modulation

By changing the magnitude of the vector, one can control the magnitude of the 3-phase supply [40]. The SVPWM is preferred to the sinusoidal PWM because it produces reduced harmonic distortion in the output voltage or current waveforms. Also, it better utilises the available DC bus voltage.

3.2.2 Effects of Inverter switching frequency on Induction motor losses

According to [31], the harmonics in the output voltage of the waveform from the inverter appear as sidebands, centered around the switching frequency and its multiples. The total harmonic distortion of a sinusoidal PWM waveform decreases with an increase in switching frequency [41] [42] and according to [43] increasing switching frequency reduces current harmonics too. This analysis does not take into account the switching losses, which increase with switching frequency [44]. Higher frequencies can also damage stator insulations due to steep fronted voltage waveforms associated with the higher frequencies [36] and there are other problems like bearing degradation associated with higher frequencies. Higher pulse frequency will reduce current harmonics and harmonic losses too [43]. Figure 3.6 gives a graphical representation of the effects of switching frequency on the motor losses

and the converter losses. It is evident from the figure, a reduction of the harmonic losses in the motor by increasing the switching frequency does not imply a reduction in converter losses, and hence there is the need for motors to be designed specifically for converter applications in order to obtain an optimised system (motor and drive combination).

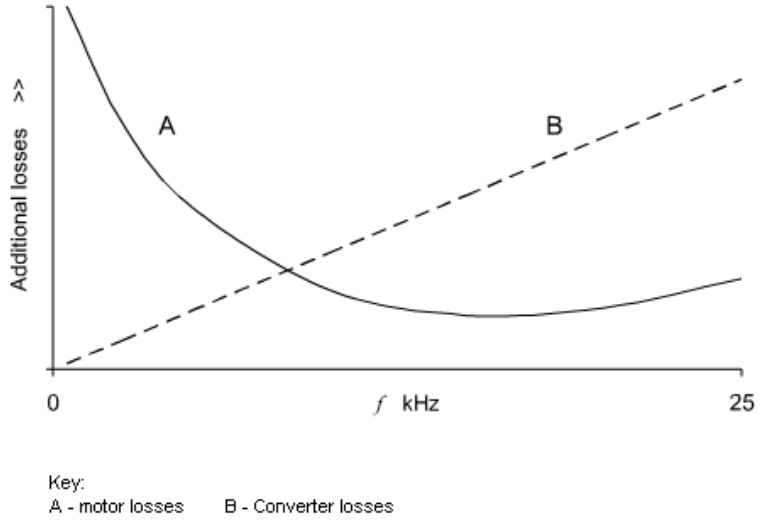

Figure 3.6 Variation of Harmonic losses with switching frequency [45]

3.2.3 Effects of the modulation index on losses

The amplitude modulation index (m_a) of the PWM inverter is the ratio of the peak control signal voltage to the peak triangular waveform voltage.

For values of modulation index less than 1.0, the amplitude of the fundamental frequency voltage varies linearly as the modulation index. This region is classified as the linear region. Overmodulation occurs when m_a is increased beyond 1.0. In this region, the output voltage contains more harmonics in the sidebands than in the linear region. This is illustrated in Figure 3.7. In addition to the fact that the harmonics with dominant amplitudes in the linear region may not be dominant in the overmodulation region, the amplitude of the fundamental frequency voltage does not vary linearly with the amplitude modulation ration [34].

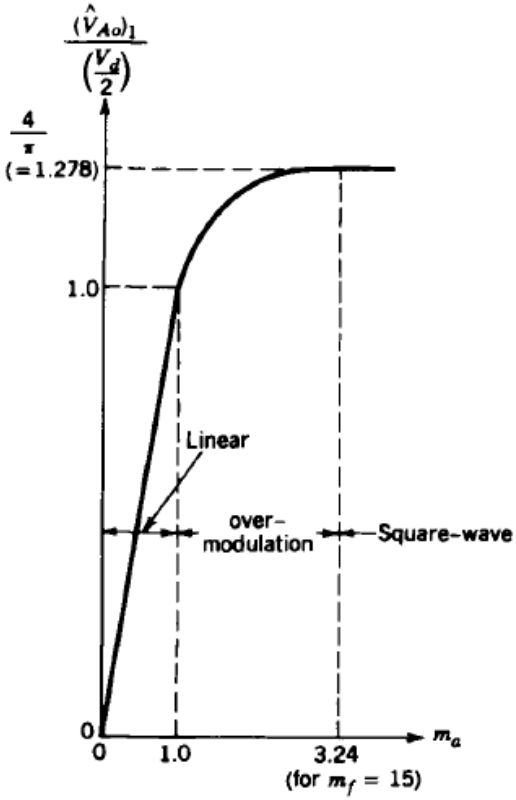

Figure 3.7 Voltage control by varying m_a [34]

According to [44], an increase in modulation index of a PWM VSI drive, decreases the core losses present in the induction motor under the VSD supplied. This is evident from the no-load core loss determined from the constant losses in the machine. For a constant dc bus voltage, the total harmonic distortion drops heavily in regions of modulation index less than unity but the variation is slower in over-modulated regions [41] .

3.3 Equivalent circuit modelling of inverter fed induction motors

The IEEE recommended equivalent circuit of an induction motor is shown in Figure 3.8. [19]. It gives V_1 as the fundamental voltage at the stator terminals, R_1 and X_1 as the per-phase stator winding resistance and leakage reactance respectively, R_2' and X_2' as the per-phase rotor resistance and leakage reactance referred to the stator winding respectively, X_m as the magnetizing reactance and s as the slip.

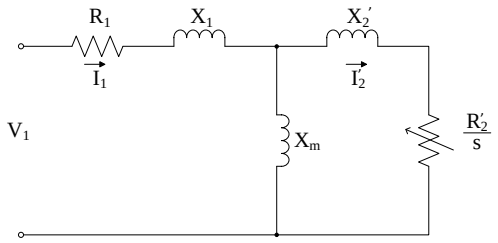

Figure 3.8 IEEE recommended equivalent circuit of an induction motor [19]

To account for the impact of harmonics, the fundamental per-phase equivalent circuit already considered has to undergo some modifications. Since the space and time harmonics have different effects on the induction machine, separate equivalent circuits are considered to account for these harmonics within the machine. Though there are some models that make adjustments for the magnetizing reactance with flux variation, skin effect and deep bar effect, this model was adopted because it is more versatile and though simplified, it is backed by relevant previous work.

The space harmonic equivalent circuit of an induction motor is shown in Figure 3.9:

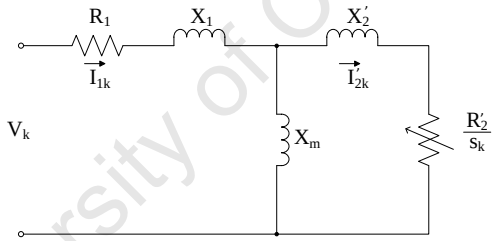

Figure 3.9 Space harmonic equivalent circuit of an induction motor [46]

The fundamental synchronous speed is *k* times the synchronous speed of the k^{th} order space harmonics [46], hence

$$\omega_k = \frac{2\pi n_k}{60} = \frac{2\pi \frac{n_1}{k}}{60} = \frac{\omega_1}{k} \tag{3.1}$$

For forward rotating space harmonics, the harmonic slip is given as

$$S_k = \frac{n_k - n}{n_k} = (1 - k) + kS_1 \tag{3.2}$$

Where

S_k and S_1 are the harmonic and fundamental slips respectively

k is the harmonic order.

Similarly, for the backward rotating space harmonics, the harmonic slip is given as

$$S_k = \frac{n_k + n}{n_k} = (1 + k) - kS_1 \tag{3.3}$$

Where

S_k and S_1 are the harmonic and fundamental slip respectively.

Using the impedance of the harmonic equivalent circuit, the harmonic stator current can be defined as

$$I_{1k} = \frac{V_k}{(R_1 + jX_1) + \frac{\left(\frac{R_2'}{S_k} + jX_2'\right)(jX_m)}{\frac{R_2'}{S_k} + j\left(X_2' + X_m\right)}} \tag{3.4}$$

Likewise, the harmonic current in the rotor circuit, as referred to the stator circuit is given as

$$I_{2K}' = \frac{jX_m}{\frac{R_2'}{S_k} + j(X_2' + X_m)} I_{1k} \tag{3.5}$$

Using the equations derived above, harmonic component of the electromagnetic torque T_{emk} is defined as

$$T_{emk} = \frac{3R_2' \left| \frac{jX_m}{\frac{R_2'}{S_k} + j(X_2' + X_m)} \right|^2 I_{1k}^2}{\frac{1}{k}\omega_1 S_k} \tag{3.6}$$

Likewise, the mechanical power from the motor can be defined as

$$P_{mechk} = 3\frac{R_2'(1 - S_k)}{S_k} \left| \frac{jX_m}{\frac{R_2'}{S_k} + j(X_2' + X_m)} \right|^2 I_{1k}^2 \tag{3.7}$$

Similarly, the time harmonic equivalent circuit for an induction motor derived from the fundamental per-phase equivalent circuit is shown in Figure 3.10 [46].

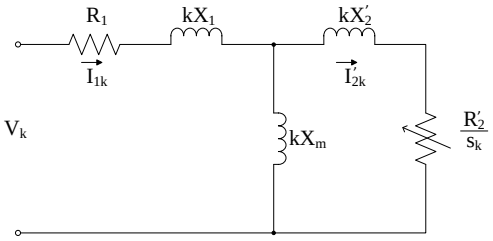

Figure 3.10 Time harmonic equivalent circuit of induction motor [46]

Unlike the case of the space harmonics, the fundamental synchronous speed is 1/*k* times the synchronous speed of the k^{th} order time harmonics [46].

$$\omega_k = \frac{2\pi n_k}{60} = k\frac{2\pi n_1}{60} = k\omega_1 \tag{3.8}$$

The harmonic slip for the forward rotating time harmonic is given as

$$S_k = \frac{kn_1 - n}{kn_1} = \frac{(k-1) + S_1}{k} \tag{3.9}$$

Similarly, for backward rotating time harmonics, the harmonic slip is given as

$$S_k = \frac{kn_1 + n}{kn_1} = \frac{(k+1) - S_1}{k} \tag{3.10}$$

Where

S_k and S_1 are the harmonic and fundamental slip respectively.

The harmonic current in the stator circuit is defined as

$$I_{1k} = \frac{V_k}{(R_1 + jkX_1) + \frac{\left(\frac{R'_2}{S_k} + jkX'_2\right)(jkX_m)}{\frac{R'_2}{S_k} + jk\left(X'_2 + X_m\right)}} \tag{3.11}$$

Likewise the harmonic current in the rotor circuit as referred to the stator is defined as

$$I'_{2k} = \frac{jkX_m}{\frac{R'_2}{S_k} + jk(X'_2 + X_m)} I_{1k} \tag{3.12}$$

The harmonic electromagnetic torque is given by the equation

$$T_{emk} = \frac{3R'_2 \left| \frac{jkX_m}{\frac{R'_2}{S_k} + jk(X'_2 + X_m)} \right|^2 I_{1k}^2}{k\Omega_1 S_k} \tag{3.13}$$

The mechanical power derived from the motor as a result of time harmonics is

$$P_{mechk} = 3\frac{R'_2(1 - S_k)}{S_k} \left| \frac{jkX_m}{\frac{R'_2}{S_k} + jk(X'_2 + X_m)} \right|^2 I_{1k}^2 \tag{3.14}$$

3.4 Impact of VSDs on Induction Motor Losses

For an induction motor operating under a PWM supply, the motor may experience a decrease in efficiency and an increase in vibration, noise, losses and temperature levels depending on the property of the PWM type employed [38]. The additional losses introduced in the machine due to the presence of harmonics, estimated to range between 10% to 20% of the total power losses at rated load [34]. The impact of the harmonics associated with the VSD on the motor losses varies with respect to the specific loss under consideration. Figure 3.11 gives the performance of a 37kW 50Hz motor powered from a 50Hz sinusoidal and 5.5kHz VSI supply [45].

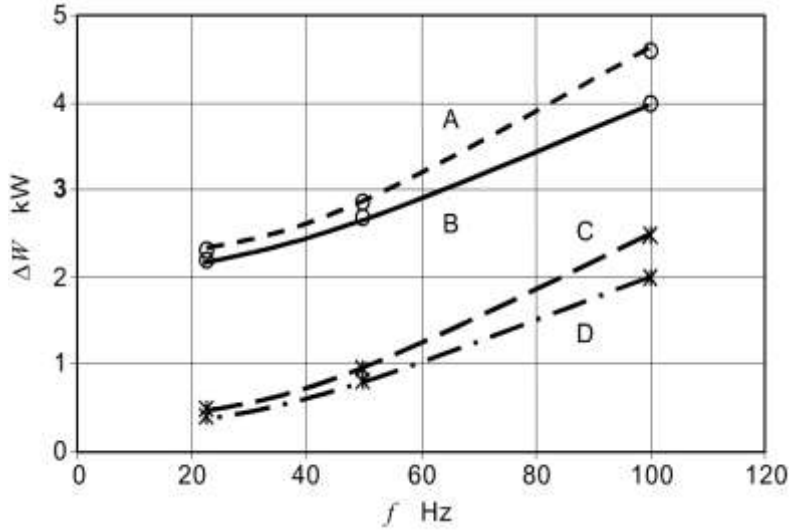

Figure 3.11 Measured losses [W] as a function of frequency & supply. A: full load, PWM supply B: full load, sinusoidal supply C: no-load, PWM supply D: no-load, sinusoidal supply [45]

With the exception of the friction and windage losses, which are assumed to remain constant once they are stabilized [47], the other losses explore increase with an increase in harmonics present. The following sub-sections explore the impact of harmonics on these losses.

3.4.1 Core losses

The core loss (P_{fe}) in an induction machine can be expressed as [47]:

$$P_{fe} = k_h f B_m^2 + k_e (f B_m)^2 \tag{3.15}$$

Where

The first and second terms account for the hysteresis losses and eddy current loss respectively

B_m is the maximum flux density

k_h and k_e are constants that depend on the property of the lamination material

Since the core loss is a function of frequency, the impact of harmonics on the core loss is additive. The estimation of these additional core losses due to the harmonics are complicated since they are dependent on the harmonic order [34]. These may be optimised during the motor design process for a particular fundamental frequency; 50Hz because it depends on the motor's geometry, type of magnetic material,

lamination thickness, etc. The presence of time harmonics results in higher saturation of the magnetic paths, hence increasing the core losses [47].

3.4.2 Copper losses

Since the copper loss in the stator and the rotor are functions of current and resistance, the presence of harmonics causes a rise in the total stator and rotor copper losses. The harmonic copper loss is the greatest proportion of all harmonic losses. The per phase additional copper loss of the stator and rotor windings due to harmonics ($\Delta P_{cu\,h}$) can be approximated as [48]:

$$\Delta P_{cu\,h} = \sum_{h=2}^{\infty} I_h^2 R_h \tag{3.16}$$

Where

I_{1h} represents the harmonic current

R_h is the resistance of the motor at the *h*th harmonic

The resistance given in the approximated equation (3.16) ignores the contribution of skin effect on the harmonic losses. This however needs to be accounted for when looking at the impact of very high harmonics on copper losses.

3.4.3 Stray Load Losses

Like the copper and core losses, the stray load losses in the induction motor increase in the presence of harmonics. The additional stray load losses associated with the presence of harmonics can be estimated as [48]:

$$\Delta P_{SL\,loss} = \sum_{h=2}^{\infty} (I_h)^x (hf_1)^y \tag{3.17}$$

Where x and y are constants that depend on the machine construction.

It can be concluded that the presence of harmonics can be very detrimental in terms of induction motor losses.

3.4.4 Friction and Windage Losses

These losses are assumed to be constant once they are stabilized at base speeds [47]. With the variation of motor speed with VSDs, friction and windage losses tend to reduce below base speeds and increase above base speeds [49]. In the case of increased motor temperature as a result of reduction of motor speed, external cooling fans are needed to prevent excessive heating of the induction motor.

3.5 Impact of VSDs on other induction motor performance parameters

- **Efficiency**

Increased losses and heating in induction machines when operated with VSDs result in a drop in motor efficiency. The additional losses associated with the use of VSDs tend to have negative effects on the efficiency of the induction machines under their supply. The drive system though, which is consists of induction machine(s) coupled to a VSD, provides higher energy savings in speed and process control compared to alternatives such as valves, dampers and throttles. Other factors, as discussed in the preceding sections, determine the degree of efficiency drop for the induction machine when operated with a VSD. There are studies being undertaken into the prospects of designing induction machines specifically for VSD applications. In this case, the optimum drive and motor properties are considered in attaining the highest efficiency for the drive system can be identified.

- **Heating**

The losses in an induction machine are dissipated as heat; since energy cannot be destroyed but merely transformed from one form to another. The presence of harmonic currents and voltages increase the copper and iron losses in the machine. This leads to higher temperatures in the stator windings and rotor bars [50]. To be able to quantify the rise in temperature, one needs to analyse the stator and rotor harmonic currents. Cooling in induction motors is reduced at low speeds. Applications involving VSDs that require the motor to run at reduced speeds, will in addition to the increasing the temperature rise; reduce the effective cooling of the

induction machine. Such applications require external cooling or derating of the machine.

- **Power factor**

The ratio of real power to the apparent power is defined as power factor. Induction motors draw reactive power to support their magnetic field to create rotation. Extreme reactive current is detrimental because it results in additional resistance losses and may acquire the use of large transformers [51] while decreasing the power factor. Furthermore, power providers penalize consumers with low power factors. One way of correcting lagging power factors is through the introduction of power factor correction capacitors. These reduce the reactive currents measured upstream the capacitor and hence improve power factor. Since VSDs have capacitors on the DC bus, this provides a means of isolating the induction motor load from the grid, improving the overall power factor of the system. [51].

- **Torque and Speed Ripples**

The presence of harmonics presents torque pulsations in the stator excitations. The effects of these torque pulsations are minimal at high frequencies. Torque pulsations at low frequencies can cause speed fluctuations and shaft fatigue [48]. The effect of torque ripple on the ripple present in the rotor speed can be expressed as follows (assuming no resonance occurs) [34]:

$$\text{Amplitude of Speed Ripple} = \text{k} \times \frac{\text{Amplitude of Torque Ripple}}{\text{Ripple frequency} \times \text{Inertia}} \tag{3.18}$$

Where k is a constant.

From the preceding equation, it can be deduced that a given value of torque ripple may result in negligible speed ripple at high ripple frequency and vice versa.

- **Starting Characteristics**

The start-up current of an induction machine is about 6 times its rated current when connected to a rated voltage supply. This current remains until the motor approaches full speed.

By contrast, when a VSD starts a motor, it initially applies a low frequency and voltage to the motor. Thus under these conditions avoids the high inrush current that occurs when a motor is started directly online. After the start of the VSD, the applied frequency and voltage are increased at a controlled rate to accelerate the load without drawing excessive current [52]. The torque throughout acceleration is approximately equal to the breakdown torque, and hence the usual strain of fixed voltage, fixed frequency and acceleration does not apply. This greatly affects the service life of the machine [35].

3.6 Mitigation of Harmonics Associated with VSDs

Customers are responsible for limiting the current distortion caused by their equipment and power utilities are responsible for limiting the voltage distortion at the point of common coupling in distribution systems [53]. The IEEE 519 stipulates allowable levels of harmonic distortion in a system, and hence necessary measures should be put in place to control the harmonics associated with the used of VSDs.

The following sections present some of the notable means of mitigating harmonics associated with VSDs.

3.6.1 Installation of Output Passive Filters

Harmonics in power systems are usually corrected using shunt passive filters [54].

These filters usually have a cut off frequency that lies below the lowest harmonic frequency of concern. The filter performance is based on system impedance and load characteristics [54]. Aside the increased cost of installation of these filters, they result in voltage drop and hence a reduction in motor horsepower [38].

A typical example of such a filter is described by [54]. The notch filter as it is called, is an LC filter and could either be single or double tuned. Figure 3.12 shows some passive filters that can be installed to mitigate the harmonics generated with the VSD.

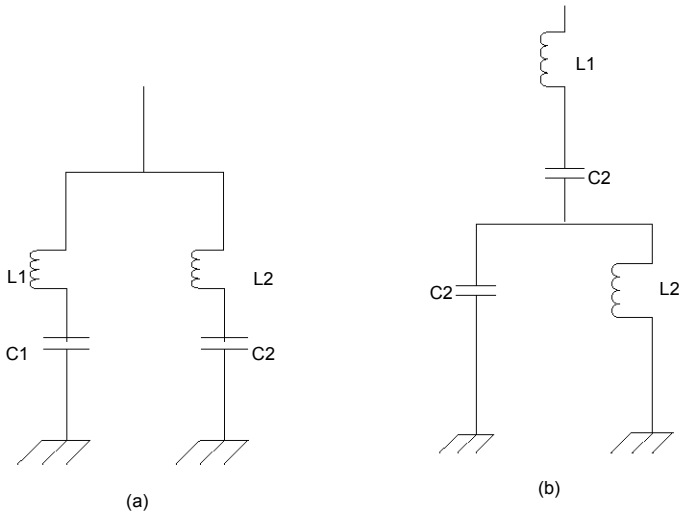

Figure 3.12 Two Single and double tuned passive filter construction respectively [53]

With the right filter parameters, the total harmonic distortion of the current waveform can be reduced from 17.2% to 3.35% [54]. Resonance conditions must be avoided since they result in significant additional losses.

Output reactors are also used because they are less expensive and still produce adequate performance in many cases.

3.6.2 Increasing Switching Frequency

As illustrated in the previous section, it is possible to obtain a decrease in the total losses in a motor supplied by VSD by increasing the switching frequency. One drawback of this method however, is the increase in inverter switching losses.

3.6.3 Pulse-width modulation quality improvement

With the advancement in power electronics, there has been the development of active power filters for the mitigation of harmonics. These devices curb harmonic distortion by injecting current or voltage that make up for the waveform distortion. An example of such a technique consists of overmodulating 15% of the sinusoidal and adding 27% of the third harmonic in phase and 2.9% of the ninth harmonic in counterphase [53]. The resulting wave is given as:

$$y = 1.15\sin(\omega_m t) + 0.27\sin(3\omega_m t) - 0.029\sin(9\omega_m t) \quad (2.26)$$

Where

ω_m is the fundamental frequency

This technique decreases the harmonics and increases the value of the fundamental term [53].

CHAPTER FOUR: LABORATORY SETUP AND TEST PROCEDURE FOR INVERTER-FED INDUCTION MOTOR TESTING

This chapter takes a detailed look at the various laboratory instrumentation and equipment that were used in the testing of the induction machines. The various test procedures that were undertaken are presented in detail in this chapter. The chapter then considers the design differences between standard and energy efficient motors.

4.1 Laboratory setup for motor efficiency determination

This section takes a look at the setup in the laboratory; the instrumentation involved and the procedure followed in testing the range of induction motors. The setup was arranged in a way to ensure conformity with the international standards for testing induction motors in terms of structure, accuracy and safety, while also ensuring consistency of test results. Figure 4.1 gives a block representation of the setup used in the laboratory for the testing of the induction machines under VSD supply. The following subsections will take a look at the various components.

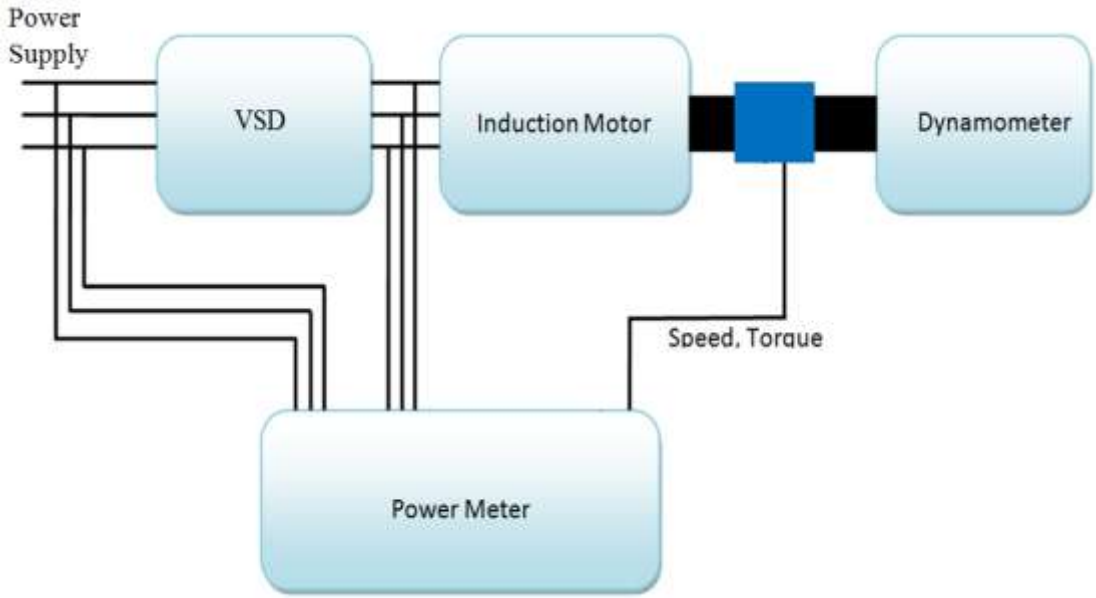

Figure 4.1 Laboratory set up for testing induction motors under VSD supply

4.1.1 Specifications for Induction Motors Tested

The study covered standard and EE (premium plus) squirrel-cage induction motors with output ratings of 3kW, 7.5kW, 11kW and 15kW. All of these motors are manufactured by WEG and are four-pole, 380/400V, 50Hz, totally enclosed fan cooled (TEFC) IC 41 machines. Table 4.1 presents some of the motor specifications.

Table 4.1 Specifications of EE and Standard Motors used in the laboratory

	Standard Motor	**EE Motors**
Service Factor	1	1.15
Speed	1450rpm (15kW, 11kW, 7.5kW) 1390rpm (3kW)	1460rpm (15kW, 11kW, 7.5kW) 1425rpm (3kW)
Insulation Class	F	H
Ingress Protection rating	55	66

4.1.2 Variable Speed Drive Specifications

Two commercial PWM VSI drives were used in the laboratory during the test process. These drives are rated 7.5kW and 15kW with voltage ratings of 342-440 V and 380/415V respectively. Figure 4.2 shows the two industrial VSDs that were used. The 15kW was needed because of the 15kW and 11kW motors, though the 7.5kW provided more flexibility in manipulating the drive properties for the purpose of this research.

Figure 4.2 (a) 7.5kW Allen-Bradley Powerflex 70 drive (b) 15kW Telemecanique Altivar 5 drive

4.1.3 Power Supply

A 520kW, 6-pole three phase synchronous generator is available in the laboratory for the generation of balanced voltages that comply with the minimum total harmonic distortion of 5% and a maximum voltage unbalance of 0.5% according to the IEEE 112 and IEC 60034-2-1 standards. By controlling the speed of the generator, the frequency was kept within ±0.1% of 50Hz during normal operating conditions and 12.5Hz for the blocked-rotor test. With a 6.6kV/400V transformer, the 6.6kV generated at the terminals of the synchronous generator is stepped down to the level suitable for this application. The synchronous generator is driven by a 250kW DC motor.

4.1.4 Dynamometer System

The induction motors were loaded using a separately excited DC machine. The machine was run as a generator whereby torque is adjusted by controlling the armature current of the machine. A 15kW three phase four-quadrant DC drive is used to control the armature current of the dynamometer which also feeds the energy back to the grid.

The dynamometer is coupled to the induction machine under test though an inline torque transducer. Figure 4.3 shows a 11kW energy efficiency induction motor coupled to the dynamometer through the torque transducer.

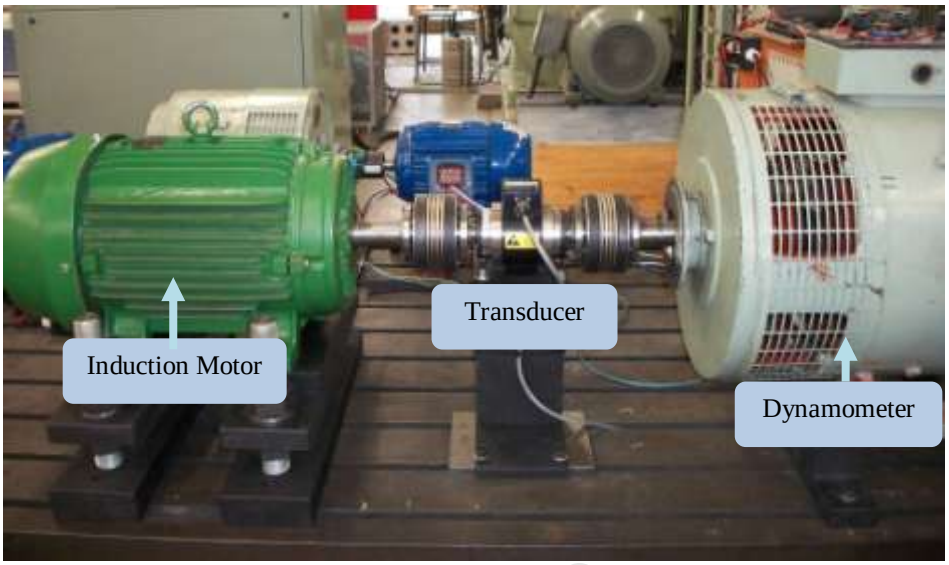

Figure 4.3 Induction Motor Coupled to a Dynamometer

In instances when testing the 11kW and 15kW motors, an external resistor bank is switched in when extra loading was needed to dissipate the additional energy that could not be absorbed by the drive.

For accuracy in load measurements, the torque transducer was calibrated. A calibration arm 509.81mm in length was used for this purpose. The shaft was locked and weights hung on the calibration arm as shown in Figure 4.4. Since the length of the calibration arm is known, for a calibrated mass *m*, the torque *T* is calculated as follows

$$T = F \times d = m \times g \times d \tag{4.1}$$

Where

d is the calibration arm length

g is the acceleration due to gravity for Cape Town (9.796 m/s^2)

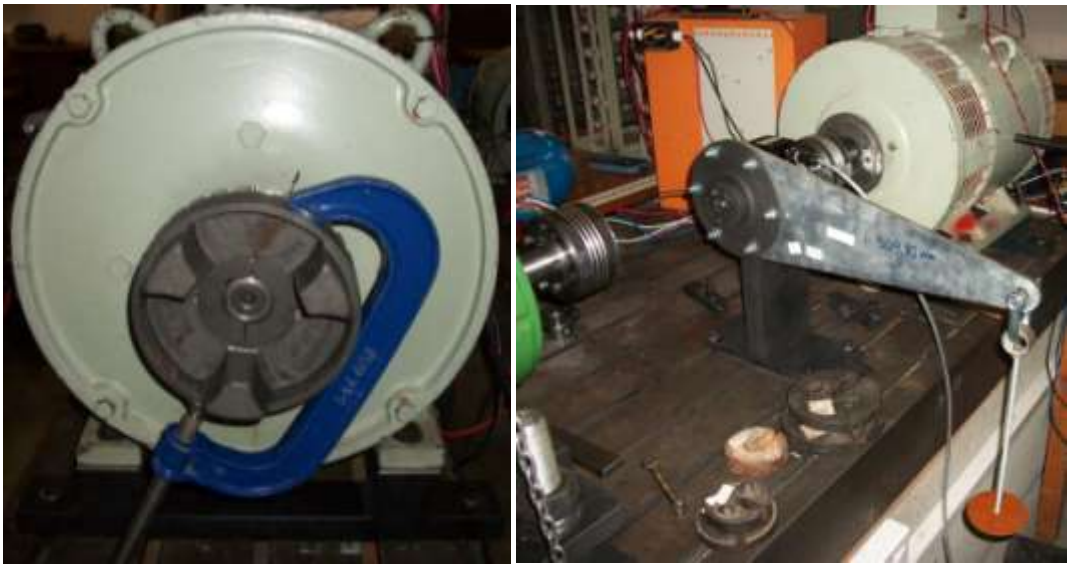

Figure 4.4 Torque Calibration Setup [10]

This is the process used to calibrate the torque transducer

4.1.5 Torque Transducer

A Magtrol TM 312 inline torque transducer with speed sensing was used in measuring the torque on the shaft of the motor. The device falls within a 0.1% accuracy class and it is rated for 200Nm. The measuring system is based on the principle of a variable torque-proportional transformer coupling. It consists of two concentric cylinders shrunk on the shaft of each of the shaft's deformation zones, with two concentric coils attached to the housing. Both cylinders rotate with the shaft. An alternating current of 20Hz frequency flows through the coil. The integrated conditioning electronic module outputs a full scale analogue voltage of ± 5V. The non-contraction differential transformer torque measuring technology is employed; hence no electronic components operate during operation. A 10kΩ pull-up resistor is used in taking speed from an open collector pin. The speed is read on a toothed wheel by an optical sensor. A frequency signal proportional to the rotational speed of the shaft is output by the electronic conditioner. An active circuit compensates the zero offset and the temperature sensitivity drifts within a tolerance of 0.1%/10K.

4.1.6 Machine Alignment

The induction machine under test is coupled to the dynamometer via two Bellows couplings with the torque transducer in-between them. This arrangement is radially and angularly aligned to prevent excessive vibrations. These vibrations can result in a reduction of energy in the drive and cause a reduction in efficiency. These vibrations also introduce noise in the speed and torque signals captured by the transducer attributing to measurement uncertainties. A misalignment of 0.3mm and 1º is tolerated radially and angularly respectively. To cater for this tolerance level, a dial gauge is used in the alignment. Figure 4.5 shows a picture of the dial gauge used in the laboratory for the alignment of the motor and dynamometer shafts. The gauge is used to check both vertical and horizontal alignment of the shafts.

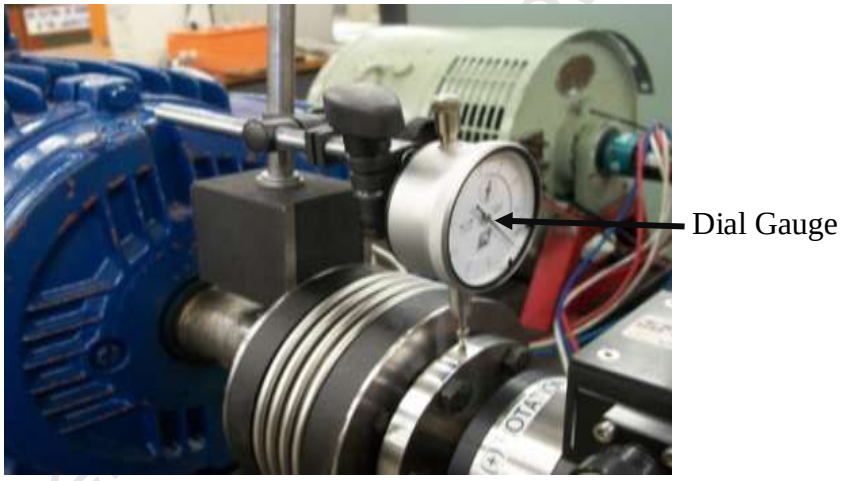

Figure 4.5 Dial Gauge for Shaft Alignment

4.1.7 Power Meter

A Yokogawa WT 1600 digital power meter (as shown in Figure 4.6) was used to record voltage, current, power, speed and torque during the test.

Figure 4.6 Yokogawa WT 1600 Digital Power Meter

The device has six input channels for voltage and current measurements and a special motor evaluation unit to measure speed and torque from the torque transducer. The first three input units had the generator as the source and the VSD as the load, to measure the voltage, current and power into the VSD. The remaining three units had the VSD as the source and the induction machine under test as the load, in this case measuring the voltage, current and power input of the motor; which doubles as the output of the VSD. The output power on the shaft of the motor was recorded using the torque and speed signals from the torque transducer. The wiring configuration selected, allowed the device to record three values of voltage and current as shown in Figure 4.7.

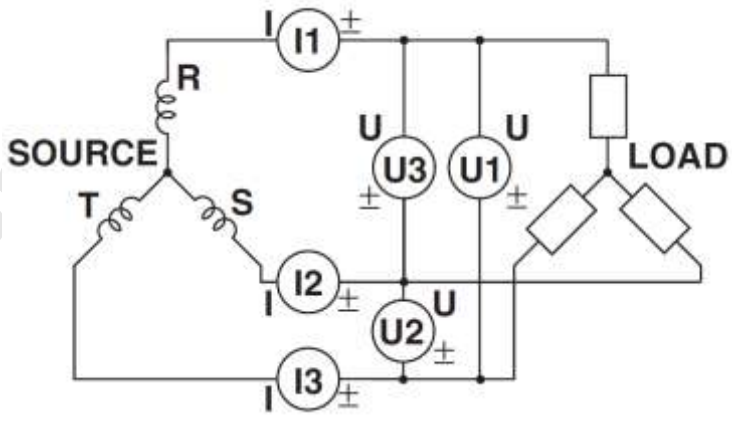

Figure 4.7 Wiring Configuration of Digital Power Meter [33]

4.1.8 Temperature Measurement

In a quest to measure the effective machine temperature, three K-type thermocouples were installed in the drive-end of the stator end windings of each machine. These thermocouples were carefully inserted at identical spots in all the machines in order

to facilitate comparison of results. Care was taken during the installation process in order not to damage the insulation on the windings. The thermocouples are strategically located close to the areas where the highest winding temperatures were expected. Figure 4.8 shows the placement of these thermocouples in the machine.

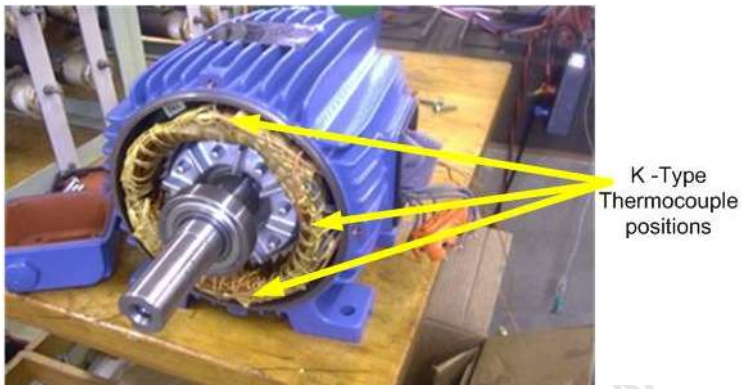

Figure 4.8 Thermocouple placements on Stator end Windings

The temperature readings were captured using an 8 channel TC-108 Pico logger. The device records the temperature at 1s intervals and the data saved on the PC in a CSV format through the device's USB interface. A picture of the logger is shown in Figure 4.9.

Figure 4.9 TC-08 Pico logger with Thermocouples

4.1.9 Winding Resistance Measurement

The measurement of resistance during the test procedure is essential since an error in resistance measurement greatly affects values of losses and efficiency as a whole. In view of this a Hewlett Packard 34401A digital multimeter (as shown in Figure 4.10) was used for resistance measurement during the test. The device has a 6.5 digit resolution.

Figure 4.10 Digital Multi Meter for Winding Resistance Measurement

The four wire method of resistance measurement was utilised since it effectively eliminates the four contact and lead resistances. Figure 4.11 gives a pictorial representation of the wiring configuration used in the resistance measurement, where R_{Lead} is the lead resistance and R_x is the unknown winding resistance.

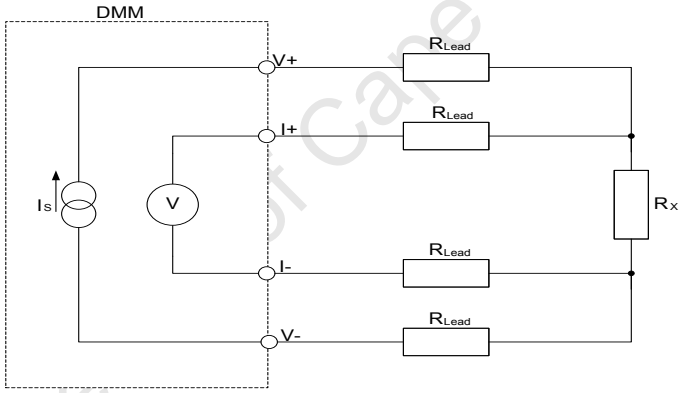

Figure 4.11 Four Wire Resistance Measurement

4.2 Test Procedure

The induction motors were tested in the laboratory according to the IEEE 112 and IEC 60034-2-1. Specific measures were taken in order to assure the accuracy of the readings taken. In testing the machine under the VSD supply, adjustments were made to the procedures required by the standards since these standards specify conditions for sinusoidal voltage supply. The IEC 60034-2-3 standard is also consulted in such situations. The following are the procedures followed:

4.2.1 Cold Winding Resistance

Before the thermal test is performed on the machine, the stator winding resistance of the entire machine are measured. The temperature of the windings is also recorded by means of the thermocouples described in section 4.1.8. The ambient temperature is measured at this point.

4.2.2 No-Load Test

Two sets of no-load tests are performed on the machine.

Firstly, the motor is run uncoupled from the shaft of the DC machine and under the generator supply. With the machine running at rated frequency (50Hz), the voltage to the machine is varied from 125% of the rated voltage (475V) down to the point when further voltage decrease caused a rise in current. The line-to-line voltage, current, power and temperature are measured.

The test is repeated, but with the VSD connected in-between the generator set and the induction motor. This test is carried out to determine the additional no-load losses in the machine as a result of the harmonics associated with the VSD. The additional harmonic losses are obtained by the difference between the no-load powers recorded during the two tests [55]. In the second test however, due to the presence of undervoltage protection in the drive, the variation of voltage does not get as low as in the first instances.

In both tests, the machine is run until the measured input power at no-load did not vary by more than 3% between two successive readings taken at the same voltage at 30 minute intervals. This process was to ensure that the no-load losses were stabilised before the tests were carried out.

4.2.3 Blocked-Rotor Test

To obtain the leakage reactance and the rotor resistance of the equivalent circuits, a blocked rotor test was carried out on each of the induction motors. After confirming the direction of shaft rotation, the shaft of the motor was clamped using a G-clamp. With frequency kept at 25% of its rated value (12.5Hz), the voltage is slowly

increased until the rated current of the machine is reached. Values of voltage, current, power and temperature are recorded in the process. This test is carried out as fast as possible to avoid overheating of the motor windings.

4.2.4 Temperature Test

Since temperature affects the losses in the machine, accuracy of the power measurements taken was maintained by carrying out a temperature test at the rated load. The induction motor was coupled to the dynamometer and rated torque applied. It was left to run at the rated load until the temperature rise was not more than 1°C over a period of thirty minutes. Once thermal equilibrium was established, the power supply to the motor and the dynamometer are switched off. When the machine came to a standstill, the resistance of the windings were recorded, within 30 seconds after the power is turned off. The winding temperatures are recorded at the same time. In order to shorten the time taken for the machines to reach the expected final temperature, it is acceptable by the standards used to overload the machine by 25% to 50% at the initial heating periods.

As in the case of the no-load test, the temperature test was carried out twice on each motor; with and without the VSD connected.

4.2.5 Variable Load Test

In carrying out the variable load test, the temperature of the windings was kept within 5°C from the rated temperature determined from the temperature test. Though the IEEE standard only states a 10°C difference, the 5°C difference was kept since the IEC standard requires these more stringent measures. In that case, one set of readings could be taken for both standards. The machine was placed under six loading conditions ranging from 25% to 150% of rated torque, with equal loading intervals between them. The machine was loaded in descending order and the voltage, current, power, speed, torque and the stator winding temperature recorded. Once again, to limit the effects of temperature variations that may affect the accuracy of the test results, the test was carried out as quickly as possible.

The variable load test was carried out again with the machines under VSD supply.

4.2.6 Test to Evaluate the Impact of Inverter Characteristics on Efficiency

To analyse the impact of VSD switching frequency on the efficiency of the motor and overall system, two 3kW standard and premium efficiency induction motors were tested using the 7.5kW VSD described in section 4.1.2. The switching frequency was varied from 2 kHz to 10 kHz since this is the range of frequencies available on the drive used in the test. At each point, a variable load test was carried out on the machines. The voltage, current and power into the VSD was measured using three of the inputs on the power analyser and the remaining three inputs used to measure the voltage, current and power between the VSD and the motor. In this case it is possible to analyse the effects of switching frequency on the induction motor and the overall motor drive system.

4.3 Design Differences between Standard and EE Motors

Induction motors have undergone numerous changes, some of which are major and others minor. It is these changes that set the standards between a standard motor and an energy efficient motor. The changes in design range from the quality and types of materials used to the sizing of certain parts of the motor, all of which contribute to an improvement in the efficiency.

Figure 4.12 shows a typical TEFC motor with the various parts of the motor that may be altered to affect the machines' efficiency.

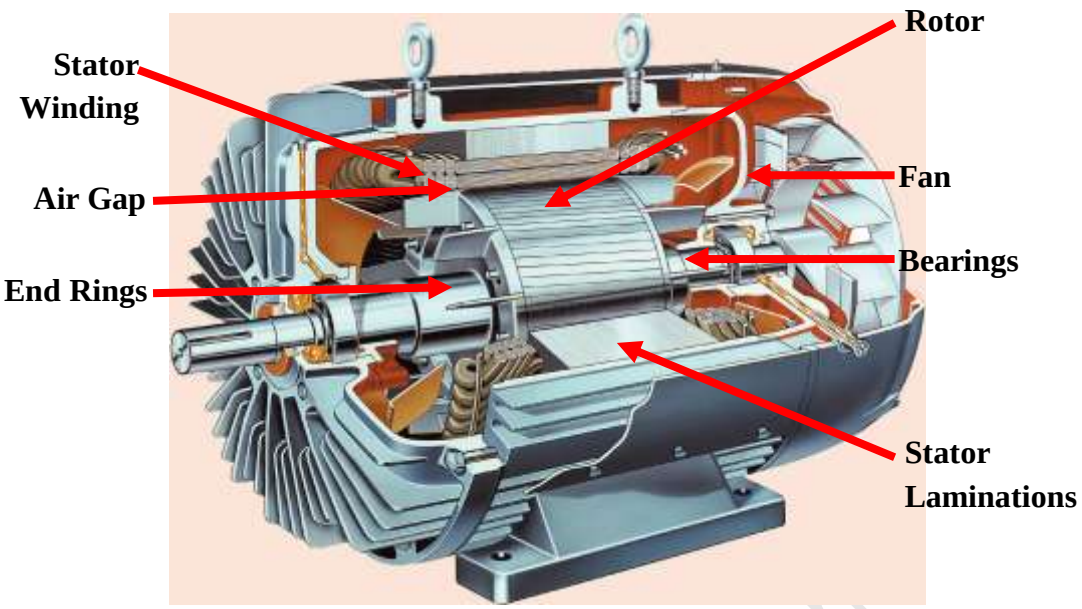

Figure 4.12 A typical NEMA Design B motor showing components modified to increase efficiency [48]

- **Quality of core material**

In terms of design, the quality of the steel lamination that is used for the core stack is of utmost importance. The quality of the magnetic material is dependent on the permeability and specific loss per kilogram [56], [57]. The ferromagnetic core of energy efficient motors is manufactured from higher-grade silicon steel, which is able to withstand high temperature conditions [58]. On the other hand, the core of standard motors is made of low cost annealed steel, which is more prone to temperature and environmental conditions.

Over the years, the quality of the magnetic material used has improved. The main advancement is with the quality of the steel used. This is necessary as hysteresis and saturation losses are reduced by replacing lower-cost plain carbon steel with steel containing up to 4% silicon for laminations [59]. There has also been a development of electrical grade lamination steel over the years. Reduction in the lamination thickness, for instance, replacing the 24-ga steel found in standard efficiency motors with 26-ga or 29-ga steel enhances the efficiency of the motor. Table 4.2 displays values of specific losses per kilogram associated with different grades of steel that is used in the manufacturing of stator laminations.

Table 4.2 Typical values for non-oriented fully processed electrical steel [52]

Steel Grade	Loss Breakdown	Watts Loss/lb @ 15kG 60Hz		
		29ga	26ga	24ga
M1 Silicon	Hysteresis	1.10	1.21	1.36
	Eddy	0.50	0.52	0.60
	Total	1.60	1.73	1.96
M36 Silicon	Hysteresis	1.26	1.49	1.69
	Eddy	0.72	0.79	0.91
	Total	1.98	2.28	2.60
Carbon Steel	Hysteresis	-	2.17	2.67
	Eddy	-	1.37	1.62
	Total	-	3.54	4.29

The coatings of laminations have also improved from basic organic (C3) to various inorganic/combination configurations (C4/C5/C6) and to oxide coatings recently. Hence losses in the steel have reduced to less than 4.41W per kilogram from 8.82-11W per kilogram. Figure 4.13 indicates the history of iron losses, whereby it is evident there has been a reduction in core losses over the years.

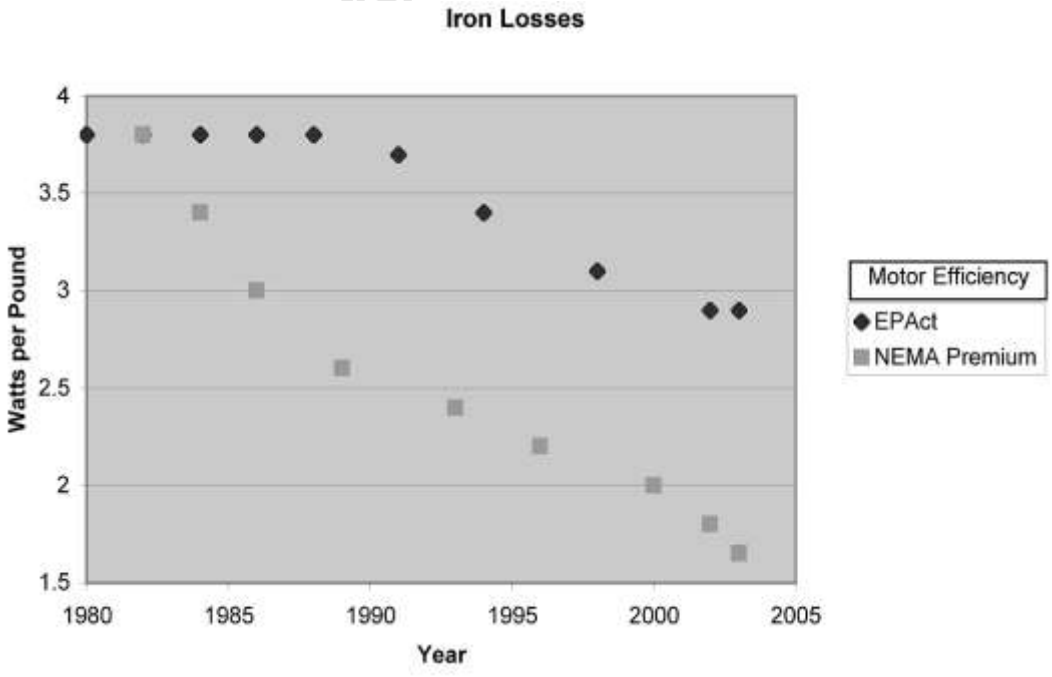

Figure 4.13 History of Iron Losses [53]

Power loss in the stator of an induction motor makes up about 35% of the total loss in the motor [60]. Consequently energy efficient motors contain more copper than standard efficient motors of the corresponding rating because an increase in copper diameter and hence, mass of the stator material reduces its resistance. Rotor losses are minimised by the decrease in the degree of slip. This is achieved by the increase in the mass of the rotor conductor bars and end plates and also by increasing their conductivity [59].

The length of the lamination core stack has seen an increase since this reduces the magnetic flux density within the core stack and as a result reduces core losses [59]. Figure 4.14 shows a rise in the rotor and stator length (and the amount of copper in the motor) as efficiency increases.

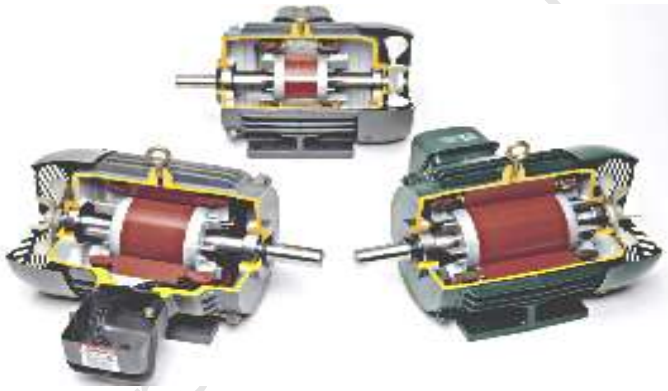

Figure 4.14 Three different efficiencies for the same horsepower rating. Top: standard-efficiency pre-EPAct motor; lower left: EPAct-level motor; lower right: NEMA Premium efficiency motor. [59]

- **Temperature Rise**

The IEEE 841 standard stipulates guidelines for cast-iron housings that are finned for enhanced heat dissipation. A fully rounded diameter of the stator lamination stack provides increased thermal conductivity to the outer housing. Figure 4.15 illustrates newer cast - iron moulding designs that have more ribs and as a result increased surface area.

Figure 4.15 New moulding designs showing more ribs to increase surface area and improve heat transfer [61].

Laminations found in the energy efficient motors are rounded on the outer diameter, which provides better thermal conductivity to the motor housing. The ribs are increased for energy efficient motors compared to the standard motors.

Some energy efficient motors are mounted with smaller sized internal and external fans. This is as a result of the reduced total losses. Smaller sized fans can go a long way in reducing the friction losses. In addition, some manufacturers increase the contact between the wound stator core and the frame to increase heat transfer.

- **Bearing and grease**

Around 60% of premature motor failures involve the motor bearing system [62]. Over the years, motor manufacturers have seen the rising of hybrid bearings that have ceramic balls instead of steel balls. These hybrid bearings further reduce the friction losses. Experiments have revealed that these hybrid bearings run cooler with longer life relative to the usual deep-groove ball bearings [62]. With adjustable speed drive applications, these ceramic balls are able to isolate the shaft and avoid bearing fluting from circulating currents.

The quality of grease has improved over the years. Current research continues to explore the possibility of improving the quality of grease used in induction motors. The IEEE 841 stipulates a polyurea-based grease to be used in motors.

- **Air Gap**

  Some designers increase the air gap in order to minimise the stray load loss and as a result maximise efficiency [63]. But in doing so, there is a drop in power factor as a result of the increase in magnetising current.

CHAPTER FIVE: COMPARISON OF EFFECTS OF VSDs ON STANDARD AND EE INDUCTION MOTORS

This chapter examines the effects of the VSDs on the efficiency of the induction motors. To be able to effectively access the effects of the VSD on the EE motors, the standard motors are compared with the EE motors based on the major standards previously discussed. The harmonic equivalent circuit is used to determine the efficiency of the motors and this is compared to the results obtained from using the direct method. The chapter then examines the impact of varying the VSD switching frequency on the efficiency of the motor.

Extensive work on the comparison between standard and EE motors using the IEEE 112-B, IEC 60034-2, the IEC 60034-2-1 and the direct method has previously been done in [10]. However, in this study, similar results are required to understand the impact of VSDs on EE motors. In [10], Van Wyk compared the efficiencies of standard and EE motors of the same ratings firstly under balanced conditions and then under the unbalanced conditions. Van Wyk carried out no load tests and blocked rotor tests in determining the no load losses and the equivalent circuit parameters. From the comparison made on the different standards used in the efficiency tests, Van Wyk concluded that in all cases the IEC 60034-2 overestimates the efficiency. This he associated with the low estimation of the stray load loss relative to the other standards. The IEEE 112-B and IEC 60034-2-1 gave similar efficiency results because the stray load loss were calculated in a similar manner. The direct method however underestimated the efficiency in all cases. He further compared the standard and EE motors using the IEEE 112-B standard. He concluded that the EE motors had higher efficiencies than standard motors. The tests were carried out at six different loading points, ie 25%, 50%, 75%, 100%, 125% and 150% of the rated load of each machine. Making use of trend lines on the experimental results, Van Wyk estimated that the peak efficiency for the 15kW standard and EE motors occurred at 60% of the rated load, with an approximated 1% difference between the efficiencies of the standard and EE motors. The 11kW EE motors and standard motors however recorded their peak efficiencies at 75% and 60% of rated load respectively with an approximated 3.5% difference between their

highest efficiencies. In the case of the 7.5kW and 3kW standard and EE motors, Van Wyk concluded that the peak efficiencies of the EE and standard motors occurred at 70% and 60% of the rated load respectively. Also, the differences between the highest efficiencies of the 7.5kW and 3kW standard and EE motors were given as 2% and 3.7% respectively. He further presented the component losses in the induction machine.

The temperature at which the no-load tests are performed affects the motor parameters obtained from the equivalent circuits. From the results of the no-load test results, it is identified that since the tests were carried out after the rated temperature test, the temperature readings at the different voltages were higher than in the case when the tests were carried out at on a cold machine. Though the tests were carried out on the same machines, this could result in a difference in the equivalent circuit parameters derived, the associated no-load losses.

A section of the results from the tests are appended to the document.

5.1 Differences between Standard and EE Motors Tested

This section takes a look at the different induction machines that were tested in the laboratory in terms of their steady state operating characteristics, efficiency and loss components.

5.1.1 Resistance and Temperature Differences

This section considers the differences between the induction motors that were used in terms of their winding resistance, rated torque and operating temperature.

- **Cold Winding Resistance**

According to the IEEE 112-B and IEC 60034-2-1 standards, the stator winding resistance of each of the induction motors was taken before the tests were carried out. Table 5.1 displays the cold stator winding resistance of the eight induction motors used in the tests.

Table 5.1 Cold Stator Winding Resistances

	3kW	7.5kW	11kW	15kW

Standard	1.810Ω	2.065 Ω	0.972 Ω	0.703 Ω
EE	1.499 Ω	1.643 Ω	0.809 Ω	0.612 Ω

- **Rated Torque**

When conducting the thermal test on each of the motors, it is required that the motor is run at rated conditions; including rated torque, until the temperature is stabilized. Using the power rating of each motor, the rated torque was calculated by using the torque-speed relationship. The rated torques of the motors are presented in Table 5.2.

Table 5.2 Rated Torque of Motors

	3kW	**7.5kW**	**11kW**	**15kW**
Standard	20.61Nm	49.39Nm	72.44Nm	98.45Nm
EE	20.11Nm	49.05Nm	71.95Nm	98.11Nm

- **Operating Temperature**

The induction motors were run at rated loads and the temperature was recorded using the pico logger and the embedded thermocouples. Thermal equilibrium was reached once the temperatures did not change for more than 1°C over a period of thirty minutes. The highest temperature recorded in each case is presented in Table 5.3. This process was carried out again when the motor was run via the VSD supply. In this case the resulting temperature readings were higher than in the initial case when the motors were run under sinusoidal supply.

Table 5.3 Steady state Temperature of Motors with and without VSD supply

		3kW	**7.5kW**	**11kW**	**15kW**
Standard Motor	With VSD	132.40°C	122.60°C	139.66°C	142.36°C
	Without VSD	123.80°C	113.00°C	120.52°C	124.50°C
EE Motor	With VSD	106.90°C	114.45°C	96.90°C	139.88°C
	Without VSD	95.61°C	105.13°C	86.92°C	109.02°C

It is evident from the table that, there is an increase in induction motor temperature when connected to the VSD. This can be attributed to the additional harmonic losses in the motor introduced by the VSD.

5.1.2 No-Load Tests

The friction and windage losses and the core losses in the induction machine are assumed to be independent of the load; hence these losses are estimated based on the no-load test. In this test, the input voltage is varied by means of a variac from 125% of the rated voltage (in this case 380V) to the point where further voltage reduction caused an increase in current. The recorded values for voltage, power, current and temperature for the 3kW standard and EE motors are presented in Table 5.4. The remaining results have been appended to the document.

Table 5.4 No-Load values for 3kW Standard and EE Motors

Standard Motor			
Temp (°C)	Voltage (V)	Current (A)	Power (W)
85.570	457.370	5.668	532.741
85.930	380.070	3.303	229.581
85.770	302.900	2.253	131.256
85.440	265.580	1.939	101.309
84.690	191.680	1.382	60.196
84.240	114.640	0.857	33.666
83.660	77.515	0.632	26.157

EE Motor			
Temp (°C)	Voltage (V)	Current (A)	Power (W)
71.19	447.680	3.921	266.638
71.337	380.050	2.748	179.764
71.19	304.390	2.077	138.377
71.08	267.320	1.804	120.287
71.06	266.520	1.803	122.236
70.88	196.720	1.326	101.573
70.87	193.130	1.321	101.656

According to [55], for a voltage source converter with an output voltage and pulse pattern which is load independent, the sum of the additional losses in the induction motor due to the converter supply is generally independent of the load. Therefore, the additional losses introduced in the motor as a result of the harmonics introduced by the VSD can be determined as the differences between the input powers recorded during the no-load tests when the motor was supplied with and without the VSD. That is , the additional harmonic losses ($P_{hamonic}$) is given as

$$P_{harmonic} = P_{VSD} - P_{sinusoidal} \quad (5.1)$$

Where

$P_{sinusoidal}$ is the no-load power when the motor is supplied without a VSD

P_{VSD} is the no-load power when the motor is supplied via a VSD

The no-load test was therefore repeated; with the induction motor supplied via the VSD and readings for voltage, current, power and temperature taken.

The additional harmonic losses for each of the motors were calculated as the difference in the no-load input powers at rated voltage conditions. These results are presented in Table 5.5.

Table 5.5 Additional harmonic losses for motors from no-load test

	3kW	7.5kW	11kW	15kW
Standard Motor	58.683W	51.853W	33.592W	27.523W
EE Motor	17.559W	14.521W	9.335W	7.247W

5.1.3 Blocked-Rotor Test

As stated earlier in section 4.2.3, the blocked-rotor test is carried out to obtain the leakage reactance and the rotor resistance of the motor circuits. The test procedure was followed as stated according to the IEEE 112 and the IEC 60034-2-1. Table 5.6 presents the results of voltage, input power and temperature at rated current that was recorded during the test.

Table 5.6 Blocked-Rotor Test Results

Motor		Temp (°C)	Voltage (V)	Current (A)	Power (W)
3kW	Standard	24.530	92.233	6.640	490.560
	EE	24.090	79.505	6.161	357.098
7.5kW	Standard	20.460	34.952	15.098	749.759
	EE	24.670	27.921	14.361	547.148
11kW	Standard	21.21	33.648	22.863	941.826
	EE	21.92	29.91	22.36	792.89
15kW	Standard	23.89	32.617	29.995	1202.450
	EE	19.75	31.307	29.648	1103.530

5.1.4 Equivalent Circuit Parameters

The per-phase equivalent circuit parameters of the induction motors used in the tests were obtained using the readings from the no-load test and the blocked-rotor test according to the IEEE 112 standard. These parameters were then adopted for the harmonic equivalent circuit. The parameters are given in Table 5.7 - Table 5.10:

Table 5.7 Equivalent Circuit Parameters for 3kW Motors

Standard Motor	
R_1	1.815
R_2'	2.101
X_1	3.655
X_2'	3.655
X_m	63.245
R_{fe}	694.183

EE Motor	
R_1	1.507
R_2'	1.770
X_1	3.545
X_2'	3.545
X_m	76.829
R_{fe}	1445.40

Table 5.8 Equivalent Circuit Parameters for 7.5kW Motors

Standard Motor	
R_1	2.067
R_2'	2.411
X_1	4.686
X_2'	4.686
X_m	115.302
R_{fe}	1827.3

EE Motor	
R_1	1.689
R_2'	1.929
X_1	4.215
X_2'	4.215
X_m	128.328
R_{fe}	2708.5

Table 5.9 Equivalent Circuit Parameters for 11kW Motors

Standard Motor	
R_1	0.975
R_2'	1.475
X_1	3.712
X_2'	3.712
X_m	61.809
R_{fe}	853.54

EE Motor	
R_1	0.811
R_2'	1.304
X_1	3.462
X_2'	3.462
X_m	68.006
R_{fe}	1670.7

Table 5.10 Equivalent Circuit Parameters for 15kW Motors

Standard Motor	
R_1	0.713
R_2'	1.084
X_1	2.721
X_2'	2.721
X_m	52.502
R_{fe}	612.088

EE Motor	
R_1	0.613
R_2'	1.045
X_1	2.724
X_2'	2.724
X_m	55.117
R_{fe}	1506.4

The equivalent circuit parameters acquired correlated with the design differences between the standard and EE motors, as mentioned earlier. In all the motors tested, it was observed that the stator and rotor resistances are smaller in the EE motors than in the standard motors. This is attributed to larger sized conductors used in the EE motors. Though the stator and rotor referred leakage reactance are almost equal in both motor types, the magnetising reactance values are higher in the EE motors than in the standard motors. A look at the core loss resistance (R_{fe}) shows higher values in the EE motors than in the standard motors. Since power is inversely proportional to resistance, the values of core loss are reduced in the EE motors in comparison to the standard motors of the same rating. As already discussed, a contributing factor is the quality of material used for the core.

5.1.5 Variable Load Test

In accordance with the IEEE 112-B and the IEC 60034-2-1 methods, the load on the induction motor was varied and the relevant signals captured. However, due to limitations in size of the load available, the 15kW motors could not be loaded to the required 150% of rated load. Table 5.11 and Table 5.12 present values for the instance when the 3kW motors were operated without the VSD supply. The remaining tables can be found in the appendix.

Table 5.11 Variable Load Test Reading for 3kW Standard Motor

Load (%)	Temp (°C)	Voltage (V)	Current (I)	Power (W)	Speed (rpm)	Torque (Nm)	Slip
150.05	124.99	378.13	10.82	6166.91	1281.50	30.93	14.74
125.10	126.93	378.73	8.95	5052.01	1331.57	25.78	11.38
100.08	128.59	379.45	7.30	4018.88	1371.27	20.63	8.66
75.02	128.94	379.96	5.88	3042.92	1408.90	15.46	6.17
50.11	128.33	381.09	4.68	2151.00	1441.85	10.33	4.08
25.30	126.98	381.89	3.76	1293.70	1469.40	5.21	2.22

Table 5.12 Variable Load Test Reading for 3kW EE Motor

Load (%)	Temp (°C)	Voltage (V)	Current (I)	Power (W)	Speed (rpm)	Torque (Nm)	Slip
150.05	96.57	379.87	9.63	5539.99	1369.40	30.16	8.73
125.21	98.58	380.62	8.05	4579.16	1396.60	25.17	6.96
100.05	97.16	381.17	6.58	3640.01	1420.88	20.11	5.33
75.06	97.99	381.78	5.27	2751.79	1442.70	15.09	3.89
50.22	96.34	382.13	4.12	1889.42	1462.80	10.10	2.58
25.21	94.84	382.95	3.26	1091.76	1480.00	5.07	1.40

5.1.6 Efficiency Variation between Standard and EE Motors

After considering the differences and similarities between the different international induction motor standards, as previously discussed in section 2.3, the motors were

tested according to the IEEE 112 method B and the IEC 60034-2-1 and these results compared with the direct method. The initial set of results indicates the induction machines operated under rated conditions without the VSD connected. The graphs confirm earlier views that the IEC 60034-2-1 overestimates the efficiency. This is due to the stray load losses, which are lower than the IEEE 112-B. Since the IEC 60034-2-1 compensates for the voltage drop across the stator windings during core loss estimation, the total losses estimated are lower hence an overestimation of efficiencies.

Figure 5.1 presents the efficiency of the 3kW standard motor obtained using the three standards. From the graph, it can be confirmed that the IEC 60034-2-1 standard overestimates the efficiency, approximately 3% and 6% above the IEEE 112-B and the direct method respectively at the rated load. The margin is larger below 50% of the rated load but narrows when exceeding the rated load. The peak efficiency as estimated by the standards is at 75% of the rated load. Figure 5.2 shows the efficiency of the 3kW EE motor. It can again be confirmed that the IEC 60034-2-1 over-estimates the motor efficiency, but in this case only approximately 2% greater than the IEEE 112-B and 6% above the direct method.

The graphs for the remaining motors can be found in the appendix.

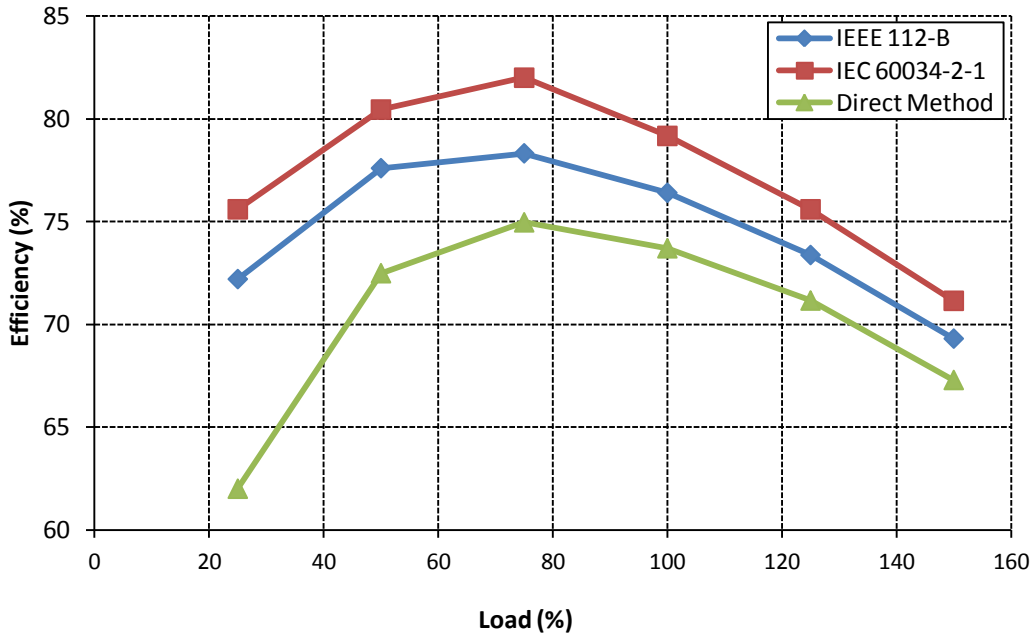

Figure 5.1 Efficiency of 3kW Standard motor derived from different standards

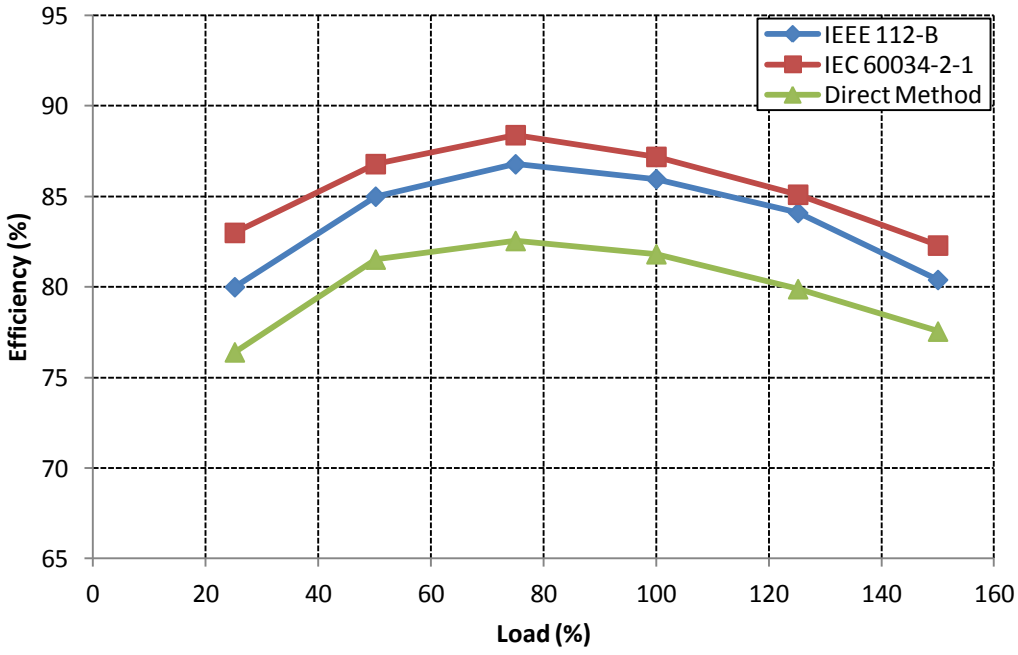

Figure 5.2 Efficiency of 3kW EE motor derived from different standards

5.1.7 Comparison of Losses

There are differences between the load dependent and load independent losses calculated for the standard and EE (premium plus) motors. The core loss and the friction and windage losses are considered load independent since they are assumed constant with varying loads. These two losses are obtained from the no-load test. The stator and rotor copper losses and the stray load losses are however load dependent since they vary with load.

The following subsections consider the various contributions of the losses in the motors under consideration.

- **Core Losses**

The core losses are obtained by subtracting the friction and windage losses from the constant losses of the machine. The constant losses are determined as the difference between the no load power and the stator winding resistance loss. From the obtained results, a graph of core loss is plotted against voltage for readings that does not show considerable saturation. These curves can then be used to obtain the core loss for any voltage point.

The IEEE 112-B does not compensate for the voltage drop across the stator winding resistance in the estimation of the core losses for the various load point. But the IEC 60034-2-1, as already discussed in section 2.3.2, compensates for the voltage drop across the stator winding resistance at the various loads. As a result of the voltage drop compensation, the core loss estimated using the IEC 60034-2-1 are higher than the IEEE 112-B.

Figure 5.3 present the results of the core loss curves obtained for the 3kW standard and EE (premium +) motors from the no-load test. It can be seen from the graphs that the core losses are higher in the standard motors than in the EE motors, as expected from literature and the initial analysis of the design differences between EE motors and standard motors. The core losses of the 3kW EE motor is averagely 50% lower than that in the standard motor. The graphs for the rest of the motors can be found in the appendix.

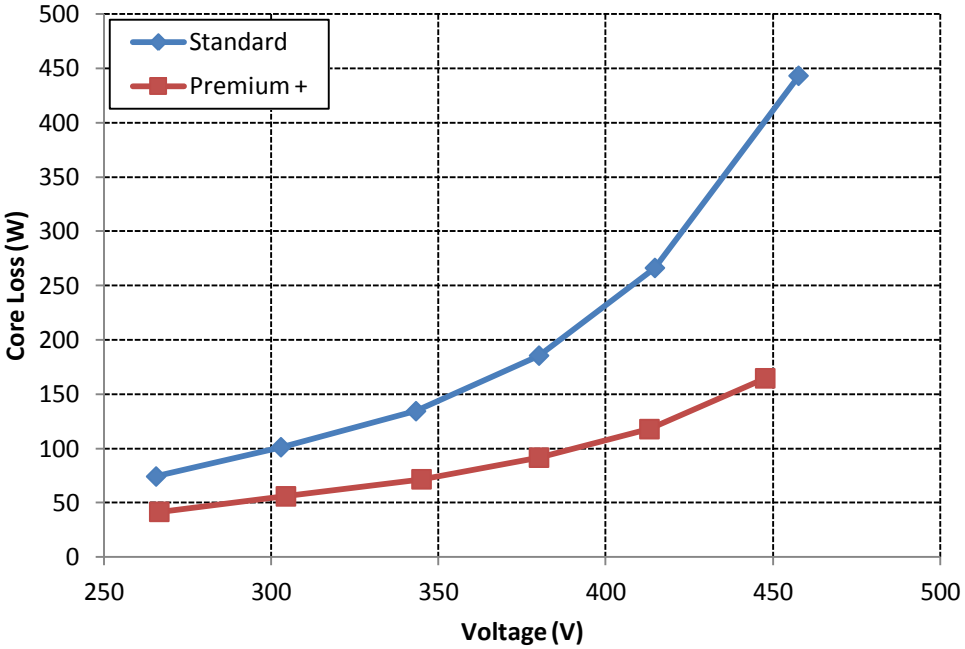

Figure 5.3 Core Loss versus Voltage curve for 3kW Motors

- **Friction and Windage Losses**

The other load independent loss to consider is the friction and windage loss. From the no-load test, the constant loss is plotted against the square of the voltage. From the resulting curve, the friction and windage losses are obtained as the intercept of the curve on the constant loss axis, since it is assumed that there are no core losses at zero voltage.

Table 5.13 Friction and Windage Losses for EE and Standard Motors

Motor Rating	EE Motor	Standard Motor
3kW	74.87W	18.74W
7.5kW	109.60W	48.92W
11kW	183.90W	99.26W
15kW	104.70W	68.36W

The EE motors have higher friction and windage losses compared to the standard motors. The EE motors used in the test are IP 66 rated machines while the standard

motors used are IP 55 rated. Therefore, the EE motors have better ingress protection against water and dust.

- **Stator Copper Losses**

  Unlike the core and friction and windage losses, which are considered to be load independent losses, the stator copper losses are considered load dependent since they vary with the loading of the motor.

  From the variable load test, the stator copper losses are determined from the product of the square of the stator current and the stator winding resistance, which has been corrected to the operating temperature.

  Just as expected, the stator copper losses are higher in the standard motors than in their equivalent EE (premium +) motors. From the graphs in Figure 5.4 and Figure 5.5 it can be observed that in the case of the 3kW motors, there is a difference of approximately 55% between the copper losses estimated in the standard and EE motors. This however decreases with the rating of the motor. The difference between the losses observed in the standard and EE motors for the 7.5kW motor is approximately 27%. This further reduces to 29% in the case of the 11kW motors.

  The graphs for the remaining motors can be found in the appendix.

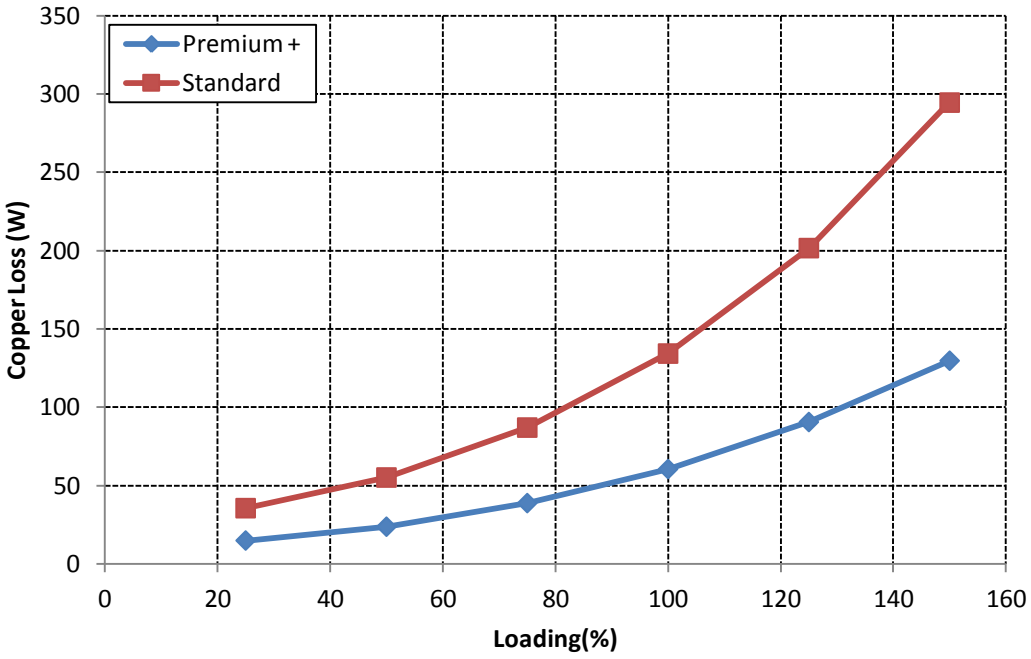

Figure 5.4Variation of Stator Copper Losses with Load for 3kW Standard and EE motors

- **Rotor Copper Losses**

Similar to the copper losses in the stator winding, the copper losses in the rotor are considered a load dependent loss.

The rotor copper loss is estimated in both the IEEE 112-B and the IEC 60034-2-1 as the product of the slip and the air gap power. The slip is corrected to the operating temperature at the specific load point. The power across air gap is estimated as the difference between the input power and the sum of the stator copper and core losses.

Figure 5.5 shows the variation of the rotor copper losses in the 3kW standard and EE motors with load as estimated by the IEEE 112-B. For the 3kW motors, there is approximately 42% difference between the rotor copper losses in the standard and EE motors at the rated load. This difference further decreases to 20% in the 7.5kW motors but it is kept at 23% in the 11kW motor. As expected, the difference between the rotor and stator losses in the two different sets of machines increase with load.

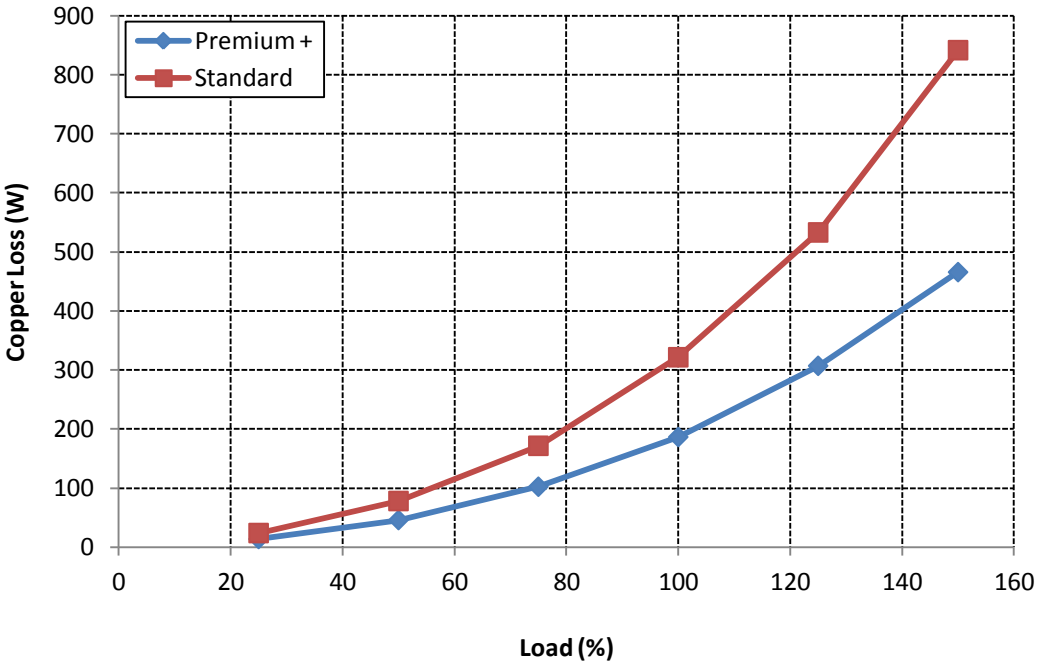

Figure 5.5 Variation of Rotor Copper Losses with Load for 3kW Standard and EE motors

- **Stray Load Losses**

The stray load losses are estimated as the differences between the total losses (ie the difference between input and output power) and the sum of the conventional losses, discussed previously, (ie friction and windage, core, and copper losses in the rotor and stator). The resultant losses are then smoothed using linear regression once plotting it against the square of the torque on the motor shaft. The regression coefficient of 0.9 is required to check the accuracy of the test procedure and the equipment according to the IEEE 112-B. However a regression factor of 0.95 is required by the IEC 60034-2-1.

The curves in Figure 5.6 represent the differences between the estimated stray load losses for the 3kW motors. The results for the remaining motors can be found in the appendix.

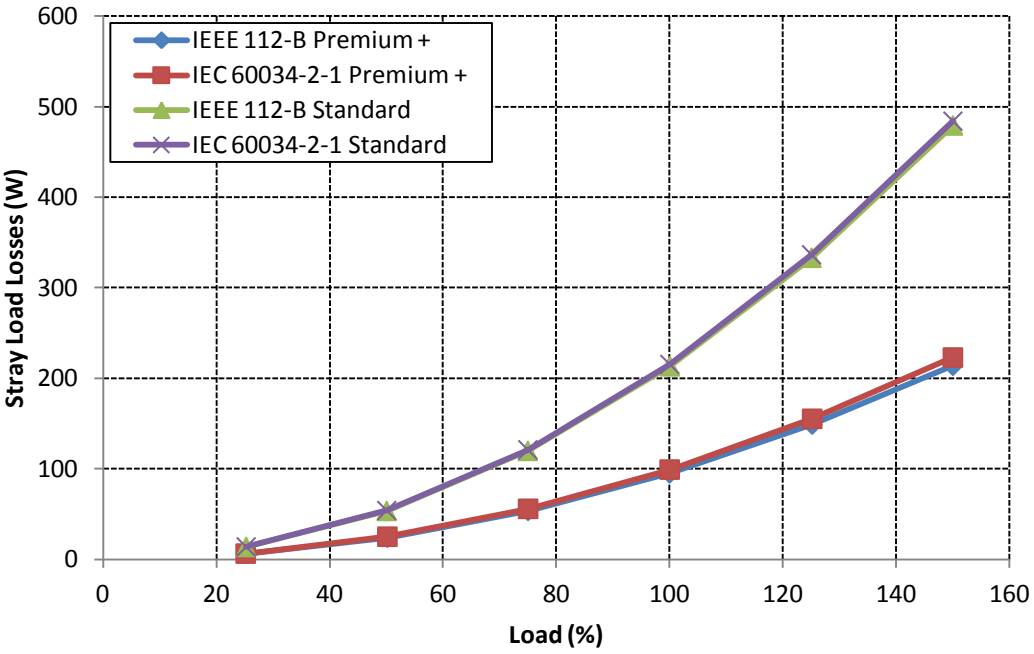

Figure 5.6 Variation of Stray Load Losses of 3kW Standard and EE motor with Load

5.2 Variation of Induction Motor Efficiency under VSD Supply

This section presents results that were obtained when the induction motors were tested with the variable speed drives. From the no-load tests, the fundamental equivalent circuit parameters were then adopted for the harmonic equivalent circuits. The switching frequency of the VSDs is varied and the tests repeated on the 3kW standard and EE motors.

5.2.1 Efficiency of induction motors with and without VSD supply

To ascertain the impact of VSD on the efficiency of the induction motors under their supply, the induction motors were supplied via VSDs and the efficiency determined using the direct method. The direct method was used because the IEEE-B and IEC 60034-2-1 are structured for machines under sinusoidal supply. The IEC 60034-2-3 Ed. 1 [55] supports using the direct method for testing induction machines under converter supply. These efficiency values were then compared to the efficiency that was presented in the preceding section when the induction motors were supplied by the generator set without the VSD connected. The VSDs were operated at a 4kHz

switching frequency. To provide a fair comparison, the efficiency values derived using the direct method was chosen since the same method was employed in determining the efficiency of the motors when supplied via VSDs.

Figure 5.7 - Figure 5.14 give a representation of the experimental results obtained in the tests.

Generally, the efficiency of the motor drive system is below the efficiency of the induction motor without the VSD connected. This is accounted for by the presence of additional harmonic losses introduced in the motor by the presence of the VSDs.

However, it can be observed from Figure 5.7 that the efficiency of the motor - drive system is approximately equal to the efficiency of the 3kW standard motor without the VSD connected between 125% and 150% of rated load.

The drop in efficiency for the 7.5kW and 11kW EE motors is smaller than in the standard motors of the same ratings when the motors are connected to the VSD supply. In the case of the 3kW the drop in efficiency is smaller in the standard motors than in the EE motors. At rated load, there is a 1.43% drop in efficiency for the 3kW EE when it is operated with and without the VSD supply. This value however drops to 1.23% for the 3kW standard motor. However, this figure stands at 2.59% and 2.66% for the 7.5kW EE and standard motors respectively. Similarly there is a drop of 2.23% and 2.93% for the 11kW EE and standard motors when they are operated with and without the VSD supply.

Generally, the EE motors tested performed better with the VSD relative to the standard motors. This can be accounted for by the fact that there are reduced losses in the EE motors than their corresponding standard motors. As pointed out in the earlier sections, the quality of magnetic material used for the core of EE motors results in lower core losses in the EE motor than in the standard motor. Since the EE motors have better slot fills and reduced resistance values, the corresponding I^2R losses will be minimal relative to the standard motors. At high frequencies, the effective resistance of the conductors is affected due to skin effect. Because there are better slot fills and larger conductor size in EE motors than in standard motors, increase in effective resistance due to skin effect on the EE motors will be lesser

than in the standard motors at higher frequencies. Hence the increase in winding resistance losses due to skin effect will be minimal in the EE motors relative to the standard motors.

It is also observed that the flatness of the efficiency curves from the EE motors is affected when there is a VSD connected to the motor.

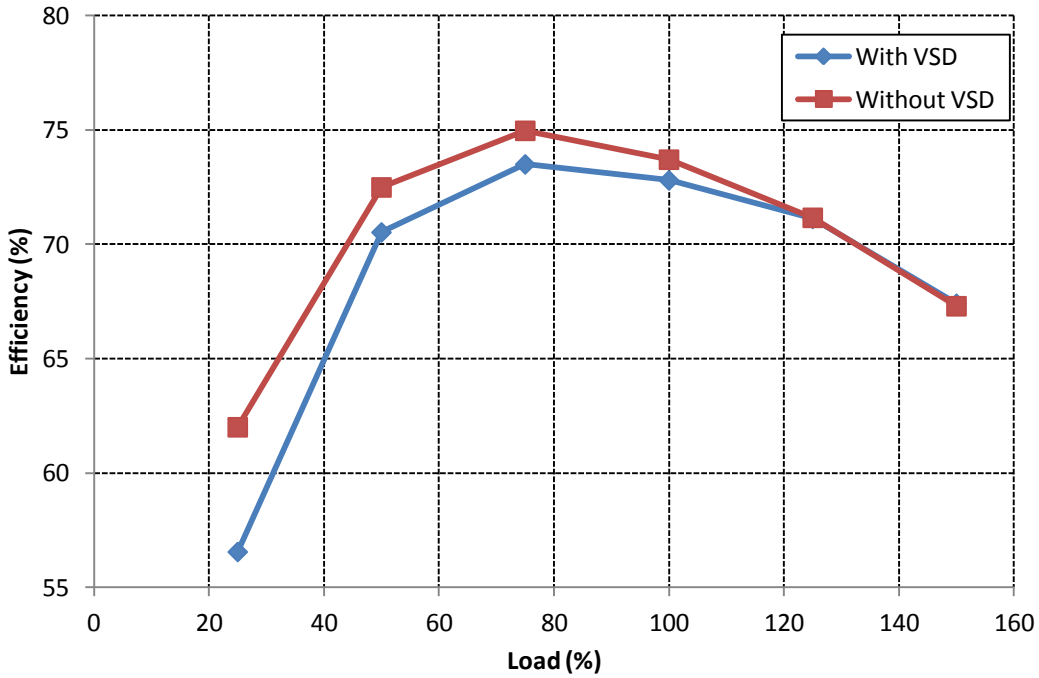

Figure 5.7 Efficiency of 3kW Standard Motor with & without VSD supply

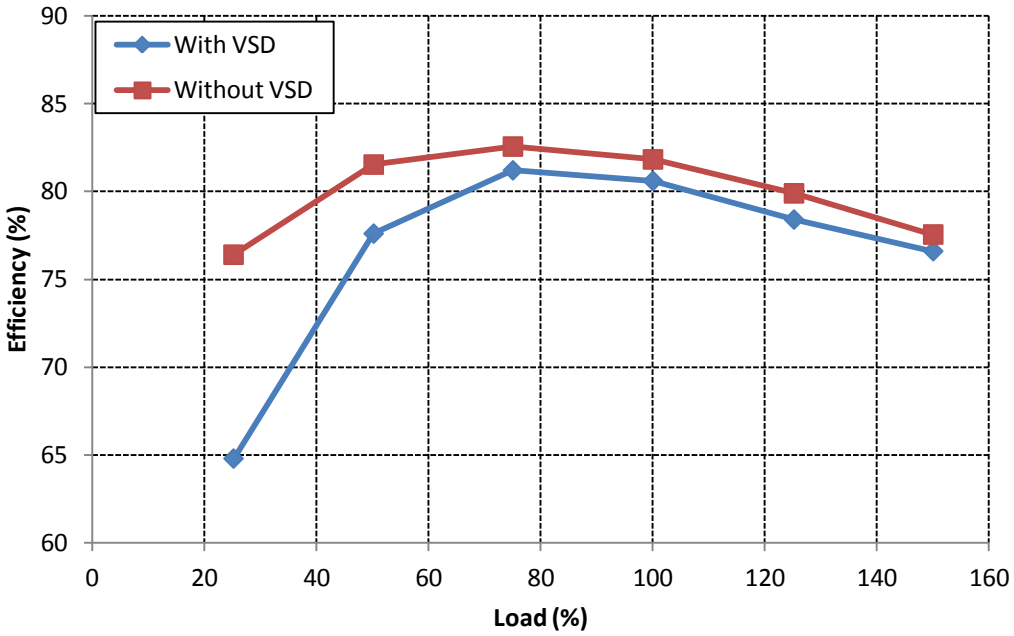

Figure 5.8 Efficiency of 3kW EE Motor with & without VSD supply

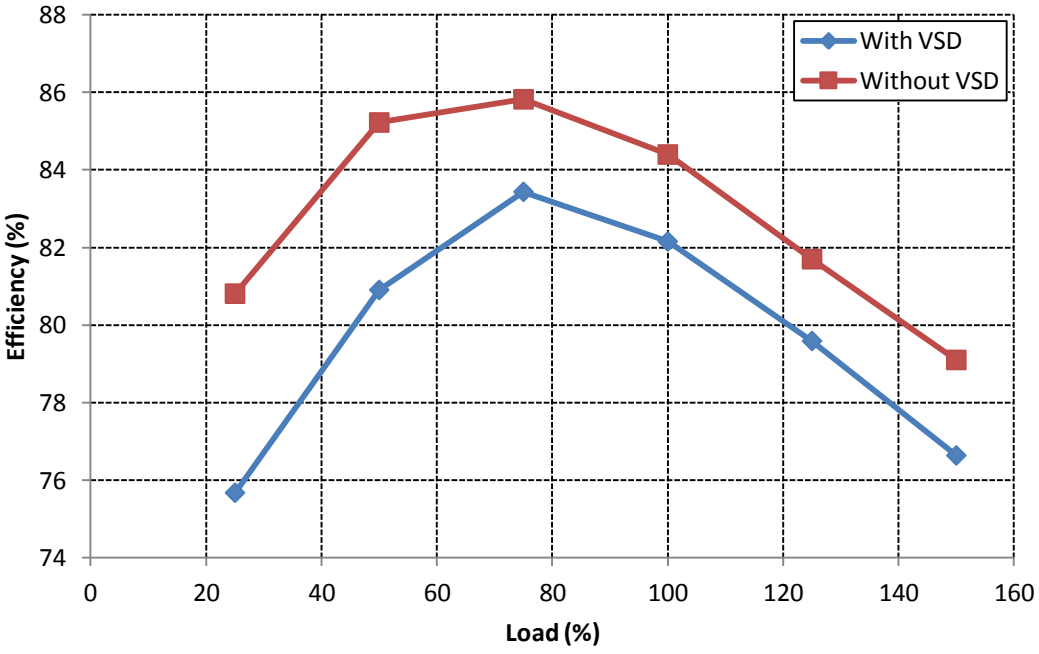

Figure 5.9 Efficiency of 7.5kW Standard Motor with & without VSD supply

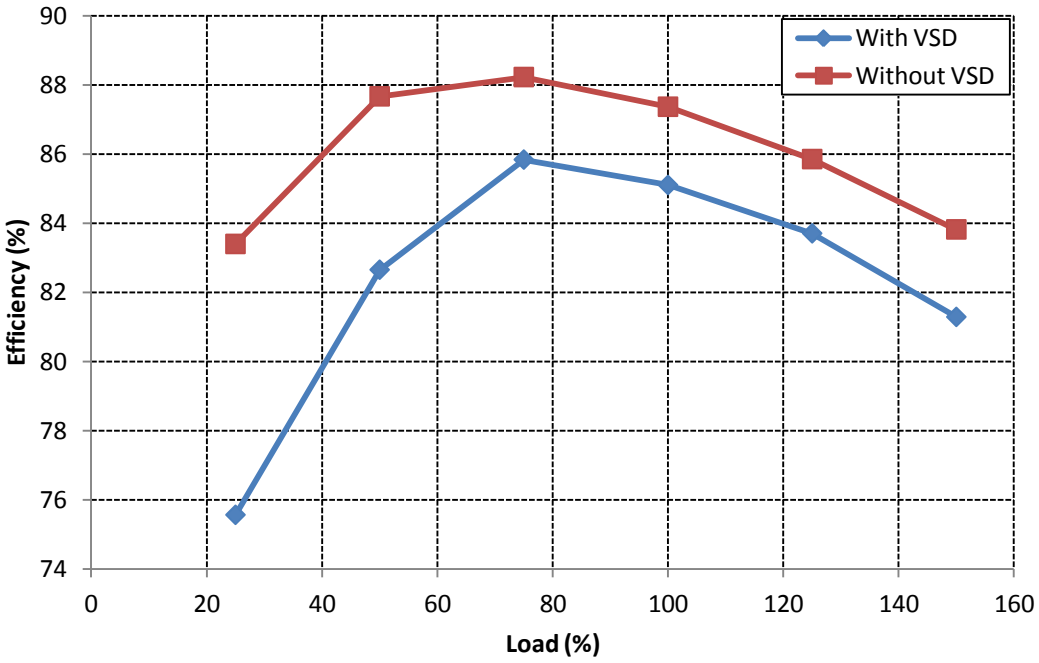

Figure 5.10 Efficiency of 7.5kW EE Motor with & without VSD supply

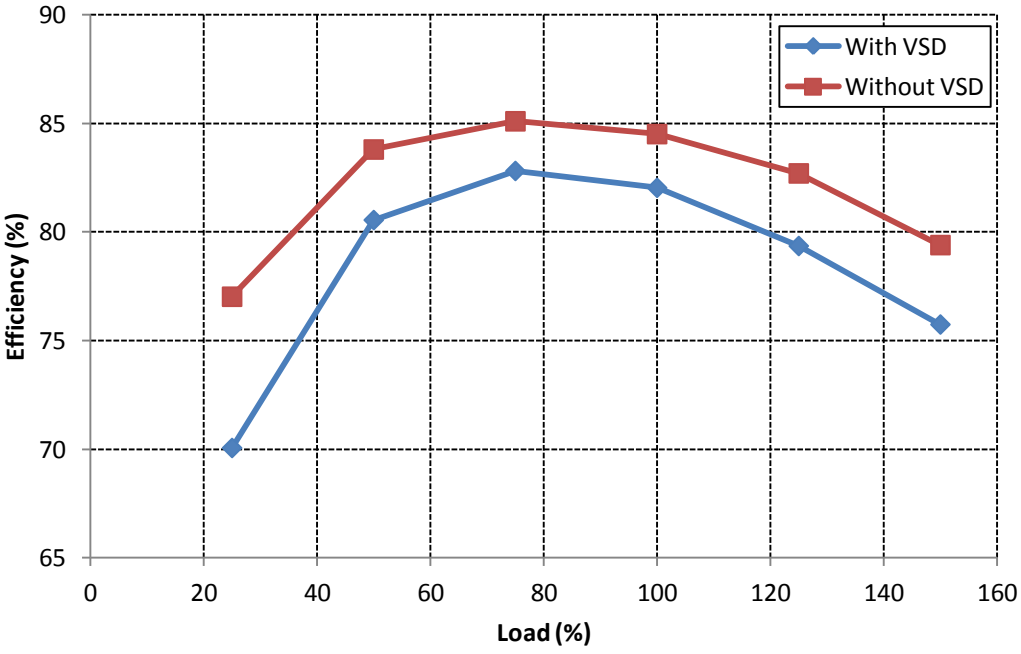

Figure 5.11 Efficiency of 11kW Standard Motor with & without VSD supply

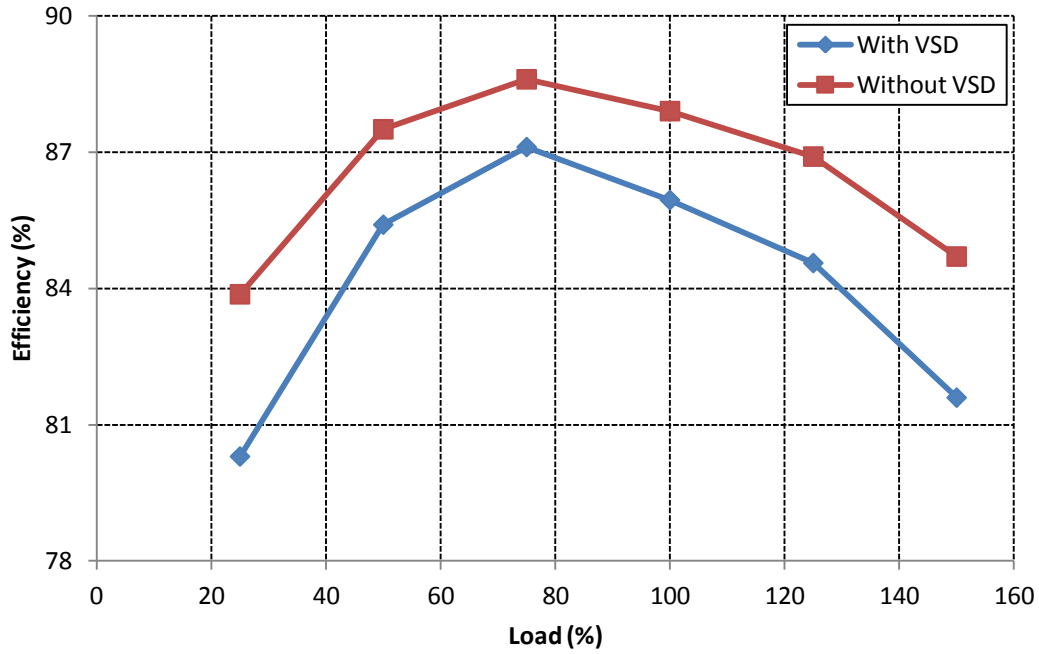

Figure 5.12 Efficiency of 11kW EE Motor with & without VSD supply

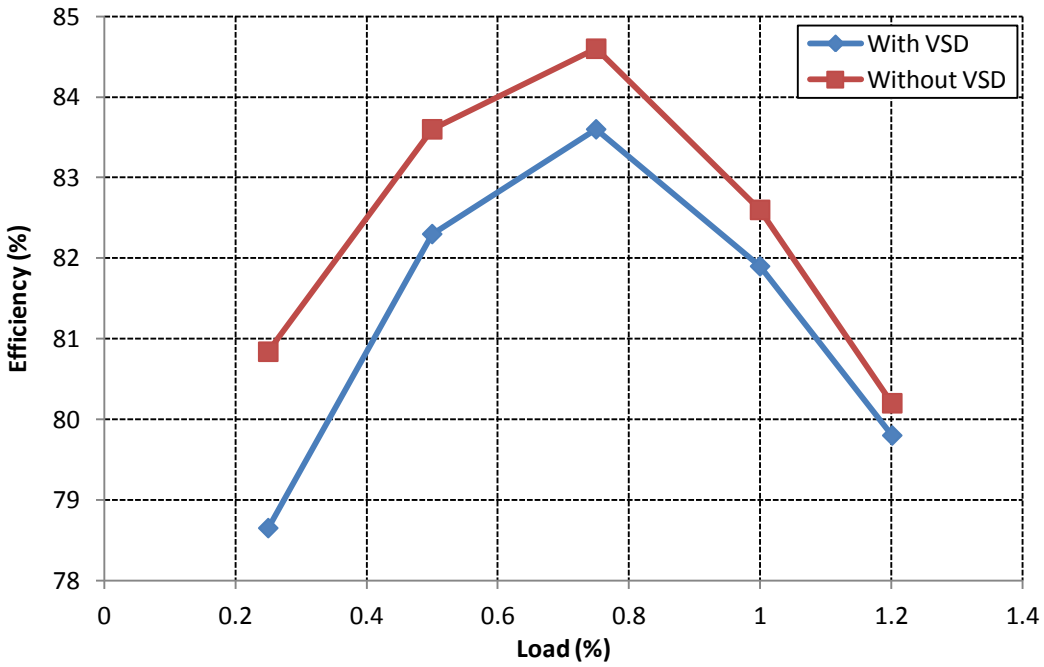

Figure 5.13 Efficiency of 15kW Standard Motor with & without VSD supply

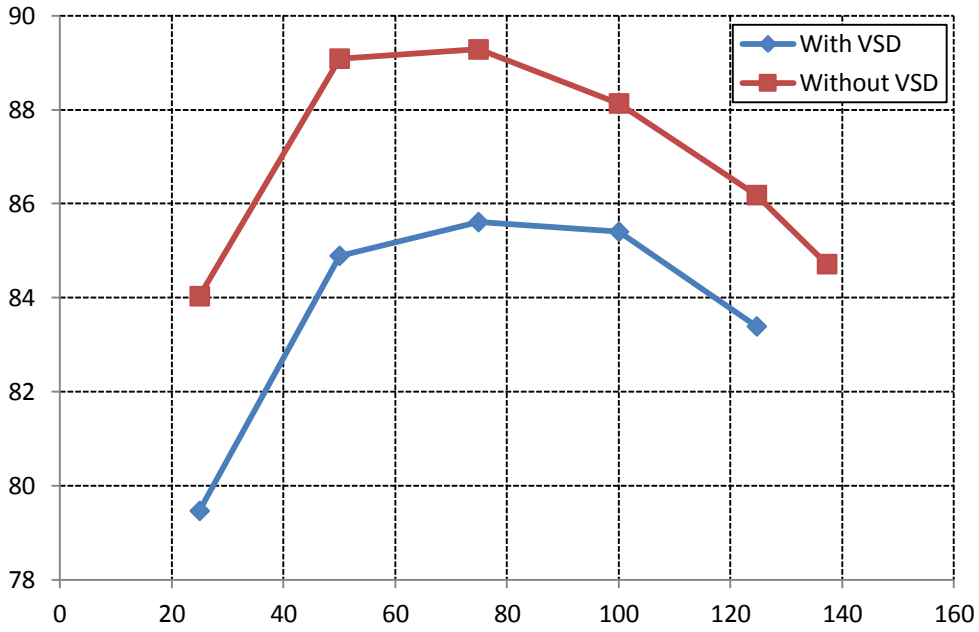

Figure 5.14 Efficiency of 15kW EE Motor with & without VSD supply

5.2.2 Efficiency Estimation Using the Harmonic Equivalent Circuit

Using the harmonic equivalent circuit developed in section 3.3, the efficiencies of the machines are calculated based on the equations associated with the circuits.

The resulting efficiency values are compared to the direct method whereby the input power is determined as in section 2.4.2 and the output power is determined from the measured shaft torque and speed. Figure 5.15 to Figure 5.22 present the curves of efficiency against rated load for the various machines obtained using both the direct method and the harmonic equivalent circuits. To show the equivalent circuit method performs relative to the other methods, the efficiency of the 3kW EE mother is calculated using the fundamental equivalent circuit. These results are then presented together with the motors efficiency when it is operated without the VSD as obtained by the direct method and the IEEE 112-B.

From the results, it is observed that the equivalent circuit method of estimating the frequency underestimates the motor efficiency relative to the direct method, when the motor is operated with a VSD. In calculating the total power on the shaft of the motor, the additional harmonic losses from the no-load test in the laboratory is

included in the calculation. This accounts for the reduction in efficiency. This difference in the recorded efficiency increases with the sizing of the motors.

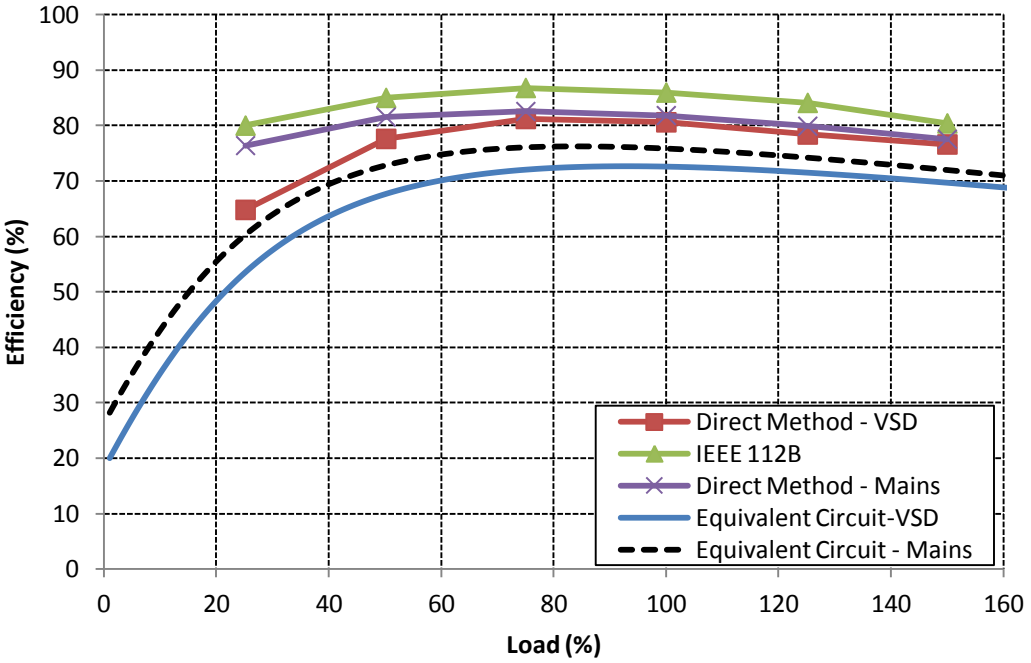

Figure 5.15 Efficiency of 3kW EE motor derived using different methods

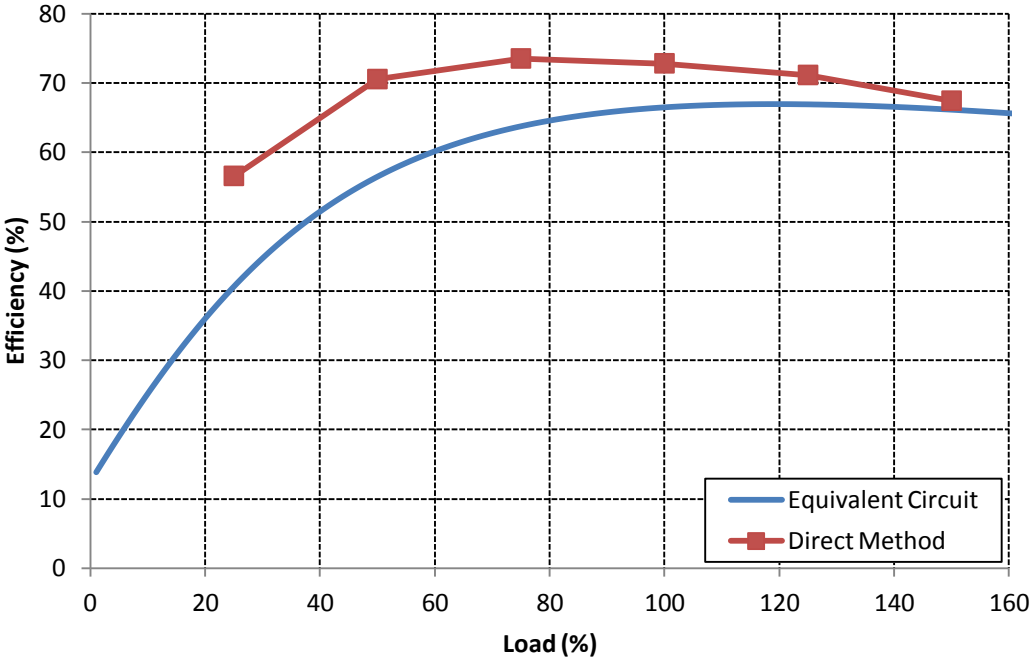

Figure 5.16 Efficiency of 3kW Standard motor derived using the direct and equivalent circuit methods when operated with VSD supply

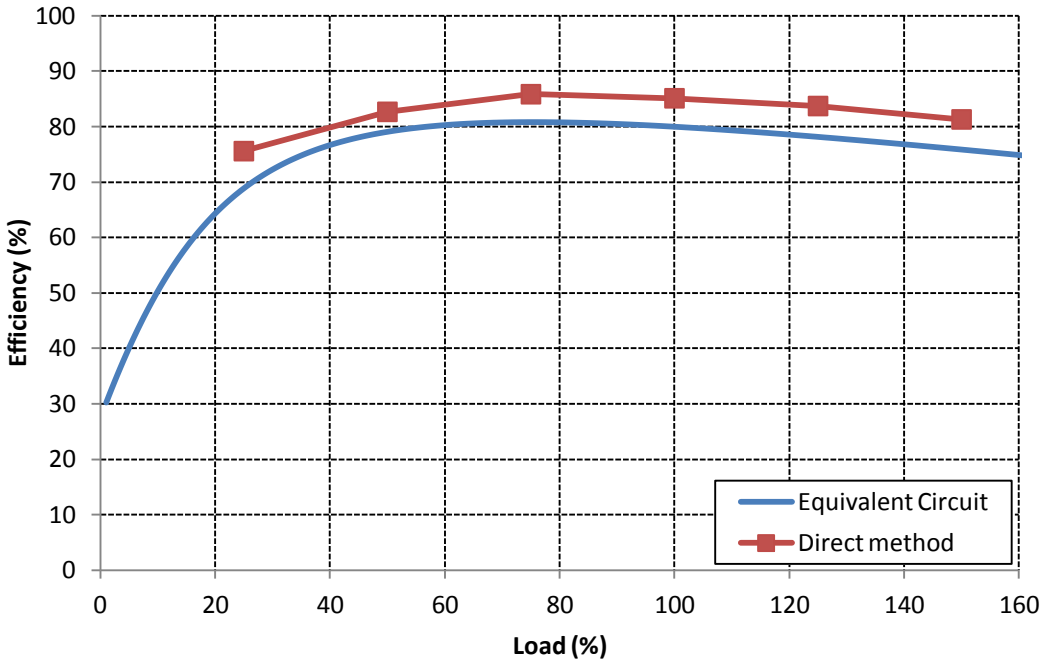

Figure 5.17 Efficiency of 7.5kW EE motor derived using the direct and equivalent circuit methods when operated with VSD supply

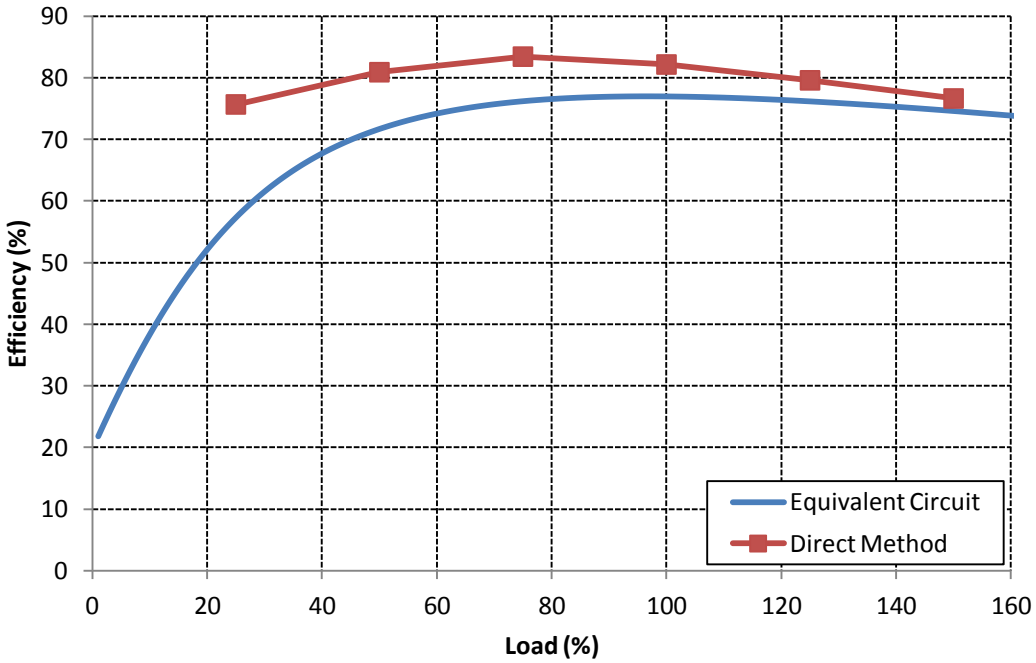

Figure 5.18 Efficiency of 7.5kW Standard motor derived using the direct and equivalent circuit methods when operated with VSD supply

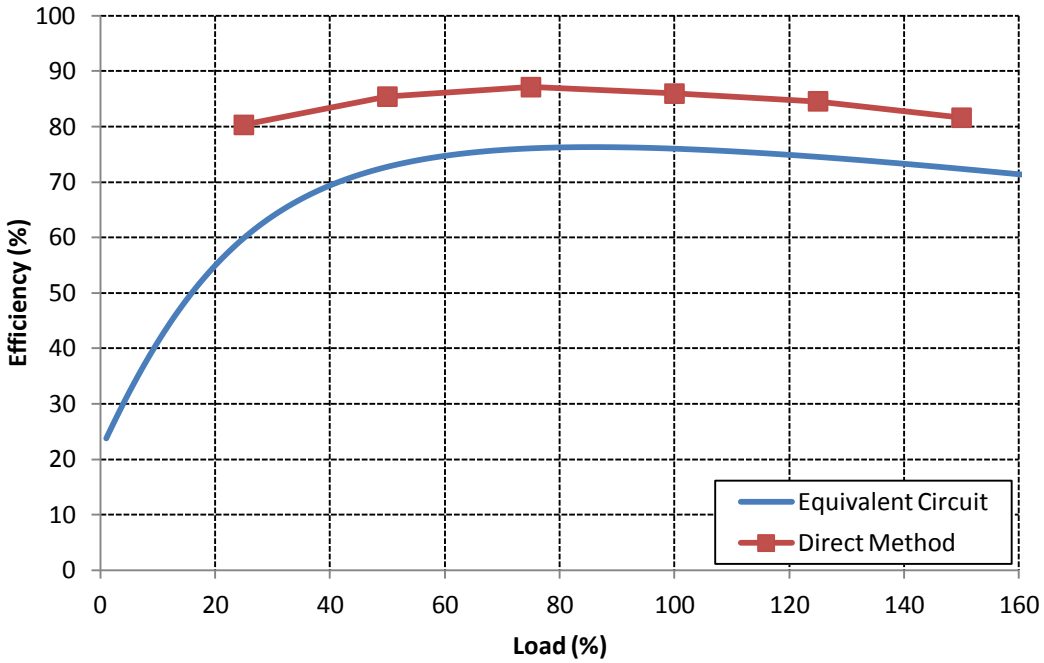

Figure 5.19 Efficiency of 11kW EE motor derived using the direct and equivalent circuit methods when operated with VSD supply

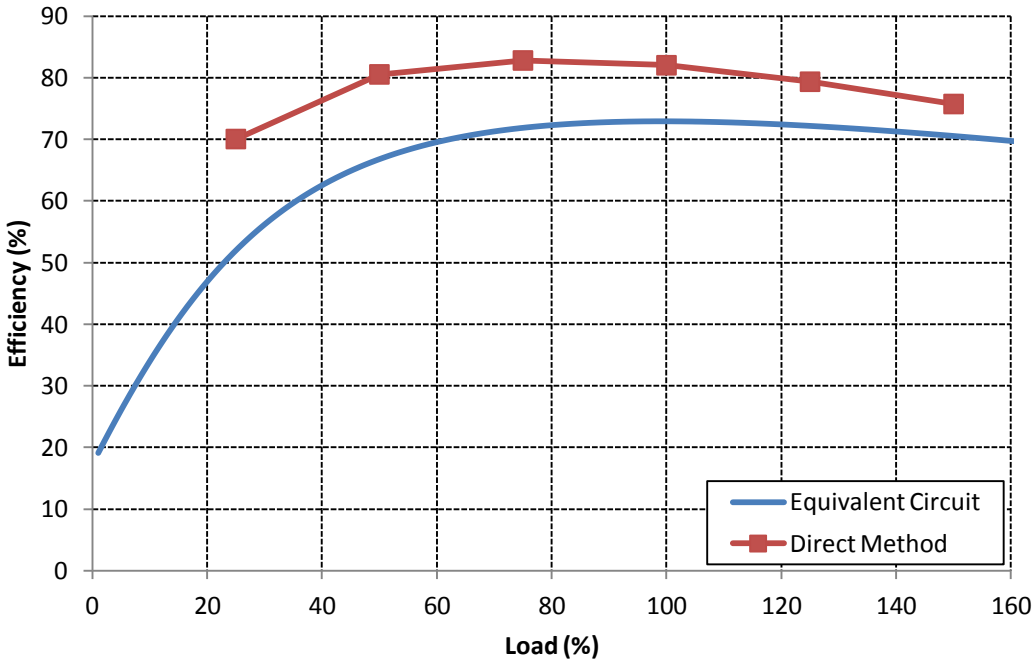

Figure 5.20 Efficiency of 11kW Standard motor derived using the direct and equivalent circuit methods when operated with VSD supply

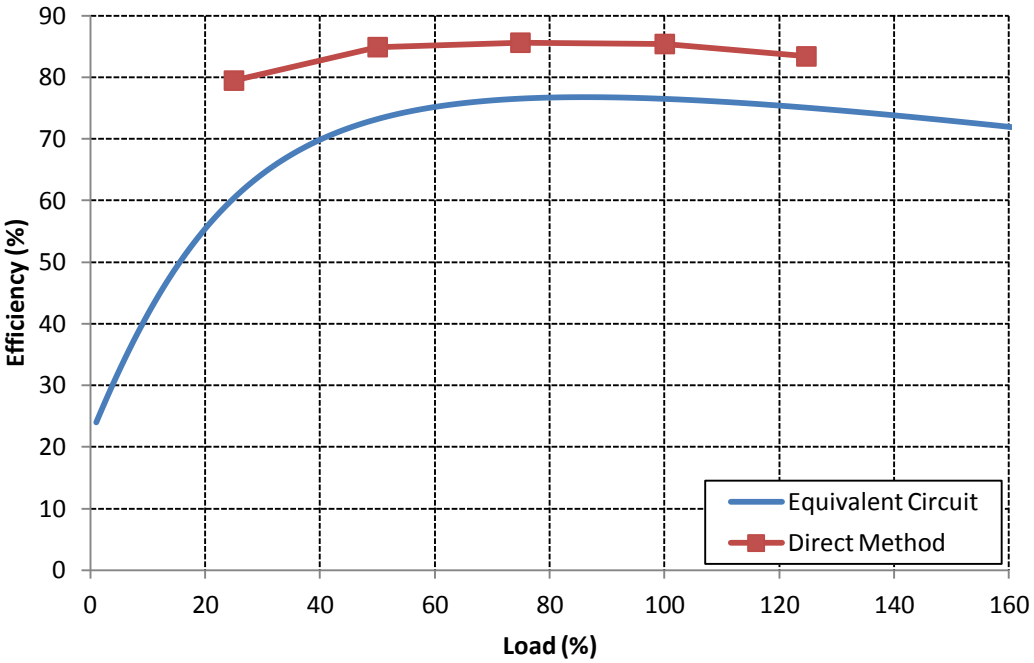

Figure 5.21 Efficiency of 15kW EE motor derived using the direct and equivalent circuit methods when operated with VSD supply

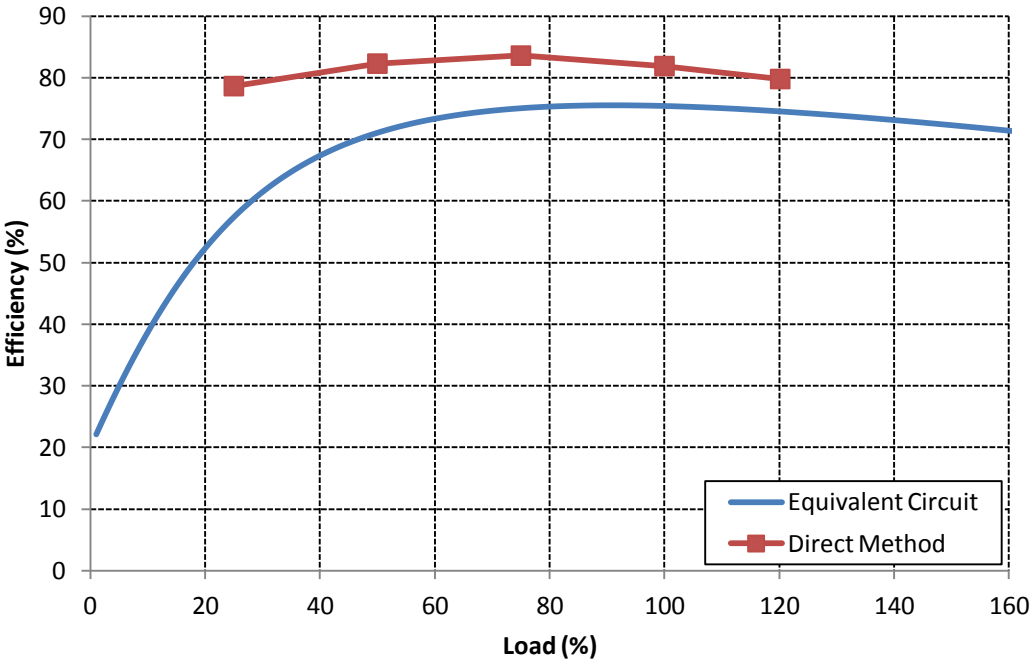

Figure 5.22 Efficiency of 15kW Standard motor derived using the direct and equivalent circuit methods when operated with VSD supply

5.2.3 Effects of Switching Frequency on Induction Motor Efficiency

The 3kW standard and EE motors were tested with the VSD under different switching frequencies to quantify the effects of variation of VSD switching frequencies on the induction motor performance. The switching frequencies were varied between 2 kHz and 10 kHz. This is the range of switching frequencies available for the VSD used for the test. These test could however not be repeated on the rest of the machines because of the rating of the VSD available. The graphs in Figure 5.23 - Figure 5.26 present the experimental results obtained.

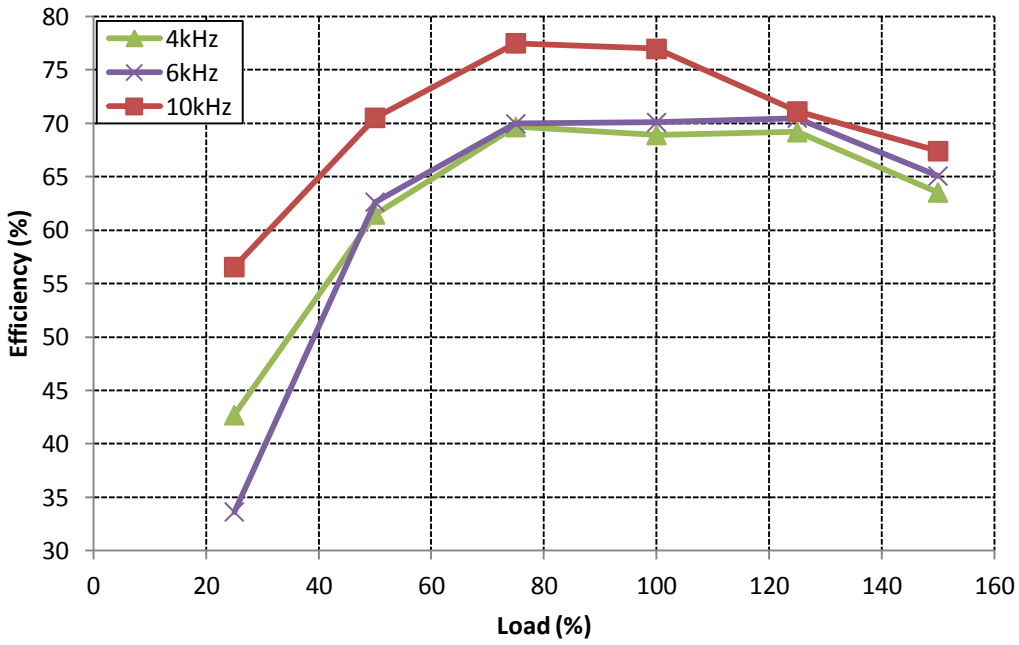

Figure 5.23 Variation of 3kW Standard motor efficiency with switching frequency

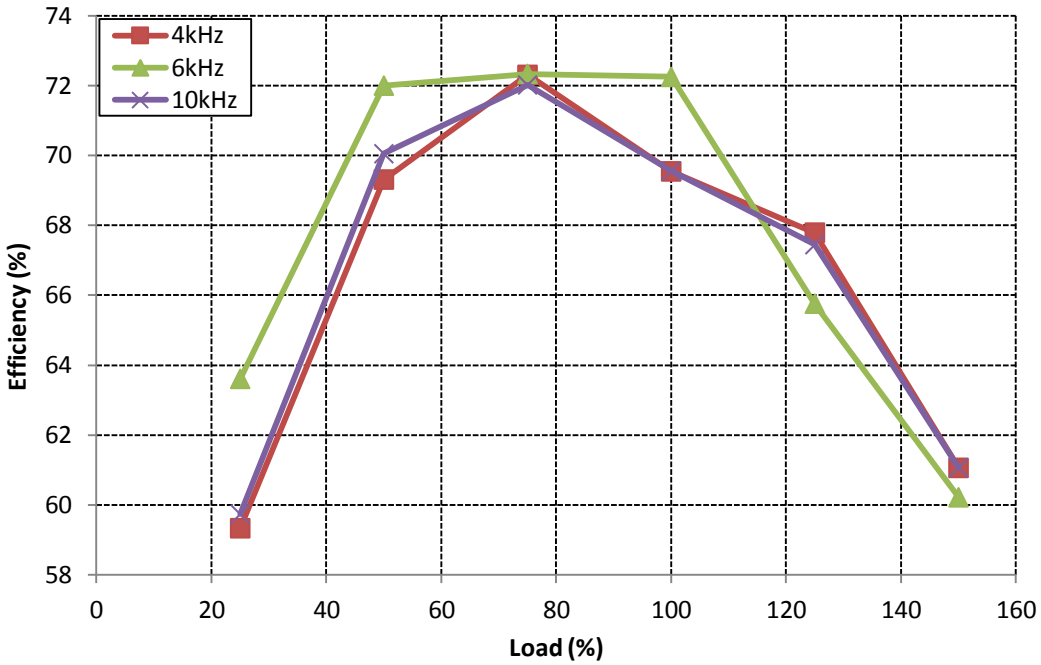

Figure 5.24 Variation of Total System efficiency with switching frequency for 3kW Standard Motor and VSD System

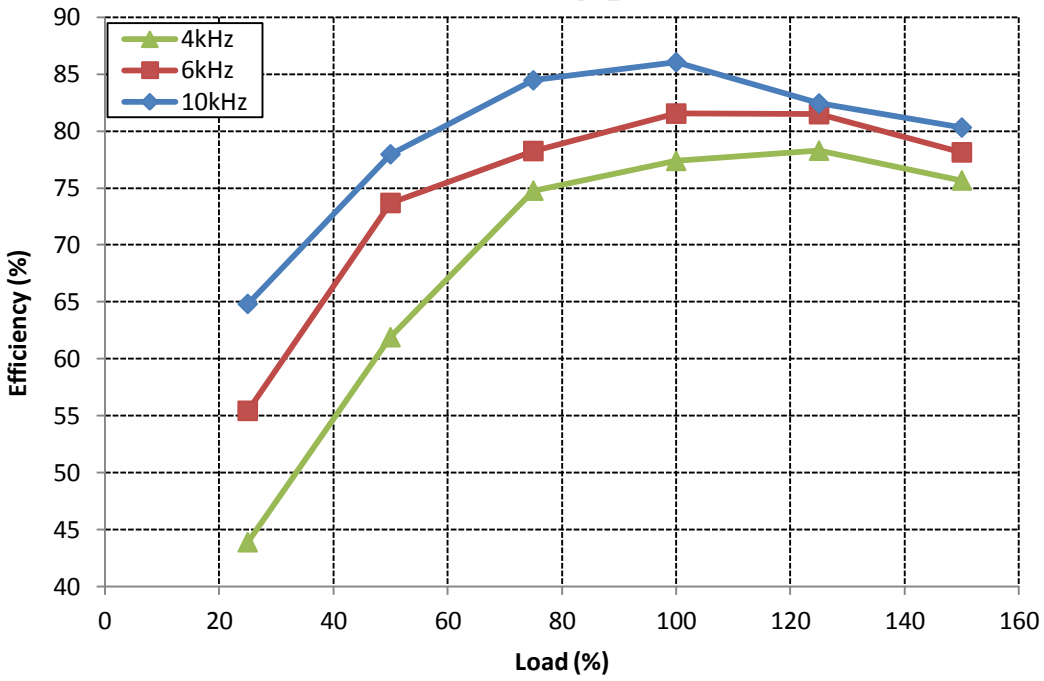

Figure 5.25 Variation of 3kW EE motor efficiency with switching frequency

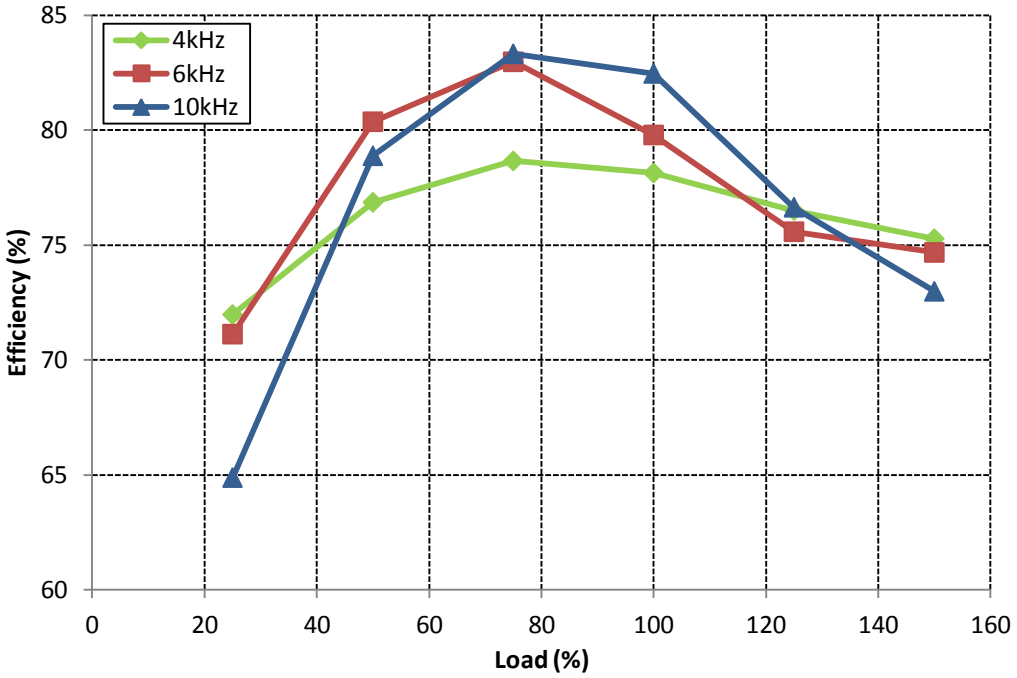

Figure 5.26 Variation of Total System efficiency with switching frequency for 3kW EE Motor and VSD System

From Figure 5.23 and Figure 5.25, it can be seen that though an increase in the switching frequency of the VSD results in an increase in the motor efficiency. This is a confirmation of what has been proposed in [41] and [42]. The total motor drive system efficiency does not follow the same format. This can be accounted for by the increase in inverter losses with increase in drive switching frequency. However, from Figure 5.24 and Figure 5.26, a linear relationship between the total system efficiency and the switching frequency is not visible, which supports the idea that an increase in switching frequency may result in an increase in motor efficiency but not necessarily an improvement in the total system efficiency.

In view of this, the drive switching frequency for optimum motor drive efficiency needs to be specified for any motor drive combination. It is therefore relevant to get a specific motor drive combination for effective system efficiency.

CHAPTER SIX: CONCLUSION AND RECOMMENDATION

6.1 CONCLUSIONS

- The process of using a wattmeter to measure power is susceptible to error in the presence of harmonics. Measurement of power in the presence of harmonics calls for more sophisticated methods of measuring power.
- EE motors have higher efficiencies than standard motors. In terms of losses the EE motors tested had lower copper, core and stray load losses than their corresponding standard motors. However, the EE motors tested had higher friction and windage losses relative to the standard motors. This can be attributed to the fact that the EE motors tested were IP 66 rated machines while the standard motors were IP 55 rated machines.
- The IEC 60034-2-1 method overestimates the efficiency of the induction motors relative to the direct method and the IEEE 112-B. The IEC 60034-2-1 method records lower core losses than the IEEE 112-B due to the compensation of voltage drop across the stator windings.
- The harmonic equivalent circuit used for estimating the efficiency of the induction motors underestimates the efficiency relative to the direct method.
- Since the harmonic equivalent circuit was adopted from the fundamental equivalent circuit, an error in determining the circuit parameters of the fundamental circuit will result in an error when the harmonic equivalent circuit is used for efficiency estimation.
- Operating an induction motor under VSD supply results in a drop in the motor efficiency. This can be associated with the additional losses associated with the harmonics introduced by the VSD.
- Relative to EE motors, the efficiency of standard motors are greatly affected by the harmonic losses when the induction motors are operated under VSD supply. Quality design features of the EE motors such as the core material, better slot fit and size of conductors makes them less prone to the additional harmonic losses that are introduced by the VSDs.

- The presence of harmonics associated with VSDs result in increase in motor losses and rise in motor temperature. The motor no-load losses increase with the introduction of VSDs.
- Increasing the switching frequency of the VSDs inverter results in an increase in induction motor efficiency. This however results in an increase in the inverter switching losses. The effect on the total system efficiency varies with the specific motor drive combination.

6.2 RECOMMENDATIONS

The following recommendations are made based on the findings of this work and the conclusions that have been drawn:

- Due to the error associated with using the wattmeter in measuring power in the presence of harmonics, more conclusive methods should be employed in measuring power in the presence of harmonics.
- Care should be taken in determining the equivalent circuit parameters of the induction motor during the no-load and blocked-rotor tests. These test results affect the efficiency estimated using the harmonic equivalent circuit.
- The direct method of efficiency determination can be adopted in determining the efficiency of VSD driven motors, but in the contest of motors without VSDs detailed tests should be carried out to quantify the individual losses.
- Though an increase in switching frequency leads to increase in motor efficiency, it is recommended that tests should be carried out on specific motor drive system to obtain the VSD switching frequency that will result in optimum system efficiency.
- It is recommended that additional cooling be applied to induction motors under VSD supply, to cater for the rise in motor temperature.
- The VSDs used for the tests are low voltage VSIs. Further research needs to be carried out on how other VSD types and control mechanisms influence the efficiency of induction machines. In other applications, operations will be at lower speeds; eg pump/fan loads where additional losses are not a problem since the load requires significantly less power and no additional cooling is needed. Also more induction motors from different vendors need to be tested with different VSDs.

- Further investigation/research is recommended in the areas of the effect of optimal flux control on the drive system efficiency; drive system efficiency at operating speeds lower than rated speed since this is the normal operating areas of adjustable speed systems. Furthermore, research into designing EE motors specifically for inverter operations for optimised efficiency is recommend.
- In addition to the above mentioned, research and further studies should be done to investigate the use of calorimeters for loss determination and also the impact of VSDs on EE and standard motors in hazardous areas.

REFERENCES

[1] Eskom DSM. (2009, October) [Online]. http://www.eskomidm.co.za/wp-content/themes/eskom/pdfs/Industrial/EE%20Motors/117102ESKD%20DSM%20EE%20Motors.pdf

[2] Alexander Eigeles Emanuel, "Estimating the effects of harmonic voltage fluctuations on the temperature rise of squirrel-cage motors," *IEEE Transactions on Energy Conversion*, vol. 6, no. 1, pp. 162-169, March 1991.

[3] Fernand G. G. de Buck, "Losses in Parasitic Torques in Electric Motors Subjected to PWM waveforms," *IEEE Transactions on Industry Applications* , vol. IA-15, no. 1, pp. 47-53, Jan/Feb 1979.

[4] K. Venkatesan, James F. Lindsay, "Comparative Study of the losses in Voltage and Current Source Inverter Fed Induction Motors," *IEEE Transactions on Industry Applications*, vol. IA - 18, no. 3, pp. 240-246, May/June 1982.

[5] Ferdinand G. G. de Buck, Paul Gistenlink and Dirk de Backer, "A Simple but reliable loss model for inverter supplied induction motors," *IEEE Transactions on Industry Applications*, vol. IA - 20, no. 1, pp. 190 - 202, January/February 1984.

[6] Daniel S. Kirschen, Donald W. Novotny and Warin Suwanwisoot, "Minimizing Induction Motor Losses by Excitation Control in Variable Frequency Drives ," *IEEE TRANSACTIONS ON INDUSTRY APPLICATIONS*, vol. IA-20, no. 5, pp. 1244-1250, September/October 1984.

[7] A. Boglietti, A. Cavagnino, M. Lazzari, M. Pastorelli, "International Standards for the Induction Motor Efficiency Evaluation: a Critical Analysis of the Stray-Load Loss Determination," *IEEE Transactions on Industry Applications*, vol. 4, no. 5, pp. 1294 - 1301 , September/October 2004.

[8] Electrical Apparatus Service Association. Understanding Energy Efficiency Motors. [Online]. http://www.empr.tfc.kg.ac.rs/rezultati%20i%20bodovi/Statkic/Glossary/ee_motors.pdf

[9] P. Giridhar Kini, R. C. Bansal, R. S. Aithal, "Impact of Voltage Unbalance on the Performance of Three-Phase Induction Motor," *South Pacific Journal of Natural Science*, vol. 24, pp. 45-50, 2006.

[10] A. L. Van Wyk , "Effects of Voltage Unbalanced Supplies on Energy-Efficient Motors," University of Cape Town, MSc Thesis November 2010.

[11] P. Pillay, P. Hofmann, "Derating of Induction Motors Operating with a Combination of Unbalanced Voltages and Over- or Undervoltages," in *IEEE Power Engineering Society Winter Meeting*, 2001, pp. 1365 - 1371.

[12] "Motors and Generators," NEMA Standards Publication MG 1-1998,.

[13] K.V. Vamsi Krishna, "Effects of Unbalance Voltage on Induction Motor Current and its Operation Performance," Lecon Systems,.

[14] Effect of Voltage Variation of Induction Motors. (2011, September) [Online]. www.landbelectric.com

[15] "IEEE Recommended Practices and Requirements for Harmonic Control in Electrical Power Systems," IEEE STD - 519, 1992.

[16] B. Lu, T. G. Habetler, R.G. Harley, "A Nonintrusive and In-Service Motor-Efficiency Estimation Method Using Air-Gap Torque With Considerations of Condition Monitoring," *IEEE Transactions on Industry Applications*, vol. 44, no. 6, pp. 1666 - 1674, Decenber 2008.

[17] W. Cao, K. J. Bradley, "Assessing the Impacts of Rewind and Repeated Rewinds on Induction Motors: Is an Opportunity for Re-Designing the Machine Being Wasted?," in *IEEE International Conference on Electric Machines and Drives*, May 2005, pp. 278 - 285.

[18] Motor Challenge Fact Sheet. Determining Electric Motor Load and Efficiency. [Online]. http://www.p2pays.org/ref/40/39569.pdf

[19] P. C. Sen, *Principles of Electric Machines and Power Electronics*, 2nd ed.: John Wiley and Sons, Inc., 1997.

[20] Reliance. AC Motor Efficiency - A guide to Energy Savings - Part 2. [Online]. http://www.reliance.com/prodserv/motgen/b7087_5/b7087_5_2.htm

[21] E. Romero, L. F. Mantilla, S. Corino, "How the Efficiency of an Induction Machine is Measured," in *International Conference on Renewable Energy and Power Quality (ICREPQ)*, 2008.

[22] B. Renier, K. Hameyer, R. Belmans, "Comparison Of Standards For Determining Efficiency Of Three Phase Induction Motors ," *IEEE Transactions On Energy Conversion*, vol. 14, no. 3, pp. 512 - 517, September 1999.

[23] H. Köfler, "Stray Load Losses In Induction Machines: A Review Of Experimental Measuring Methods And A Critical Performance Evaluation," in *International*

Conference On Renewable Energies And Power Quality (ICREPQ), 2003.

[24] A. T. de Almeida, F. T. E. Ferreira, J. F. Busch, P. Angers , "Comparative Analysis Of Ieee 112-B And Iec 34-2 Efficiency Testing Standards Using Stray Load Losses In Low Voltage Three-Phase, Cage Induction Motors," *IEEE Transactions on Industry Applications*, vol. 38, no. 2, pp. 608-614, March/April 2002.

[25] "IEEE Standard Test Procedure for Polyphase Induction Motors and Generators," IEEE 112-2004,.

[26] "Methods for Determining Losses and Efficiency of Rotating Electrical Machinery from Test," IEC 34-2, 1996.

[27] "Standard Methods for Determining Losses and Efficiency from tests (excluding machines for traction vehicles)," IEC 60034-2-1, 2007.

[28] SABS-South African Bureau of Standards. (2010) List of Published Standards. [Online]. https://sabs.co.za/business_units/standards_SA/controls/published_standards/PS61.pdf

[29] A. H. Samra, "Power Measurement in the Presence of Harmonic Distortion ," in *IEEE Southeastcon '93, Proceedings*, 1993.

[30] I. Purkayastha, P. J. Savoie, "Effects of Harmonics on Power Measurement," *IEEE Transactions on Industrial Applications*, vol. 26, no. 5, pp. 944-946, October 1990.

[31] N. Morrison, *Introduction to Fourier Analysis*.: Wiley-Interscience, 1994.

[32] W. Zhijian, Y. Zhongdong, "Power Analysis and Its Measurement Research under Harmonic Circumstances," in *International Conference on Energy and Environment Technology*, 2009 , pp. 193-196.

[33] WT 1600 Digital Power Meter User's Manual.

[34] N. Mohan, T. M. Underland, W. P. Robbins, *Power Electronics*, 3rd ed.: John Wiley & Sons Inc, 2003.

[35] T. J. Cookson, N. G. Lang, E. J. Thornton, "Adjustable Speed Drives Applied to Large AC Induction Motor and Pump Systems," in *Proceedings of The Twenty-Fourth International Pump Users Symposium*, 2008, pp. 75-80.

[36] D. A. Casada, J. D. Kueck, H. Staunton, M. C. Webb, "Efficiency testing of motors powered from pulse-width modulated adjustable speed drives," *IEEE Transactions on*

Energy Conversion, vol. 15, no. 3, pp. 240 - 244 , September 2000.

[37] R. P. Bingham, "Harmonics - Understanding the Facts".

[38] Technical Guide - Induction Motors fed by PWM Frequency Inverters. [Online]. www.weg.com

[39] D. Leggate, R. J. Kerkman, "Pulse based dead time compensator for PWM voltage inverters," *IEEE Transactions on Industrial Electronics* , vol. 44, pp. 191-197, 1997.

[40] M. Malengret, "EEE 4099F Course Notes - Space Vector Pulse Width Modulation," University of Cape Town, 2010.

[41] L. Tong, G. Wu, F. W. W. Shu, E. He, "Influence of the Inverter Characteristics on the Harmonic Losses in PWM fed Traction Motors," in *Proceedings of International Symposium on Electrical Insulating Materials*, vol. 2, June 2005, pp. 379-381.

[42] S. Khomfoi, V. Kinnares, P. Viriya, "Influence of PWM characteristics on the Core Losses due to Harmonic Voltages in PWM fed Induction Motors," in *IEEE Power Engineering Society Winter Meeting*, 2000, pp. 365 - 369.

[43] E. Nicol Hildebrand, H. Roehrdanz, "Losses in Three-Phase Induction Machines fed by PWM Converter," *IEEE Transactions on Energy Conversion*, vol. 16, no. 3, pp. 228-233, September 2001.

[44] A. Boglietti, P. Ferraris, M. Lazzari, M. Pastorelli, "Influence of the Inverter Characteristics on the iron losses in PWM Inverter-fed induction motors," *IEEE Transactions on Industry Applications*, vol. 32, no. 5, Sept/Oct 1996.

[45] "Guide for the Design and Performance of Cage Induction Motors Specifically Designed for Converter Supply," IEC 60034-25, 2004.

[46] X. Liang, Y. Luy, "Harmonic Analysis for Induction Motors," in *Canadian Conference on Electrical and Computer Engineering*, 2006, p. 172.

[47] P. K. Sen, H. A. Landa, "Derating of Induction Motors Due to Waveform Distortion," *IEEE Transactions on Industry Applications*, vol. 26, no. 6, pp. 1102-1107, November/December 1990.

[48] J. M. D. Murphy, Michael G. Egan, "A Comparison of PWM Strategies for Inverter-Fed Induction Motors," *IEEE Transactions on Industry Applications* , vol. 1A-19, no. 3, pp. 363-369, May/June 1983.

[49] M. J. Melfi, "Quantifying the Energy Efficiency of Motors fed by Adjustable Frequency Inverters," in *Petroleum and Chemical Industry Conference*, 2009, pp. 1-7.

[50] J. Fouladgar, E. Chauveau, "The Influence of the Harmonics on the Temperature of Electric Machines," *IEEE Transactions on Magnetics*, vol. 41, no. 5, pp. 1644-1647, May 2005.

[51] "Operation and Application of Variable Frequency Drive (VFD) Technology," Carrier Corporation, 2005.

[52] S. Campbell, *Solid-State AC Motor Controls*. New York: Marcel Dekker Inc, 1987.

[53] M. J. Meco-Gutierrez, F. Perez-Hidalgo, F. Vargas-Merino, J. R. Heredia-Larrubia, "A New PWM Technique Frequency Regulated Carrier for Induction Motors Supply ," *IEEE Transactions on Industrial Electronics*, vol. 53, no. 5, pp. 1750 - 1754 , October 2006.

[54] T. K. Abdel-Galil, E. F. El-Saadany, M. M. A Salama, "Implementation of different mitigation techniques for reducing harmonic distortion in medium voltage industrial distribution system," in *IEEE/PES Transmission and Distribution Conference and Exposition*, 2001 , pp. 561 - 566.

[55] IEC 60034-2-3 Ed. 1, "Rotating Electrical Machines - Part 2-3: Specific test methods for determining losses and efficiency of converter-fed AC motors," (Draft).

[56] E. Chiricozzi, F. Parasiliti, M. Villani, "New materials and Innovative Technologies to Improve the Efficiency of Three-Phase Induction Motors. A Case Study," in *International Conference on Electrical Machines*, Cracovia, Polonia, 2004.

[57] F. Parasiliti, M. Villani, C. Paris, O. Walti, G. Songini, A. Novello, A. Rossi, "Three-Phase Induction Motor Efficiency Improvements with Die-Cast Copper Rotor Cage And Premium Steel," in *Proceedings of SPEEDAM'04 Symposium*, Capri, Italy, 2004.

[58] Penrose H.P, "Anatomy of an Energy Efficient Electric Motor Repair," *IEEE Electrical Insulation Magazine paper*, February 1997.

[59] Introduction to Premium Efficiency Motors. [Online]. http://www.copper.org/applications/electrical/energy/motor_text.html

[60] D. G. Walters, I. J. Williams, D. C. Jackson, "The case for a new generation of high efficiency motors-some problems and solutions," in *Seventh International Conference on Electrical Machines and Drives*, 1995, pp. 26 - 31.

[61] A. H. Bonnett, C. Yung, "Increased Efficiency Versus Increased Reliability," *IEEE Industry Applications Magazine*, pp. 29-36, 2008.

[62] J. Malinowski, J. McCormick, K. Dunn, "Advances in construction techniques of AC induction motors: preparation for super-premium efficiency levels," *Industry Applications, IEEE Transactions on*, pp. 1665 - 1670, November 2004.

[63] A. H. Bonnet, "Understanding Efficiency in Squirrel-Cage Induction Motors," *IEEE Transactions on Industry Applications*, vol. IA-16, no. 4, pp. 476 - 483, August 1980.

APPENDIX

Comparison of Standard to EE motors Using different Standards

The following section has the tables and figures from the tests carried out in comparing the 7.5kW, 11kW and 15kW standard and EE motors using the IEEE 112-B, the IEC 60034-2-1 and the direct method.

- **No- Load Test Results**

Table A.0.1 No-Load values for 7.5kW Standard and EE Motors

Standard Motor			
Temp (°C)	Voltage (V)	Current (A)	Power (W)
41.440	454.750	10.379	936.688
41.970	380.540	5.524	348.787
41.970	303.950	3.603	184.291
41.930	216.180	2.436	116.824
41.900	189.990	2.130	101.127
41.790	115.220	1.359	69.712
41.680	75.298	0.997	58.395

EE Motor			
Temp (°C)	Voltage (V)	Current (A)	Power (W)
40.080	450.430	7.354	498.856
40.280	380.370	4.996	306.229
40.280	304.520	3.750	228.571
40.260	263.560	3.171	202.768
40.210	189.890	2.279	159.291
40.080	115.040	1.543	129.807
39.980	76.063	1.352	117.236

Table A.0.2 No-Load values for 11kW Standard and EE Motors

Standard Motor			
Temp (°C)	Voltage (V)	Current (A)	Power (W)
42.020	450.700	17.472	1484.430
42.670	380.090	10.110	670.911
42.610	312.180	7.039	409.866
42.550	269.740	5.933	313.830
42.320	193.150	4.131	213.119
42.170	109.550	2.465	137.767
42.050	74.428	1.923	118.143

EE Motor			
Temp (°C)	Voltage (V)	Current (A)	Power (W)
40.16	449.12	14.63	933.51
40.53	380.15	9.25	494.74
40.65	304.96	6.75	355.35
40.59	268.50	5.87	312.39
40.32	194.07	4.09	254.91
40.14	113.23	2.72	208.51
39.68	76.05	2.42	199.38

Table A.0.3 No-Load values for 15kW Standard and EE Motors

Standard Motor			
Temp (°C)	Voltage (V)	Current (A)	Power (W)
48.120	445.210	18.035	1506.460
48.375	380.010	11.991	820.262
48.330	304.490	8.706	493.419
48.290	267.740	7.439	364.902
48.150	184.960	4.968	199.075
47.930	115.070	3.180	116.949
47.760	76.474	2.229	90.494
48.120	445.210	18.035	1506.460

EE Motor			
Temp (°C)	Voltage (V)	Current (A)	Power (W)
36.380	442.920	17.035	895.712
36.680	380.250	11.419	454.532
36.660	302.040	8.141	283.363
36.630	256.420	6.816	252.033
36.550	191.950	5.015	180.212
36.340	113.870	3.091	135.416
36.170	77.057	2.292	120.204
36.380	442.920	17.035	895.712

- **Variable Load-Test**

Table A.0.4 Variable Load Test Reading for 7.5kW Standard Motor

Load (%)	Temp (°C)	Voltage (V)	Current (I)	Power (W)	Speed (rpm)	Torque (Nm)	Slip
1.50	115.29	378.94	23.37	13715.28	1409.10	74.00	6.07
1.25	116.63	380.11	18.96	11139.73	1429.70	61.60	4.66
1.00	117.52	381.11	15.13	8781.59	1446.70	49.29	3.49
0.75	117.56	382.41	11.74	6554.63	1460.60	37.12	2.48
0.50	116.61	384.62	8.84	4429.52	1473.23	24.79	1.57
0.25	115.31	385.87	6.65	2367.57	1485.35	12.31	0.77

Table A.0.5 Variable Load Test Reading for 7.5kW EE Motor

Load (%)	Temp (°C)	Voltage (V)	Current (I)	Power (W)	Speed (rpm)	Torque (Nm)	Slip
1.50	106.16	377.53	22.27	13148.95	25.46	1431.50	73.52
1.25	107.92	379.17	18.32	10820.23	25.96	1445.57	61.36
1.00	108.30	380.77	14.70	8585.95	27.69	1459.80	49.07
0.75	107.20	382.37	11.39	6424.84	31.56	1471.76	36.78
0.50	104.85	383.86	8.44	4332.35	39.42	1482.23	24.47
0.25	103.16	385.32	6.10	2324.82	55.20	1491.47	12.30

Table A.0.6 Variable Load Test Reading for 11kW Standard Motor

Load (%)	Temp (°C)	Voltage (V)	Current (I)	Power (W)	Speed (rpm)	Torque (Nm)	Slip
1.50	117.09	368.30	37.35	19979.15	1397.20	108.65	6.64
1.25	119.19	374.05	29.84	16317.70	1424.35	90.80	4.81
1.00	120.34	378.42	23.70	12884.26	1444.28	72.50	3.49
0.75	119.80	380.93	18.65	9668.72	1459.60	54.31	2.45
0.50	117.78	383.60	14.48	6600.15	1473.20	36.17	1.55
0.25	116.00	385.03	11.46	3682.88	1484.70	18.24	0.85

Table A.0.7 Variable Load Test Reading for 11kW EE Motor

Load (%)	Temp (°C)	Voltage (V)	Current (I)	Power (W)	Speed (rpm)	Torque (Nm)	Slip
1.50	87.94	373.55	34.31	18854.10	1427.30	107.95	4.77
1.25	88.55	377.55	28.09	15588.50	1444.50	90.21	3.66
1.00	88.84	381.25	22.54	12357.00	1458.70	71.86	2.71
0.75	88.63	383.94	17.75	9261.01	1470.30	54.03	1.92
0.50	87.39	385.96	13.75	6328.77	1480.50	36.05	1.27
0.25	85.96	387.12	10.68	3415.45	1489.87	18.05	0.65

Table A.0.8 Variable Load Test Reading for 15kW EE Motor

Load (%)	Temp (°C)	Voltage (V)	Current (I)	Power (W)	Speed (rpm)	Torque (Nm)	Slip
1.37	107.33	372.45	43.06	23651.07	1420.37	134.70	5.23
1.25	107.58	375.67	38.34	21288.97	1431.87	122.36	4.47
1.00	107.82	380.98	30.39	16910.63	1449.90	98.16	3.26
0.75	108.28	385.84	23.45	12626.36	1464.72	73.49	2.26
0.50	108.73	389.05	17.71	8522.84	1476.60	49.10	1.45
0.25	108.97	391.28	13.38	4550.67	1487.54	24.55	0.73

- **Efficiency Variation between Standard and EE Motors**

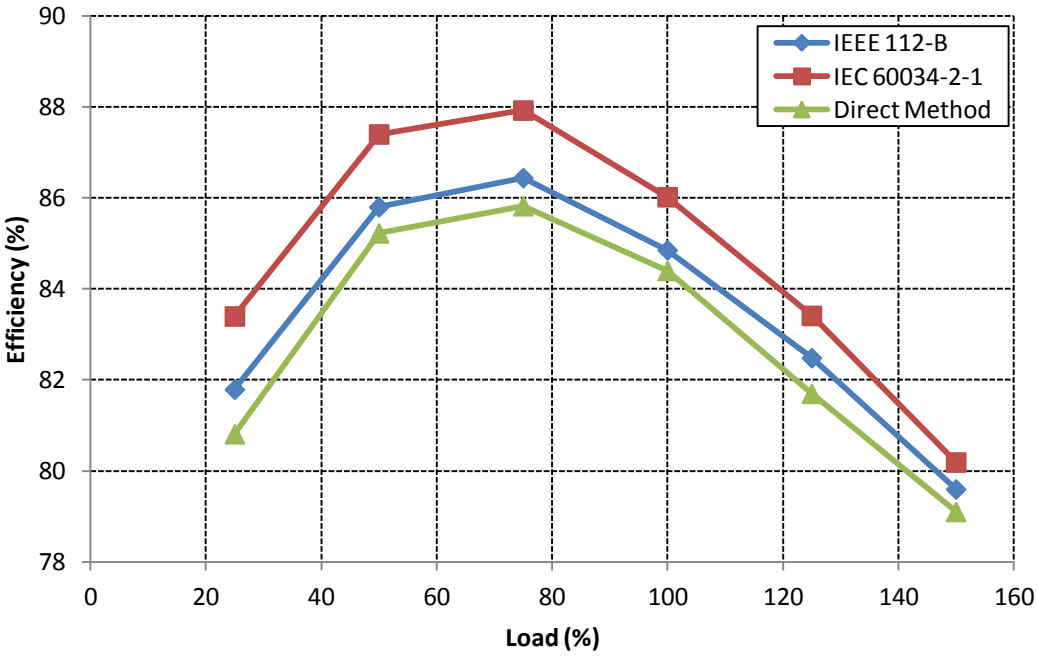

Figure A.0.1 Efficiency of 7.5kW Standard motor derived from different standards

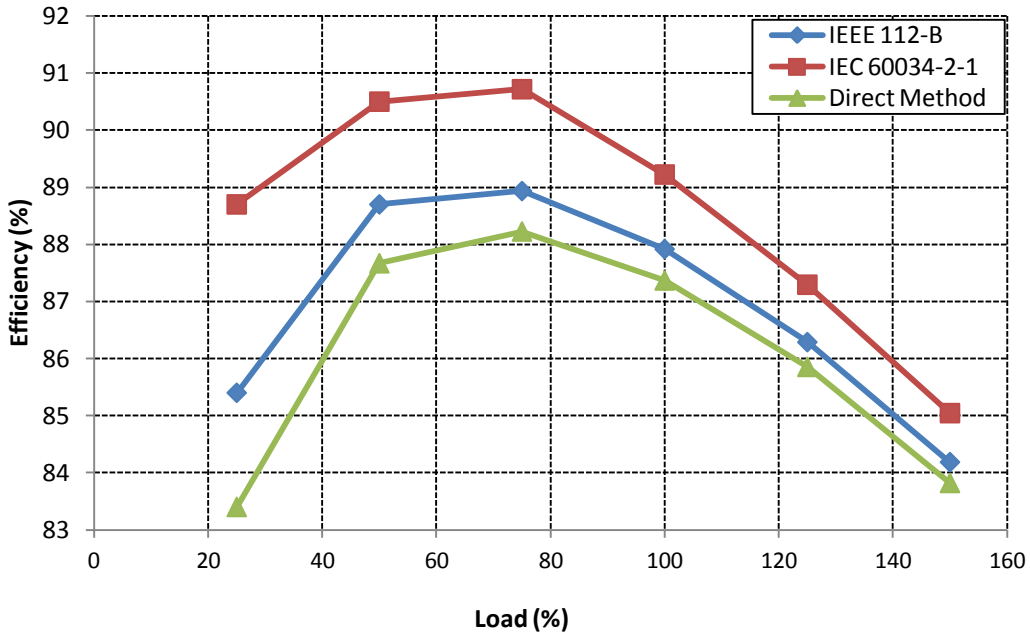

Figure A.0.2 Efficiency of 7.5kW EE motor derived from different standards

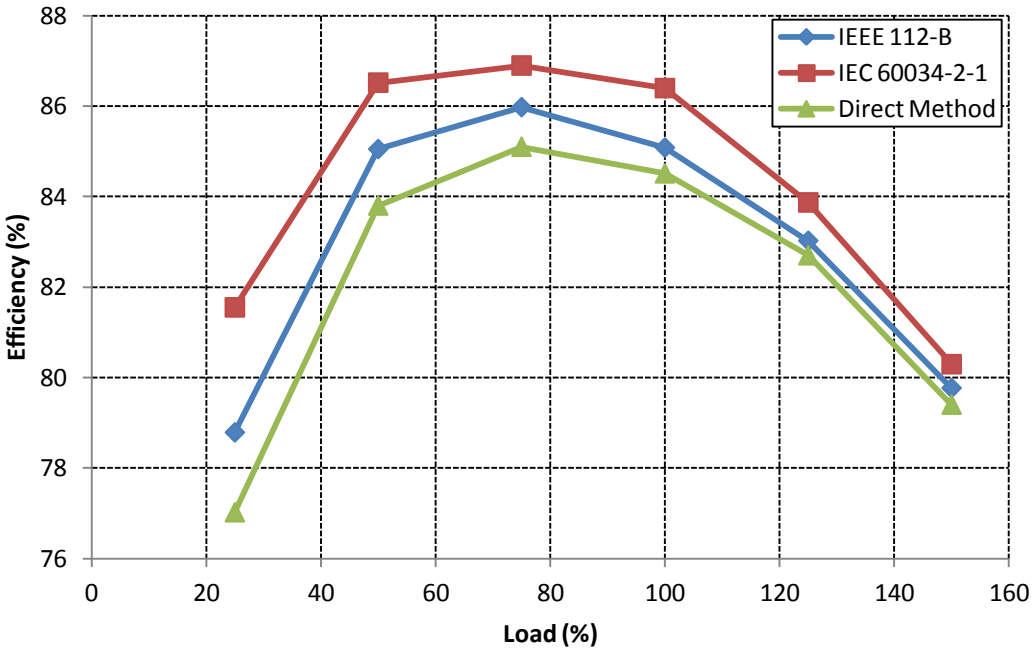

Figure A.0.3 Efficiency of 11kW Standard motor derived from different standards

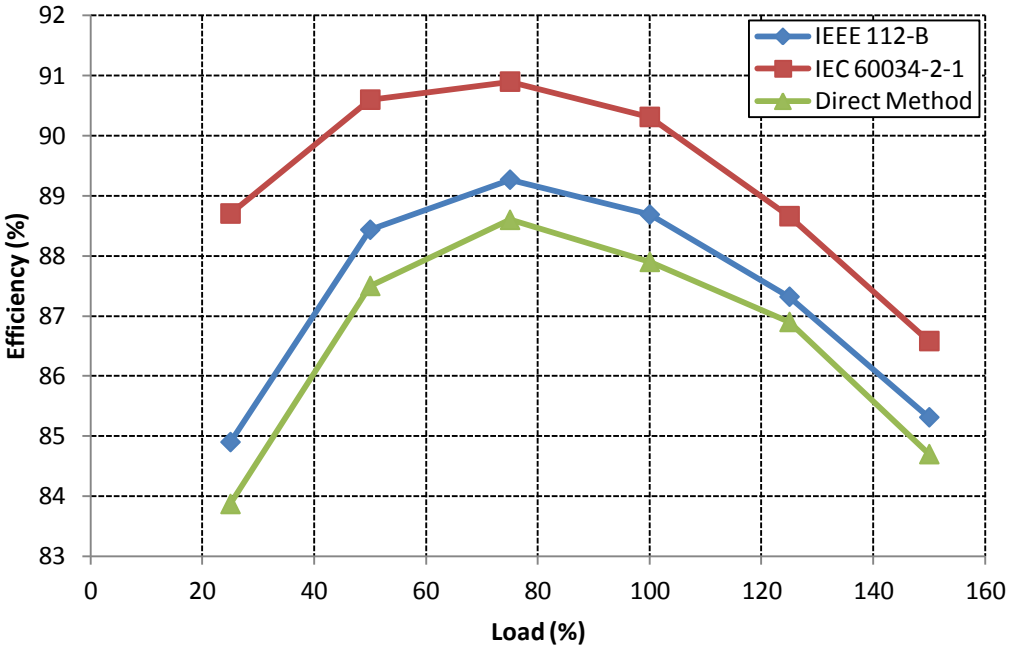

Figure A.0.4 Efficiency of 11kW EE motor derived from different standards

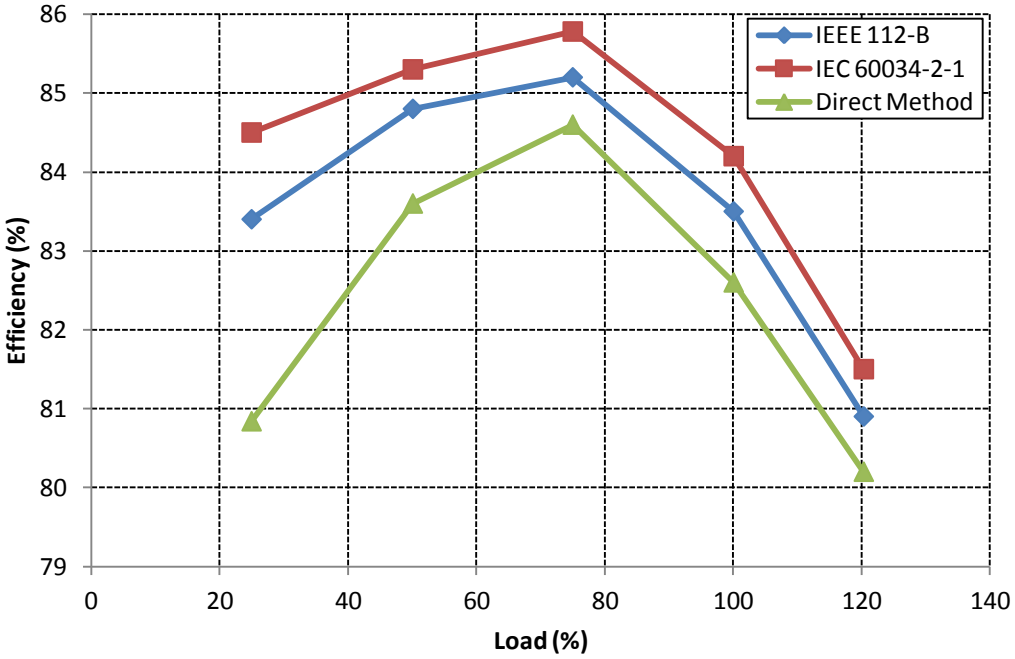

Figure A.0.5 Efficiency of 15kW Standard motor derived from different standards

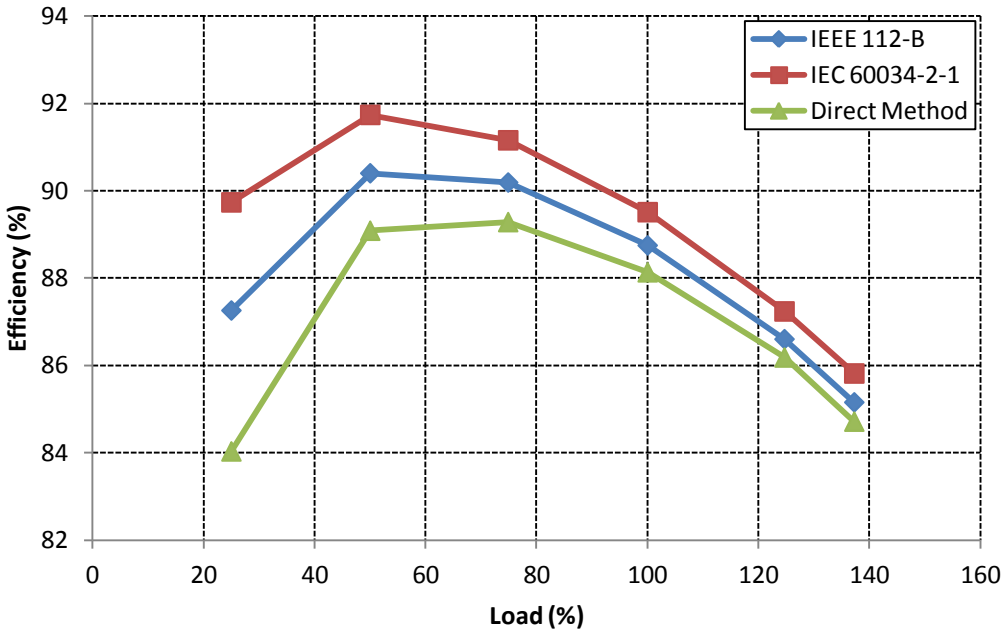

Figure A.0.6 Efficiency of 15kW EE motor derived from different standards

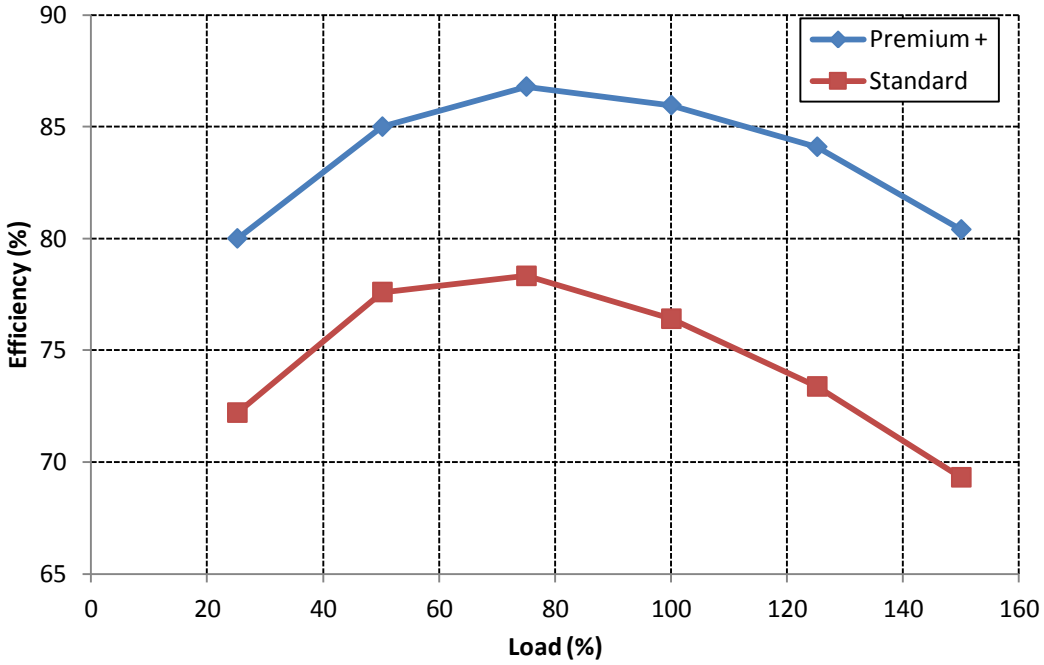

Figure A.0.7 Efficiency versus load characteristics of 3kW Standard and EE motors

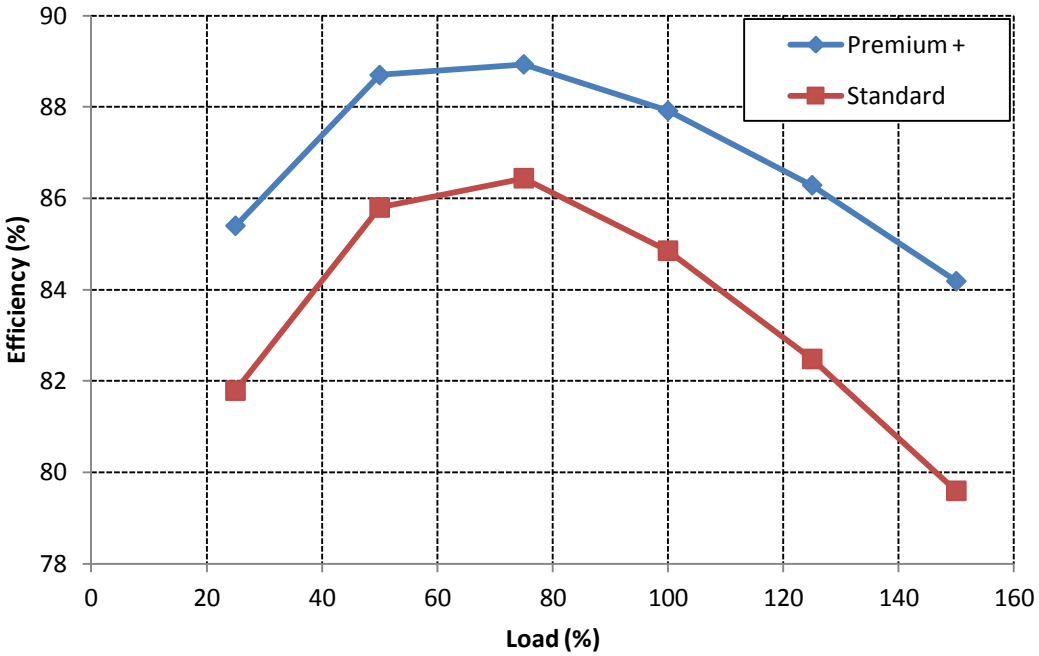

Figure A.0.8 Efficiency versus load characteristics of 7.5kW Standard and EE motors

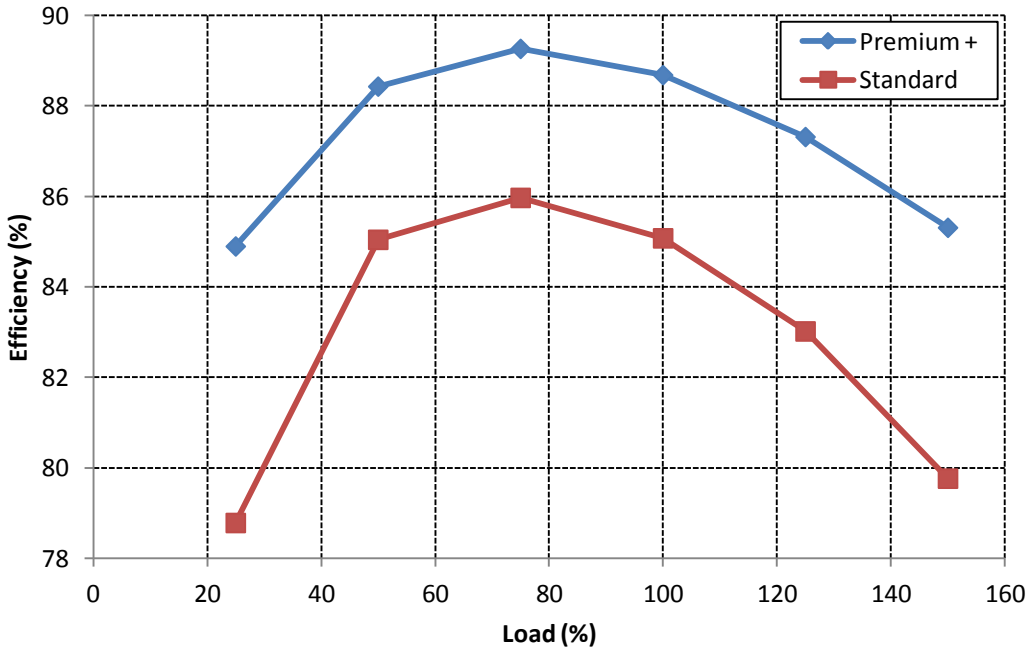

Figure A.0.9 Efficiency versus load characteristics of 11kW Standard and EE motors

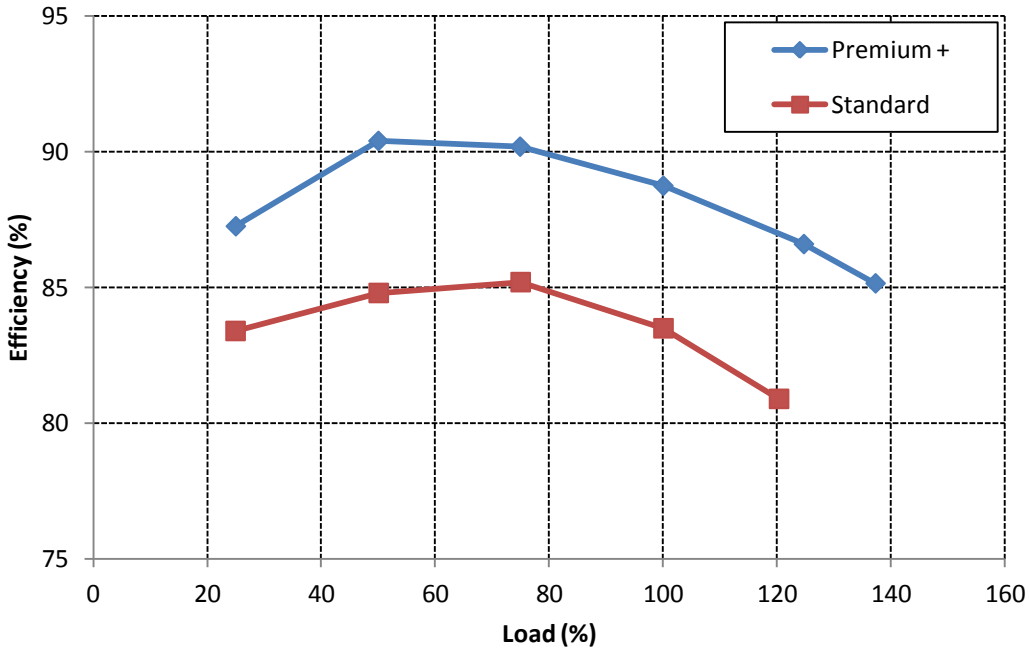

Figure A.0.10 Efficiency versus load characteristics of 15kW Standard and EE motors

- **Comparison of Losses**

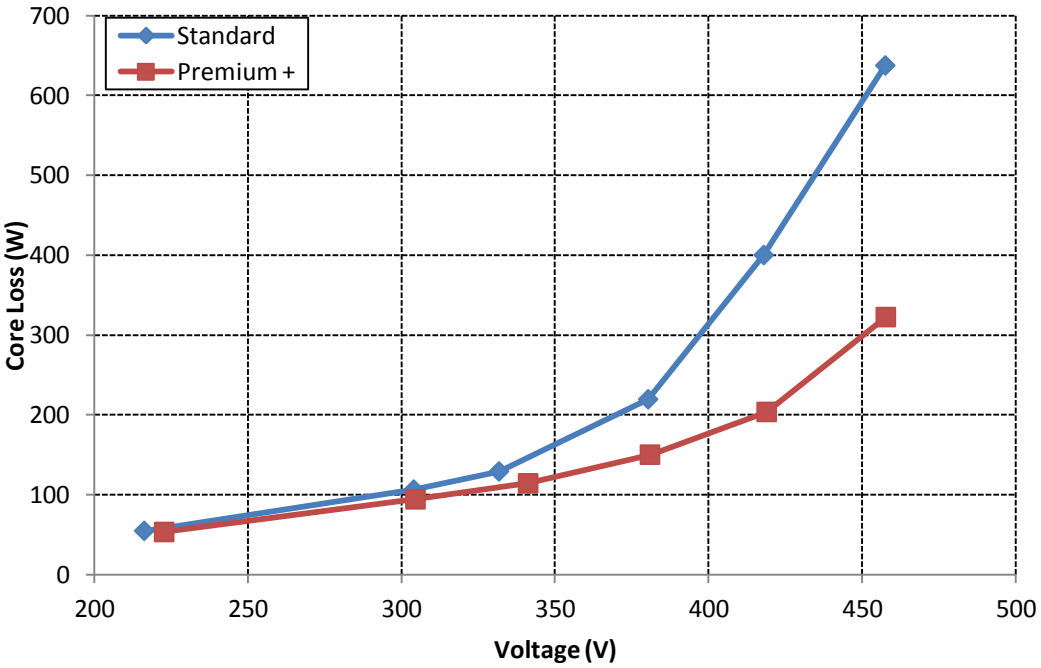

Figure A.0.11 Core Loss versus Voltage curve for 7.5kW Motors

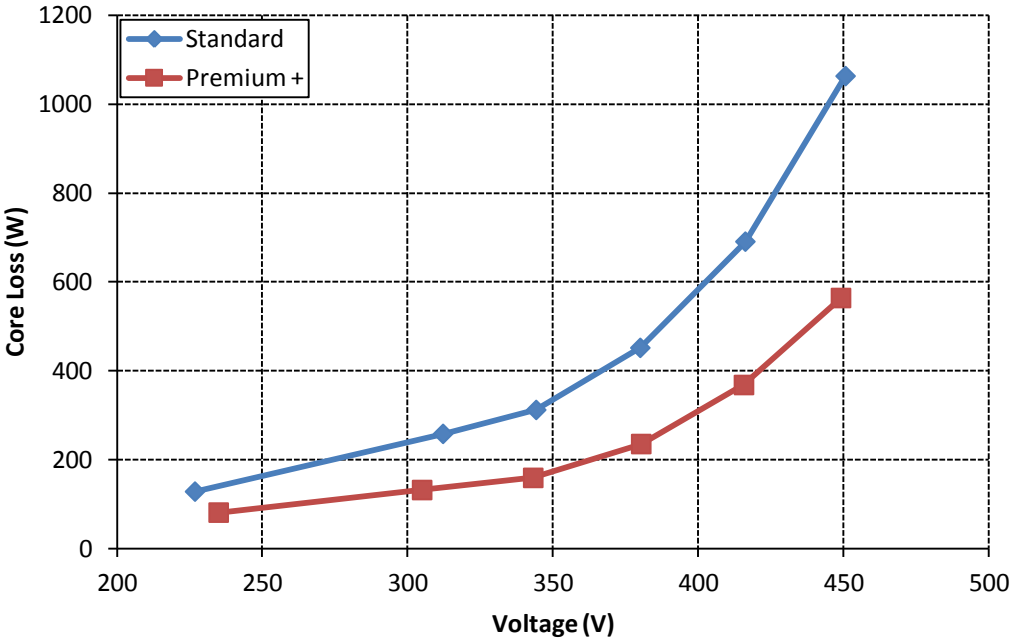

Figure A.0.12 Core Loss versus Voltage curve for 11kW Motors

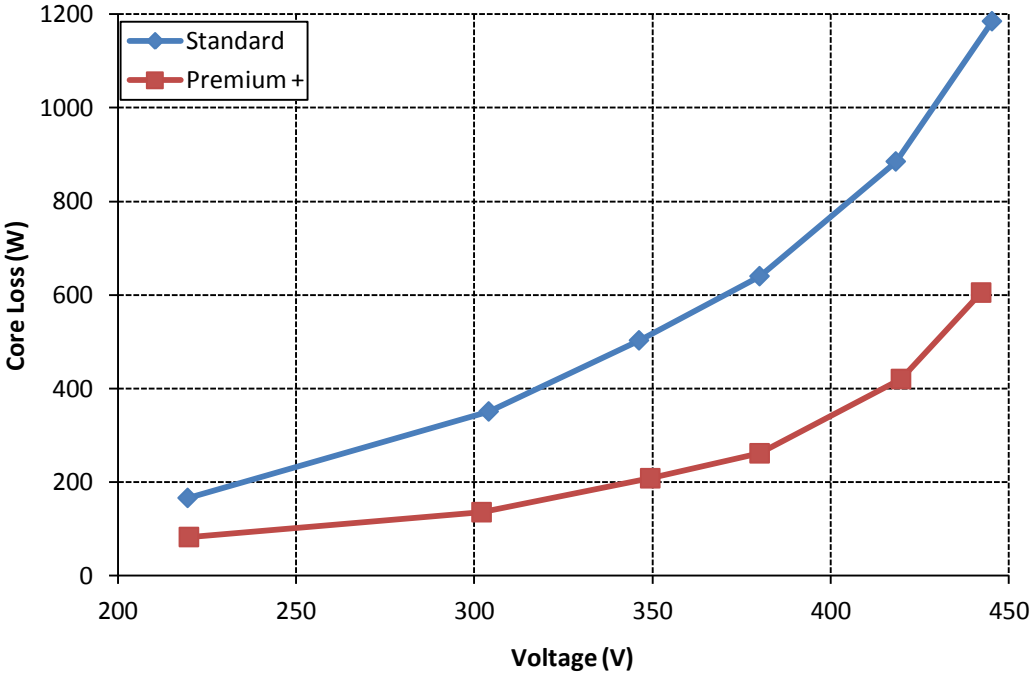

Figure A.0.13 Core Loss versus Voltage curve for 15kW Motors

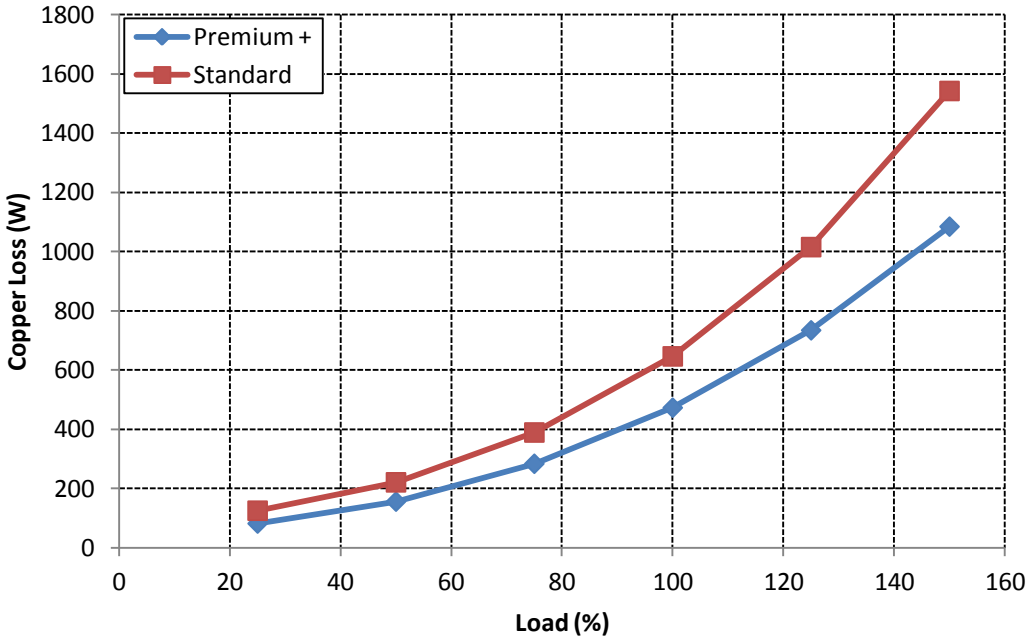

Figure A.0.14 Variation of Stator Copper Losses with Load for 7.5kW Standard and EE motors

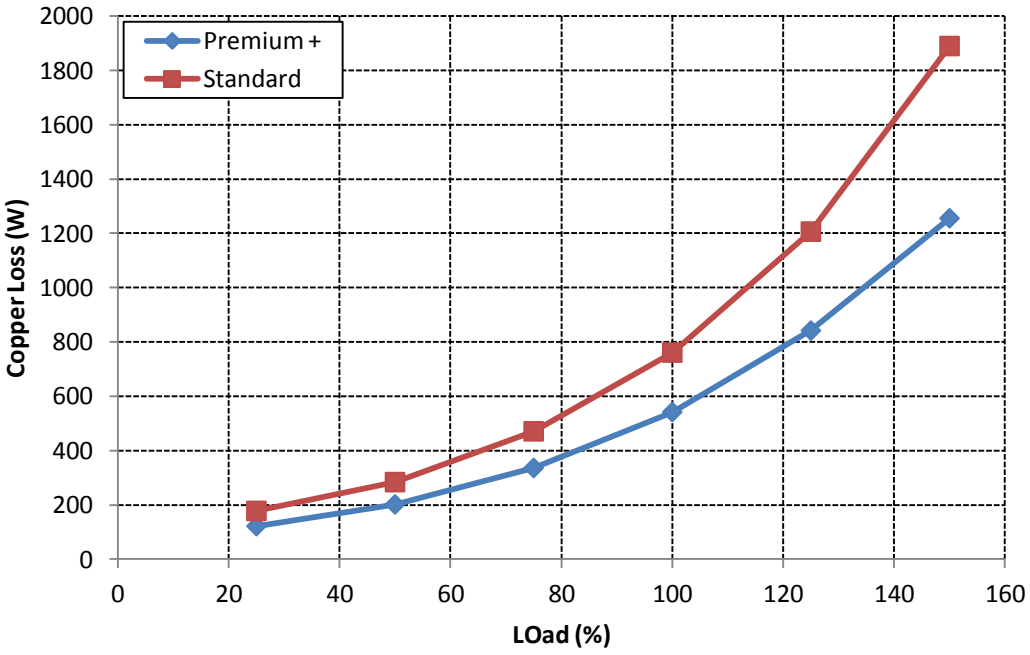

Figure A.0.15 Variation of Stator Copper Losses with Load for 11kW Standard and EE motors

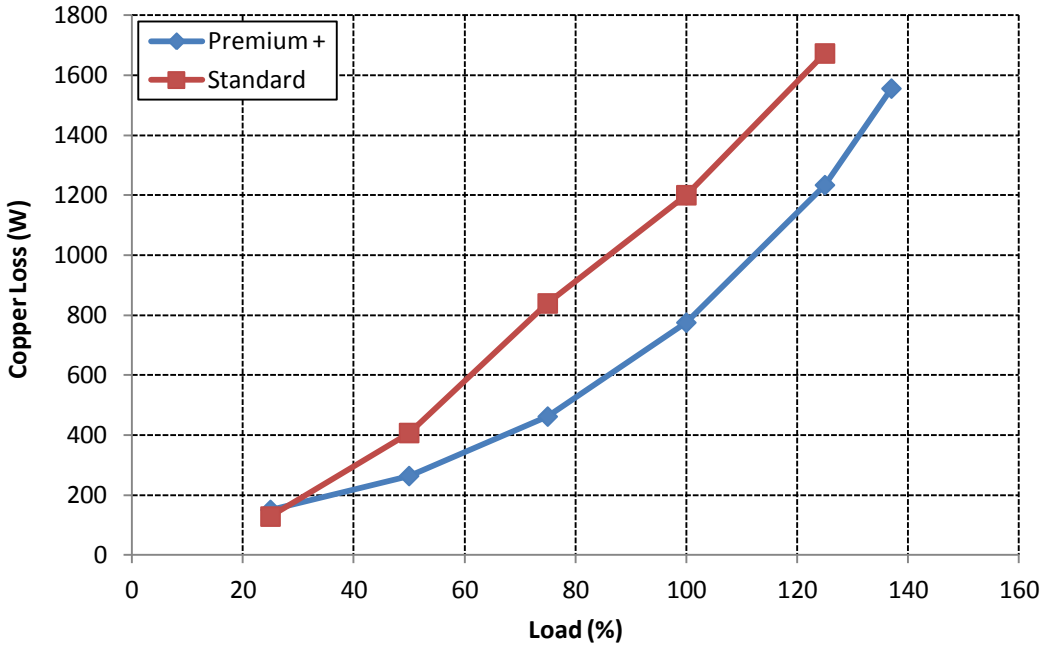

Figure A.0.16 Variation of Stator Copper Losses with Load for 15kW Standard and EE motors

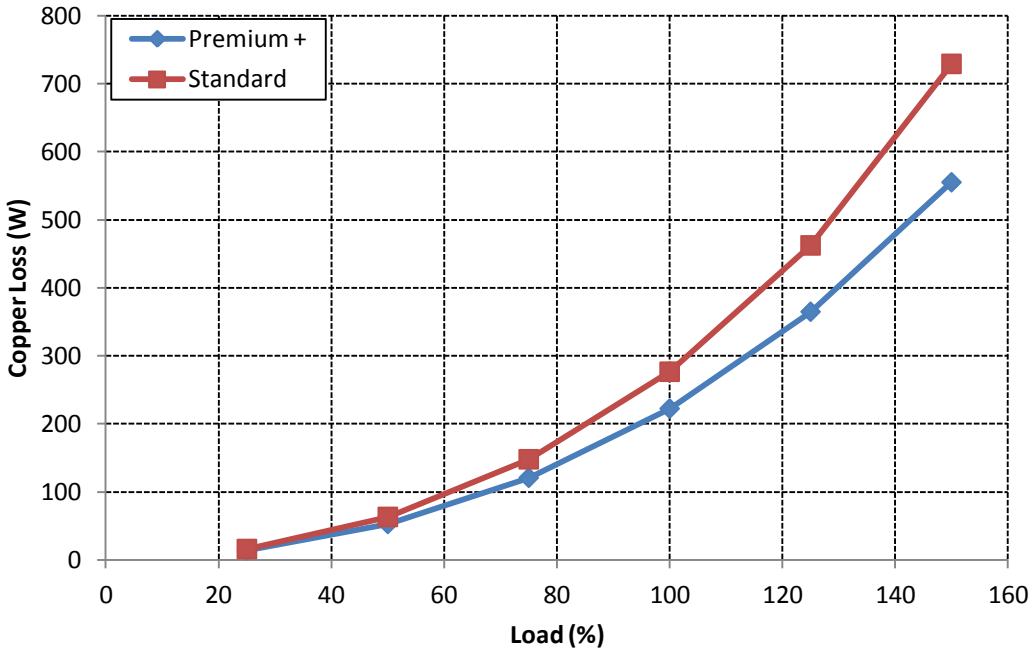

Figure A.0.17 Variation of Rotor Copper Losses with Load for 7.5kW Standard and EE motors

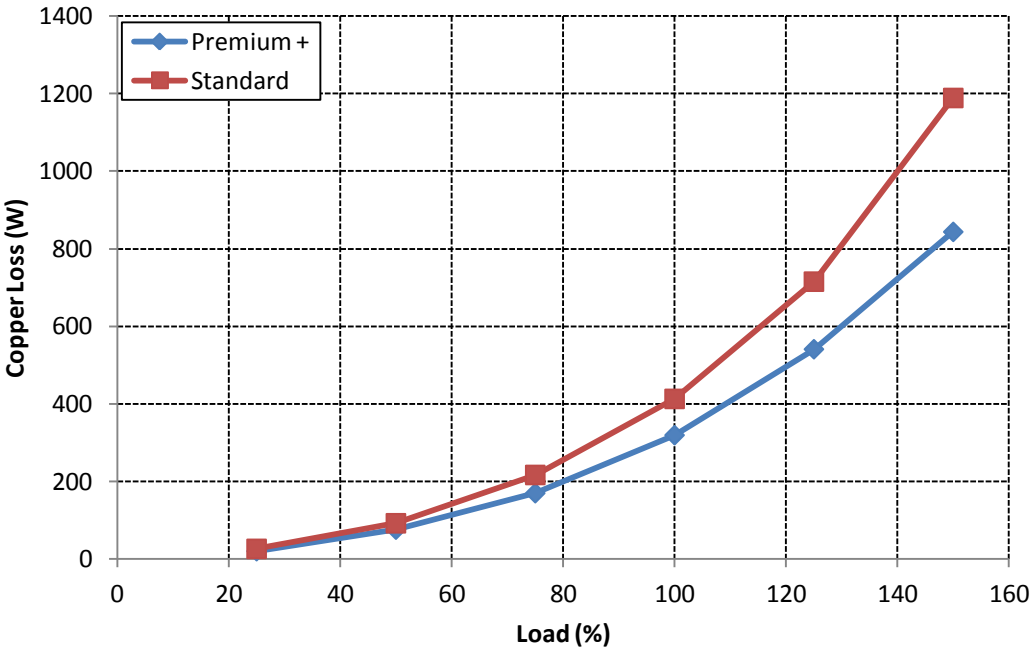

Figure A.0.18 Variation of Rotor Copper Losses with Load for 11kW Standard and EE motors

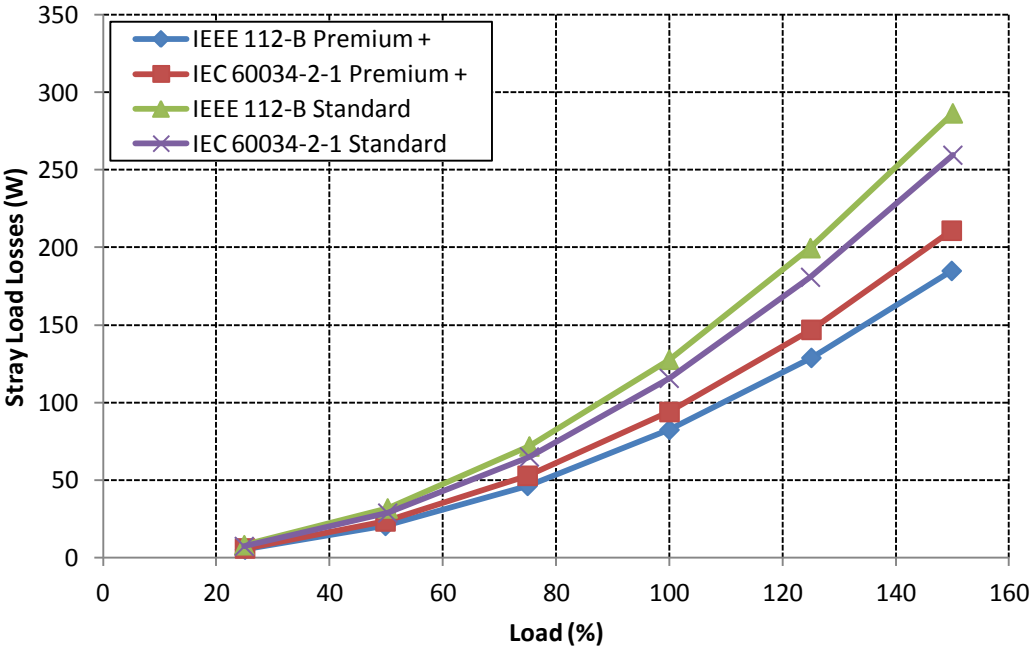

Figure A.0.19 Variation of Stray Load Losses of 7.5kW Standard and EE motor with Load

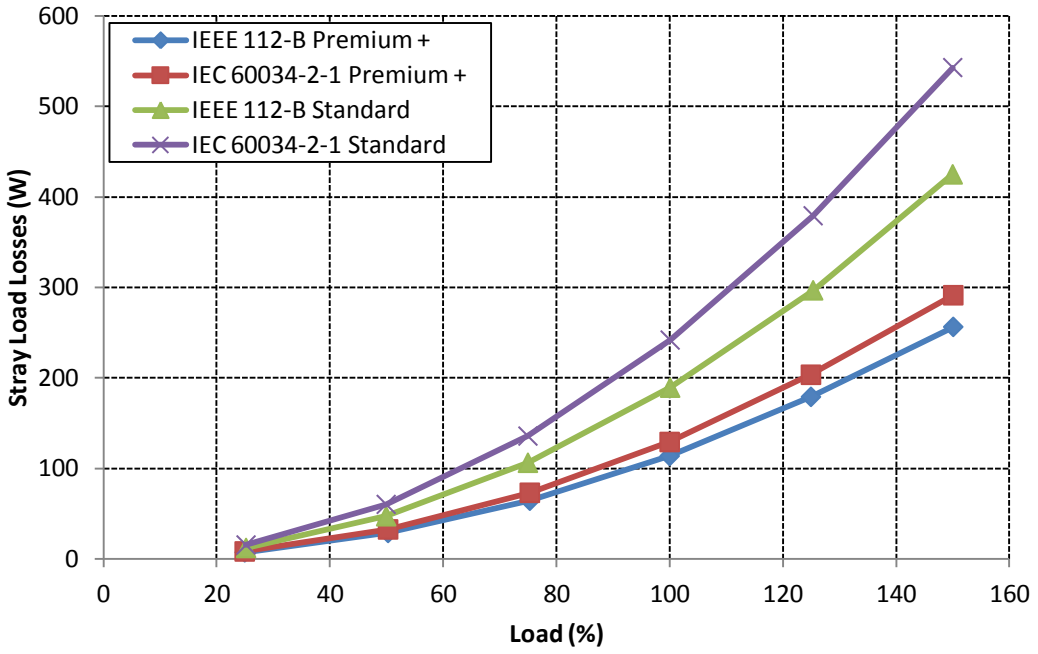

Figure A.0.20 Variation of Stray Load Losses of 11kW Standard and EE motor with Load

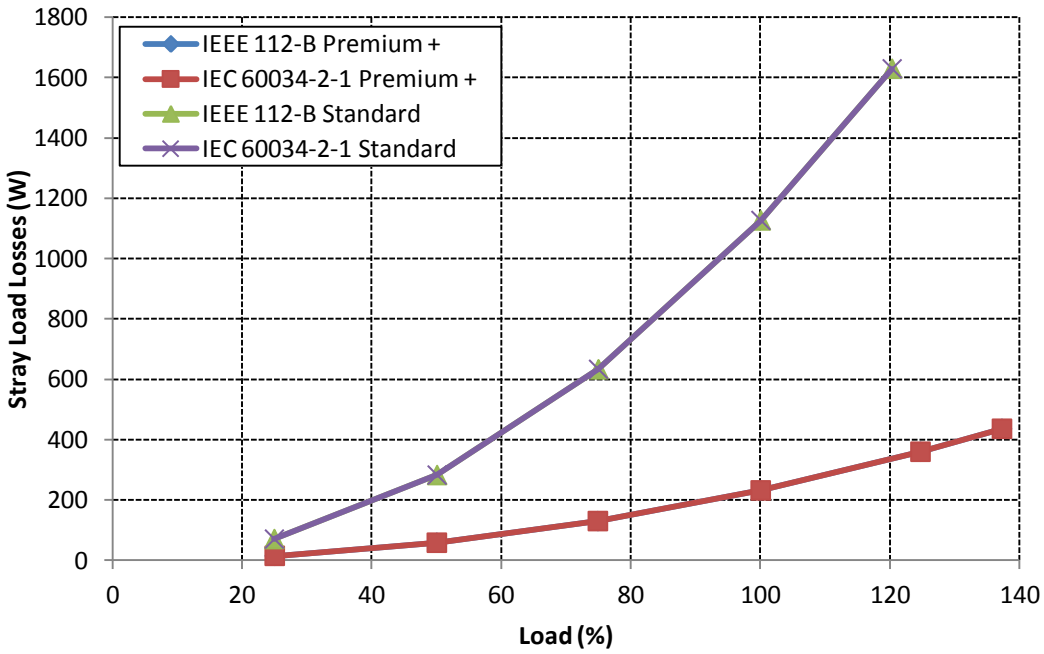

Figure A.0.21 Variation of Stray Load Losses of 15kW Standard and EE motor with Load

Matlab Code used with Harmonic Equivalent Circuit

```
clear all; close all;

%%%%%%%%%%%%%%%%%%%%%%%%%%%%%%%%%%%%%%%%%%%%%%%%%%%%%%%
%%%%%%%%

%       Determining the equivalent circuit parameters from the no-load and open circuit
tests

%%%%%%%%%%%%%%%%%%%%%%%%%%%%%%%%%%%%%%%%%%%%%%%%%%%%%%%
%%%%%%%%

m = 3;                                  % three phase motor

p=4;                                    %number of poles

a = 1; %X2 = X1                         % (X1\X2)=1 design A

f = 50;                                 % rated frequency

fL = 12.5;                              % locked rotor frequency

R1L = 2.07172;

V10 = 380;                              % no load voltage

V1L = 35.04166667;                      % locked rotor voltage (at rated current)

I10 = 5.502/sqrt(3);                    % no load current

I1L = 15.13566667/sqrt(3);              % locked rotor rated current

P0 = 307.016;                           % no load power

PL = 753.941;                           % locked rotor power (at rated current)


Ph = 8.0875e-021*V10^10 - 2.123e-017*V10^9 + 2.4178e-014*V10^8 - 1.5674e-
011*V10^7 + 6.3807e-009*V10^6 - 1.697e-006*V10^5 + 0.0002972*V10^4 -
0.033676*V10^3 + 2.3522*V10^2 - 90.905*V10 +1474.2
% core loss eq from test results for motor

Q0 = sqrt((m*V10*I10).^2 - P0.^2);            % no load reactive power

QL = sqrt((m*V1L*I1L).^2 - PL.^2);            % locked rotor reactive power

Xm = 100;  X1old = 1;  X1L = 10;  XLold = 1;  X1 = X1L; n = 0;
```

```
while (abs(Xm - X1old)/X1old > 0.000001) || (abs(X1L - XLold)/XLold > 0.000001)

   X1old = Xm;

   Xm = (m*V10.^2/(Q0 - (m*I10^2*X1)))*(1/(1 + X1/Xm).^2);

   error1 = abs(Xm - X1old)/X1old;

   XLold = X1L;

   X1L = (QL/((m*I1L.^2)*(1 + a + X1/Xm)))*(a + X1/Xm);

   error2 = abs(X1L - XLold)/XLold;

   X1 = f/fL*X1L;

   n = n + 1;

end

n;

Xm

X1

Bm  =  1/Xm;

Gfe = (Ph./(m*V10^2))*(1+X1./Xm)^2;

Rfe = 1/Gfe

R2L = ((PL./(m*I1L^2))-R1L)*(1+(X1./Xm))^2-((X1L^2)*Gfe)

%%%%%%%%%%%%%%%%%%%%%%%%%%%%%%%%%%%%%%%%%%%%%%%%%%

%Using the determined parameters to determine current, torque, speed, output power
and efficiency
%%%%%%%%%%%%%%%%%%%%%%%%%%%%%%%%%%%%%%%%%%%%%%%%%%

%c=1;   %counter for total efficiency

%d=1;   %counter for fundamental eff

%Efficiency = 0; Eff_fund =0;

%for S1=0.0005:0.00001:1                    %fundamental Slip [pu]

 S1= 0.045

ns=120*f/p;                                 %Synchronous speed [rpm]
```

```
ws=2*pi*ns/60;                    %Synchronous speed [rad/sec]
n=(1-S1)*ns;                      %Rotor speed [rpm]
w=2*pi*n/60;                      %Rotor speed [rad/sec]
R1 = R1L;
X2p = X1;
R2p = R2L;
V1 = V10;
a=1; %counter for forward rotating h
b=1; %counter for backward rotating h
%%%%%%%%%%%%%%%%%%%%%%%%%%%%%%%%%%%%%%%%%%%%%%%%%%%%%%%%%%%%%%%%%%%%%%%%
%for loop works out h components of power, torque, speed and power%%%%%%
%%%%%%%%%%%%%%%%%%%%%%%%%%%%%%%%%%%%%%%%%%%%%%%%%%%%%%%%%%%%%%%%%%%%%%%%
for m = 1:1:100
    Torqf = 0; P_output_f = 0; P_add_f = 0; P_inf_sum = 0; Skf = 0;
  for k = 6*m+1                   %forward rotating time h
    Skf      = (k-1+S1)/k;        %h slip
    Slip_f(a)  = Skf;             %storing slip values
    Vkf      = V1/k;              %h voltage
    I1kf     = Vkf/((R1+j*k*X1)+(((R2p/Skf+j*k*X2p)*(j*k*Xm))/(R2p/Skf+j*k*(X2p+Xm))));
    i1kf(a)    = I1kf;
    I2kpf     = ((j*k*Xm)/((R2p/Skf)+j*k*(X2p+Xm)))*I1kf;
    i2kpf(a)   = I2kpf;
    Pmechf     = 3*I2kpf^2*R2p*(1-Skf)/Skf;
    pmechf(a)  = Pmechf;
    P_add_f    = P_add_f + Pmechf;
    P_inf      = 3*I1kf * Vkf;
```

```
    p_inf(a)    = P_inf;
    P_inf_sum   = P_inf_sum + P_inf;
    a=a+1;
   end
    Torqb = 0; P_output_b = 0; P_add_b = 0; P_inb_sum = 0; Skb = 0;
  for k = 6*m-1                          %backward rotating time h
    Skb       = (k+1-S1)/k;              %h slip
    Slip_b(b)= Skb;                      %storing slip values
    Vkb       = V1/k;                    %h voltage
    I1kb      =
Vkb/((R1+j*k*X1)+(((R2p/Skb+j*k*X2p)*(j*k*Xm))/(R2p/Skb+j*k*(X2p+Xm))));
    i1kb(b)    = I1kb;
    I2kpb      = ((j*k*Xm)/((R2p/Skb)+j*k*(X2p+Xm)))*I1kb;
    i2kpb(b)   = I2kpb;
%       Temkb      =
abs((3*R2p*(I1kb)^2*((j*k*Xm)/(R2p/Skb+j*k*(X2p+Xm)))^2)/(k*ws*Skb));
%       temkb(b)   = Temkb;
%       Torqb      = Torqb + Temkb^2;
    Pmechb     = 3*I2kpb^2*R2p*(1-Skb)/Skb;
    pmechb(b)  = Pmechb;
    P_add_b    = P_add_b + Pmechb;
    P_inb      = 3*I1kb * Vkb;
    p_inb(b)   = P_inb;
    P_inb_sum  = P_inb_sum + P_inb;
    b=b+1;
    %%P_output_b  = P_output_b + Pmechb^2;
  end
```

```
end
%%%%%%%%%%%%%%%%%%%%%%%%%%%%%%%%%%%%%%%%%%%%%%%%%%%%%%%%%%%%%%%%%%%%%%%%%%%%
%          calculate fundamental input and developed mechanical output powers
%%%%%%%%%%%%%%%%%%%%%%%%%%%%%%%%%%%%%%%%%%%%%%%%%%%%%%%%%%%%%%%%%%%%%%%%%%%%
I1          = V1/((R1+j*X1)+(((R2p/S1+j*X2p)*(j*Xm))/(R2p/S1+j*(X2p+Xm))));
I2          = ((j*Xm)/((R2p/S1)+j*(X2p+Xm)))*I1;
%       Tem1       = abs((3*R2p*(I1)^2*((j*Xm)/(R2p/S1+j*(X2p+Xm)))^2)/(ws*S1));
P_mech_1      = 3*I2^2*R2p*(1-S1)/S1;                    %fundamental developed
mechaninal power
P_input_1     = 3*I1*V1;                                 %fundamental input power
P_input_harm   = P_inb_sum + P_inf_sum;                  %harmonic input power
P_input_total  = P_input_1 + P_input_harm ;   %total input power
P_mech_harm    = P_add_f + P_add_b;           %output harmonic power
P_mech_total   = P_mech_1 + P_mech_harm ;     %total developed mechanical power
P_output      = P_mech_total  +  P_const;
Eff_fund      = 100*abs(P_output_1)/abs(P_input_1);
Eff_total     = 100* P_output_total / P_input_total  %efficiency
%Eff(c)       = Efficiency;
%c = c+1;
%end


%S1=0.0005:0.00001:1;
%plot(S1,Eff,'r',S1,Effffff,'b')
%grid on
```